Title	Furoxan-Containing Polymeric Nanomedicines for Nitric Oxide Delivery
Author(s)	王, 騰蛟
Citation	大阪大学, 2016, 博士論文
Version Type	VoR
URL	https://doi.org/10.18910/59606
rights	
Note	

Doctoral Dissertation

Furoxan-Containing Polymeric Nanomedicines for Nitric Oxide Delivery

Tengjiao Wang

January 2016

Graduate School of Engineer

Osaka University

Contents

Chapter 6

Concluding Remarks

Chapter 1

General Introduction

Nitric oxide (NO) is the first endogenous gaseous molecule identified as a signaling mediator involved in many pathological processes in the human body.[1] The disorder of NO production has been associated with numbers of diseases such as diabetes[2], liver fibrosis[3], cardiovascular illness[4], neurodegenerative diseases[5] and several cancers[6]. However, for the therapeutic applications, systemic administration of NO is challenging due to its free radical nature and short life time. Although compounds like furoxans[7] were developed as NO donors[8] that are capable of releasing NO under physiological conditions, potential problems still exist such as the lack of tissue specificity and the short blood plasma half-life of small NO donors. In the field of drug delivery, pro-drug prepared as polymeric nanomedicine are widely exploited to improve the pharmacokinetics of small drugs. In this thesis, I aim to prepare furoxan-based polymeric NO donors and explore their potential therapeutic application. A practical protocol for removing copper impurities in furoxan-based polymeric NO donors was also developed.

Nitric Oxide

Nitric oxide (NO) has long been recognized as a toxic gas molecule as well as environmental pollutant. During the last twenty years of the 20th century, it has been found that NO plays important roles in the human body. In the year 1992, NO was selected as "Molecule of the year" due to its important regulatory roles in various physiological processes.[9] Robert F. Furchgott, Louis J. Ignarro and Ferid Murad won the Nobel Prize in Physiology or Medicine in 1998 because of the discovering of its function as a signaling molecule in the cardiovascular system. Until now, thousands of reports have been published regarding the discovery of physiological roles and potential therapeutic applications of NO.

NO is produced endogenously through both enzymatic and non-enzymatic pathways (**Figure 1**). In the enzymatic pathway, NO is generated from L-arginine and molecular oxygen by the enzymatic action of nitric oxide synthases (NOS).[10] There are three mammalian NOS isoforms: neuronal (nNOS), endothelial (eNOS), and inducible (iNOS).[11] NO produced by eNOS stimulates soluble guanylyl cyclase (sGC), which increases cyclic guanosine monophosphate (cGMP) concentration in

vascular smooth muscle cells, resulting in vasorelaxation.[12] Alternatively, NO is also produced non-enzymatically via the nitrate-nitrite-nitric oxide pathway.[13] Nitrate is converted to nitrite by oral bacteria, which disproportionates into NO after entering the acidic environment of the stomach. NO produced in this pathway reduces gastrointestinal tract infection and increases mucous barrier thickness and gastric blood flow.[14]
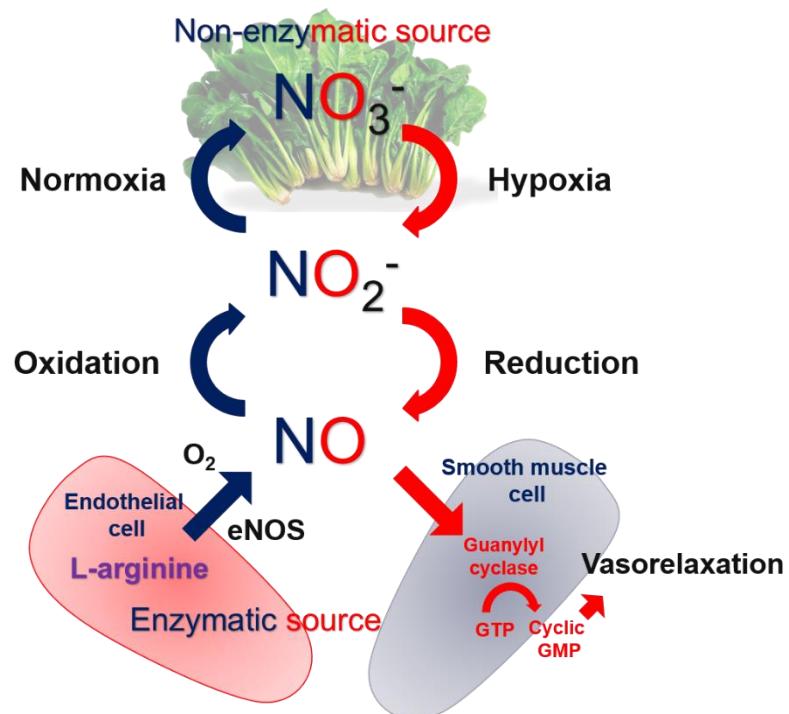
Figure 1. Two parallel pathways for the generation bioactive NO in mammals. [Ref. 13]

Due to the diverse and essential roles in many physiological processes in the cardiovascular[15], central nervous[16] and immune systems[17], NO finds application in organ transplantation[18], ischemia-reperfusion[19], and stent

restenosis prevention[20]. Furthermore, recent studies showed that the use of NO in combination with chemotherapeutic agents (cisplatin and doxorubicin) can enhance their cytotoxicity in various cancer cells[21] and also overcome drug resistance in cancer[22]. Another potential application of NO is to enhance the enhanced permeation and retention (EPR) effect in tumors.[23] Furthermore, NO was reported to enhance the chemopreventive effect of non-steroidal anti-inflammatory drugs (NSAIDs).[24] For example, NSAIDs having a NO-releasing moiety showed stronger anti-proliferative and pro-apoptotic effects in different cancer cells compared to the NSAID alone.

NO Donor

NO is a free radical having one unpaired electron, which can be oxidized in a few seconds under physiological condition.[25] NO donors, a class of compounds that generate NO upon decomposition, have been developed to study the biological properties of NO in cells.[8] NO donors can be classified into three groups based on the NO release mechanisms: a) hydrolytic decomposition; b) stimuli-sensitive decomposition (e.g., light, heat and thiol); c) enzymatic oxidation.[21] This classification is summarized

in **Table 1**. Furthermore, other important parameters to consider for a certain applications are the byproducts formed after NO release and the half-lives of NO donors.

Table 1. Classification of NO-donors based on the NO release mechanisms.

<table>
<tr><td rowspan="3">NO donors</td><td>Hydrolytic</td><td>Nitrosothiols
Diazetine dioxides
Sydnonimines
N-Nitrosamines
Oximies</td></tr>
<tr><td>Stimuli-sensitive
(i. e. thiols, light, heat)</td><td>Nitrosimines
C-Nitroso compounds
Furoxans
Oxatriazole-5-imines</td></tr>
<tr><td>Enzymatic
(i. e. Cyt-P450, peroxide)</td><td>Organic nitrites
Organic nitrates
Metal-NO complexes
N-Nitrosamines
N-Hydroxyl nitrosamines
Hydroxylamines
N-Hydroxyguanidences
Hydroxyureas</td></tr>
</table>

Furoxans

Furoxans (1,2,5-oxadiazole-2-oxides) are an important class of NO

donors that release NO by reacting with thiol-containing compounds such as cysteine and glutathione.[26] The general chemical structure of furoxan derivatives and some examples are shown in **Figure 2**. Furoxans have been reported to exert a variety of NO-related bioactivities, including cytotoxicity[27], mutagenicity[28], immunosuppression[29], central muscle relaxant properties[30], anticonvulsive effects[31], monoamino oxidase inhibition[32], and vasodilatory activities[33]. CAS 1609[34] (**Figure 2**) is one of the most bioactive furoxans and showed a potent vasodilatory effect in the femoral artery. The vasodilatory potency of the furoxans correlated well with their NO releasing capacity. Recently, a series of peptidomimetic scaffold-conjugated furoxan derivatives[35] has been synthesized and shown to exhibit neuroprotective and procognitive activities with potential applications in stroke and Alzheimer's disease. Since NO was reported to enhance the chemopreventive effect of non-steroidal anti-inflammatory drugs (NSAIDs),[24] several reports appeared concerning the conjugates of furoxans with anti-inflammatory and antimalarial drugs[36,37]. Marco L. et al. reported the furoxan-Ibuprofen derivatives (**Figure 2**) showed a reduced gastric ulcerogenicity but no altering in anti-inflammatory activity when compared with ibuprofen.[38] Meanwhile, furoxan-Aspirin derivatives[39]

6

(**Figure 2**) prepared *via* an ester bond reported by Clara C. et al that showed an antiplatelet action which is primarily contribute by the NO release activity and an anti-inflammatory trend. But these derivatives are lack of acute gastrotoxicity due to the ester nature.
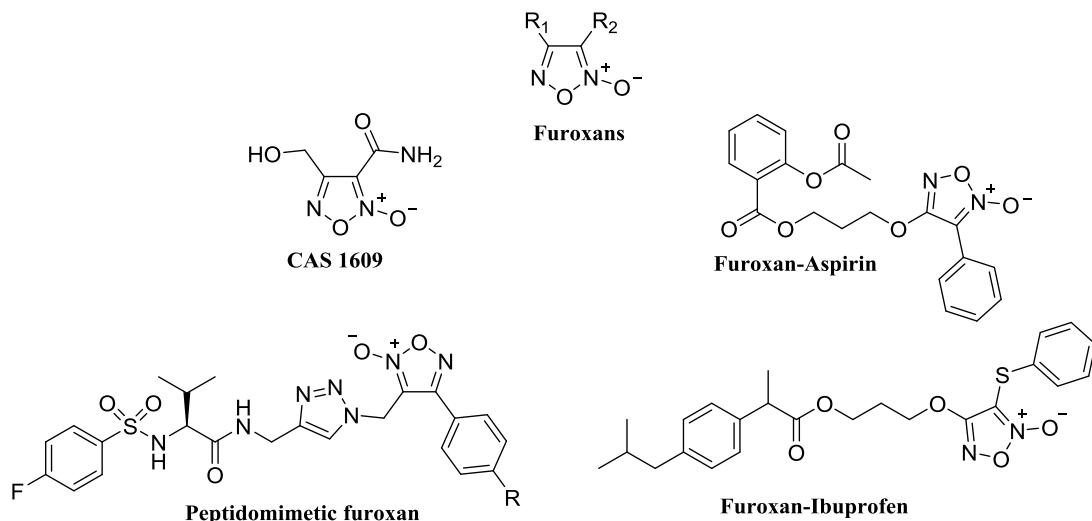
Figure 2. Chemical structures of furoxan derivatives [Ref. 8, 34, 35, 38, 39]
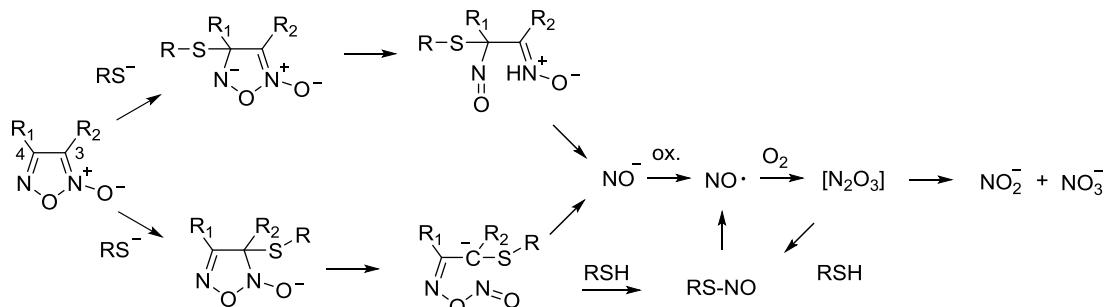
Scheme 1. NO release from furoxan under physiological condition by the action of thiols.

Furoxans are thermally stable compounds. They are also stable against acids and electrophiles. On the other hand, their stability toward bases and nucleophiles is less pronounced. In addition, it has been shown

that the NO release properties of furoxans can be modulated by changing the R_1 and R_2 groups attached to the furoxan ring (**Figure 2**). These features make furoxans attractive NO donors that have potential to deliver NO to target tissues or cells in a controlled manner. The mechanism for NO release from furoxans by the reaction with thiol-containing compounds like cysteine and glutathione has been reported by Feelisch et al.[40] (**Scheme 1**). The attack of RS⁻ at position 3 or 4 leads to formation of intermediates that undergo ring opening to the nitroso derivatives. NO is then formed by oxidation of eliminated nitrosyl anions (NO⁻). The reaction of the nitroso derivative with thiol can also result in the formation of *S*-nitrosothiol that decomposes to NO *via* radical cleavage. The generated NO reacts with oxygen to form NO_2 and N_2O_3, which can hydrolyze to form nitrite and nitrate anions. Both anions can nitrosate thiols to form *S*-nitrosothiols and nitrite.

Polymeric nanomedicine

Although the development of NO donors opens up a new strategy in NO-based therapies, one of the potential problems is the lack of tissue specificity of those low molecular weight compounds. In addition, since

NO exerts versatile roles in the body, the systemic administration of NO donors may elicit not only the desired activity but also affect other functions which could potentially cause side effects in healthy tissues. Furthermore, small NO donors generally exhibit a short half-life in the body due to rapid renal clearance and metabolic degradation. Therefore, controlled delivery of NO donors to the specific tissues or cells is necessary for practical applications.


Polymer –drug conjugates   Micelles   Vesicles

Dendrimers   Hydrogel
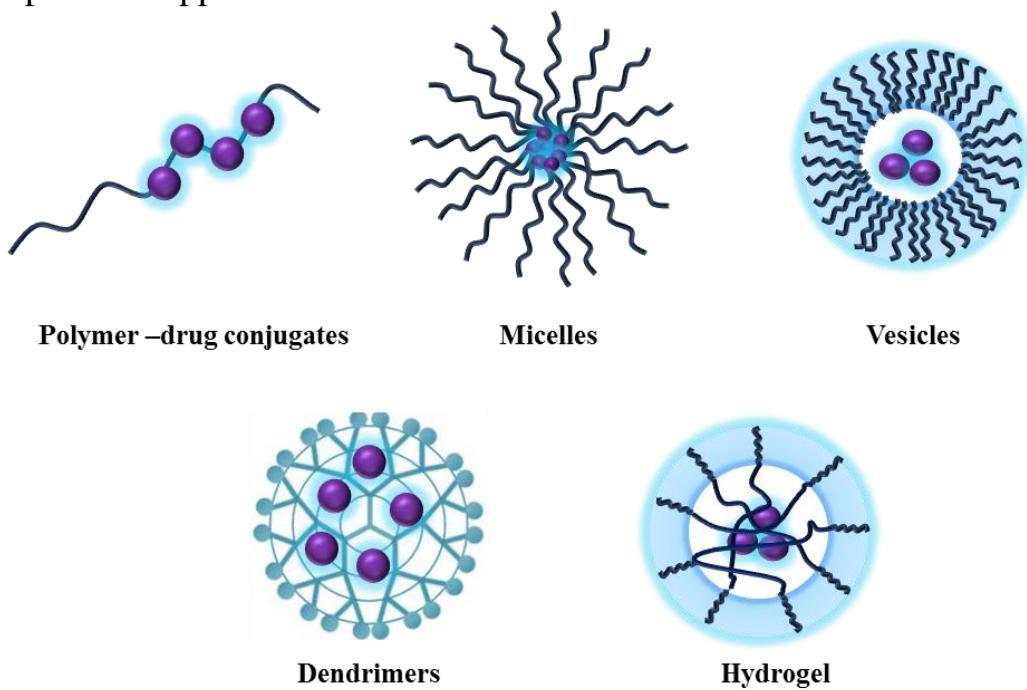
Figure 3. Schematic illustration of representative polymeric nanomedicines.

In the field of drug delivery, nanomedicine[41] refers to multi-component drug or drug delivery systems in the size range of subhundred nanometer.[42,43] A wide variety of polymeric materials including polymer-

drug conjugates,[44-47] polymeric micelles,[48-51] polymeric liposome,[52-54] dendrimers,[55-57] polymeric vesicles,[58-60] and polymeric hydrogels[61-63] (**Figure 3**) have been prepared and used to deliver drugs to the target tissues/cells in a controlled manner. [64]

The approach to use polymer-drug conjugates was first proposed by Ringsdorf (**Figure 4**). In this approach, drug molecules are bound to a hydrophilic polymer via a covalent bond, which can be cleaved at the site of interest to release drugs.[65] Additionally, modification of polymer conjugates with antibodies or targeting peptides can enhance accumulation of drugs at target tissues. Solubilizing groups can be attached to the polymer backbone to modify the bioavailability of the drug–polymer conjugate. In general, substances smaller than 5 nm, such as low molecular weight drugs are eliminated from the body by renal clearance. In addition, substances larger than 200 nm in dimension would be captured by reticuloendothelial system. Therefore, it is expected that polymer-drug conjugates in the size range of 5-200 nm show prolonged blood circulation time .[66]
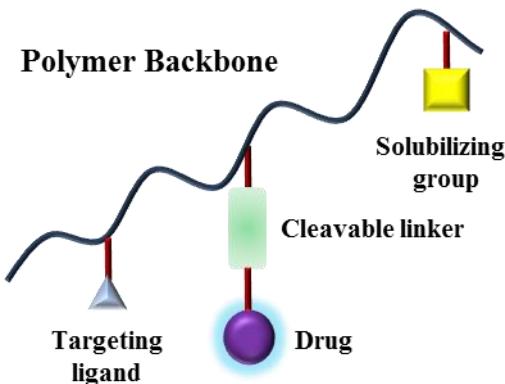
Figure 4. Ringsdorf's model on polymer-drug conjugates.

Polymeric micelles, another type of nanomedicines, are prepared from amphiphilic block copolymers having hydrophilic and hydrophobic segments by assembly in aqueous media. These block copolymer micelles has been widely used in the field of drug delivery because of the high drug-loading capacity of the core and the ability to improve solubility and bioavailability of drugs.[67,68] Polymeric micelles in the size range of 10–100 nm in diameter promote drug accumulation at tumor sites due to leaky vasculature and poor lymphatic drainage, also called "enhanced permeability and retention (EPR) effect". Another beneficial aspect of polymeric micelles is their long blood circulation time after systemic administration.

Polymeric NO donor

The use of nanomedicine is one of the strategy to improve the stability

and pharmacokinetics of NO donors.[69] NO donor-loaded inorganic nanoparticles like silica nanoparticles[70,71], gold nanoparticles[72], iron oxide nanoparticles[73] and hydrogel/glass composite[74] have been reported. These nanoparticles had sustained NO-release property and showed promise in antibacterial and antitumor therapies as well as wound healing.[75,76] Poly (lactic-co-glycolic acid) (PLGA) nanoparticles containing a NO donor, diazeniumdiolate (NONOate), has also been prepared and used to deliver NO to the vaginal mucosa resulting in improved vaginal blood perfusion, which may have implications in the treatment of female sexual dysfunction.[77] Furthermore, NONOate derivatives were encapsulated into PEG-coated polymeric nanoparticles and showed anticancer activity.[78] Compared to the nanoparticles, fewer number of reports have been published on NO-releasing polymeric micelles. The first NO-releasing micelles were reported by Jo et al. [79] in 2009. The micelles containing NONOate moieties showed extremely slow NO release. However, the potential risk in the use of NONOates due to their toxicity as well as the carcinogenic secondary amine byproduct of NONOates after NO release may limit the therapeutic application of the NONOate-based micelles.[80] Recently, Duong et al. reported nitrosothiole-bearing polymeric micelles

which enabled intracellular delivery of NO.[81] More recently, NO releasing

micelles carrying various types of NO donors including organic nitrate[82],

S-nitrosothiol[83] and photo sensitive 4-nitro-3-trifluoro-methylphenol

(NTP)[84] were also reported.

Purpose and outline of thesis

Considerable effort has been devoted to develop NO-releasing

polymeric nanomedicines where various NO donors are attached to

macromolecular nano-structures including polymers, micelles or latex

nanoparticles[70,85,86]. Despite the interesting properties of furoxan

derivatives, furoxan-containing polymeric NO donors have not been

investigated. Thus, in this thesis, I aim to prepare furoxan-containing

polymeric nanomedicines, hydrophilic polymer-furoxan conjugates and

polymeric micelles containing furoxan moieties, and explore their potential

application in NO-based therapy.

This thesis consists of six chapters including general introduction and

concluding remarks. The content of each chapter is briefly described below.

In chapter 2, "**Nitric oxide-releasing polymeric furoxan conjugates**"

is described. The polymeric furoxan conjugates were prepared by conjugating azide-functionalized furoxan derivatives to poly(ethylene glycol) (PEG) with an alkyne end group by the copper(I)-catalyzed 1,3-Huisgen cycloaddition. The NO release properties in response to cysteine, hydrolytic stability and a synergistic anti-proliferative effect with ibuprofen in human colon cancer cells were evaluated.

In chapter 3, "**Furoxan-bearing micelles for nitric oxide delivery**" is described. The furoxan-containing polymeric micelles were prepared from an amphiphilic block copolymer consisting of a hydrophobic furoxan-bearing block and a hydrophilic poly (*N*-acryloylmorpholine) (PAM) block, which was synthesized by using a combination of the reversible addition-fragmentation chain transfer (RAFT) polymerization and the copper(I)-catalyzed 1,3-Huisgen cycloaddition reaction techniques. The NO release properties in response to cysteine, hydrolytic stability and a synergistic anti-proliferative effect with ibuprofen in human colon cancer cells were evaluated.

In chapter 4, "**Copper removal from polymers by diethyldithiocarbamate complexation**" is described. In chapter 2 and 3,

furoxan-containg polymeric NO donors were prepared by using the copper(I)-catalyzed 1,3-Huisgen cycloaddition reaction. However, a drawback of this approach is the remaining trace amounts of copper catalyst in the final product, which may affect the NO releasing property of furoxans. In this chapter, new purification method using diethyldithiocarbamate (DTC) as a complexing ligand followed by size exclusion chromatography was developed to remove copper impurities from the PEG-furoxan conjugate as well as furoxan-containing polymeric micelle.

In chapter 5, **"NO-releasing micelles from amphiphilic furoxan-bearing block polymers by modification of poly(*N*-acryloylmorpholine)-*b*-poly(pentafluorophenyl acrylate) with amine-containing furoxan"** is described. Since the use of the copper-catalyzed reaction to conjugate furoxan moieties to polymers requires the additional purification step to remove the copper impurities, a new synthetic approach to prepare a furoxan-bearing block copolymer without using a copper catalyst was developed. Poly(*N*-acryloylmorpholine)-*b*-poly(pentafluorophenyl acrylate) diblock copolymer was synthesized and the pentafluorophenyl ester moieties were reacted with amine-containing

furoxan derivative to yield a furoxan-bearing diblock copolymer. The micelles were prepared from this polymer and the morphology and NO release property were characterized.

In chapter 6, the results and conclusions obtained in each chapter are summarized.

Chapter 2

Nitric oxide-releasing polymeric furoxan conjugates

Introduction

In this chapter, preparation of polyethylene glycol (PEG)-furoxan conjugates was described. To avoid side reaction and archive high degree of conjugation, copper(I)-catalyzed 1,3-Huisgen cycloaddition reaction, or copper-catalyzed azide-alkyne cycloaddition reaction (CuAAC), was used. CuAAC was known as the classic "click reaction" coined by K. Barry Sharpless in 1998, and was first fully described by Sharpless, Hartmuth Kolb, and M.G. Finn of The Scripps Research Institute in 2001.[87-90] Since the CuAAC is a very robust and orthogonal reaction, in recent years, it has been often used to prepare polymeric materials with a complex structure and functionality.

As shown in **Figure 5**, by using CuAAC, two azide-containing furoxan derivatives were successfully conjugated to alkyne group-bearing PEG. The conjugates released NO in response to cysteine and enhanced the anti-proliferative effect of ibuprofen in HT-29 colon cancer cells. Furthermore, the furoxan derivatives underwent decomposition in

physiological buffer, which can be slowed down by the conjugation of furoxan derivatives to PEG.
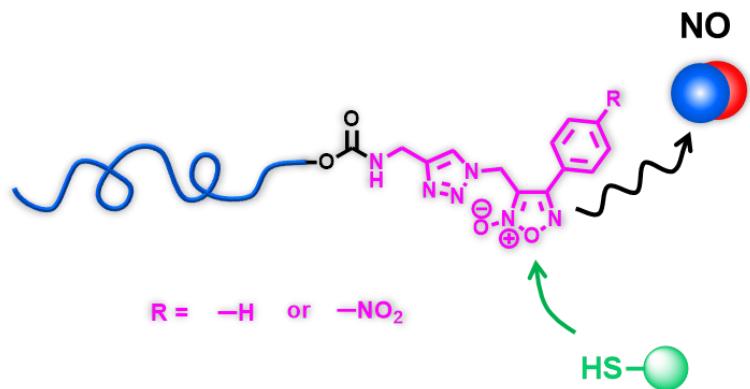
Figure 5. Nitric oxide-releasing polymeric furoxan conjugates.

Experimental

Instrumentation

NMR spectroscopy. ^{1}H NMR and ^{13}C NMR spectra were measured with a Bruker DPX400 NMR spectrometer. For ^{1}H NMR spectra a total of 32 scans were collected and the D1 was set to 10 s for the polymers and 1 s for the low molecular weight compounds. Chemical shifts are referenced to the residual undeuterated NMR solvent signal at 2.50 (d_6-DMSO) and 7.26 ppm (CDCl$_3$). For ^{13}C NMR 1024 scans were collected and the D1 was set to 2 s. Chemical shifts are referenced to the residual undeuterated (CD$_3$OD) solvent at 49.00 ppm.

UV/Vis spectroscopy. The absorbance was measured with a Tecan infinite M200 plate reader in transparent polystyrene 96 well plates and UV/Vis spectra were recorded on a Thermo Scientific NanoDrop 2000c spectrophotometer using 2 μL of sample volume or a quartz cuvette.

Attenuated total reflection infrared spectroscopy (ATR-IR). Attenuated total reflection infrared (ATR-IR) spectra were obtained on a Thermo Scientific Nicolet iS5 equipped with an iD5 universal ATR

sampling accessory.

Electrochemical detection of NO. For NO detection a 2 mm NOP-electrode was connected to a TBR4100 Four-Channel Free Radical Analyzer (WPI, United States). The measurements were recorded with the LabScribe software. The electrode was inserted in a 1–3 mL four port closed chamber. The temperature was measured with a temperature sensor and controlled through an external circulating bath.

Materials

Propargylamine, propargylamine hydrochloride, diphenylphosphoryl azide (DPPA), 1,8-diazabicyclo[5.4.0]undec-7-ene (DBU), L-cysteine, reduced glutathione, *N*-(1-naphthyl)ethylenediamine dihydrochloride (NED), diethylenetriaminepentaacetic acid (DTPA), diethylammonium diethyldithiocarbamate, 2,3-diaminonaphthalene and sulfanilamide (SA) were purchased from Tokyo Chemical Industry (TCI), Japan. Disuccinimidyl carbonate (DSC), super dehydrated dimethyl sulfoxide (DMSO), super dehydrated dimethylformamide (DMF), super dehydrated toluene, copper(II) sulfate pentahydrate ($CuSO_4 \cdot 5H_2O$), sodium ascorbate, concentrated HCl (aq.), 1 N HCl (aq.), sodium nitrite ($NaNO_2$), potassium

bicarbonate ($KHCO_3$), sodium hydrogen sulfate ($NaHSO_4$), anhydrous sodium sulfate (Na_2SO_4), ibuprofen and silica (SiO_2) were purchased from Wako Pure Chemical Industry (Japan), and 2 M HCl in isopropanol (HCl/i-PrOH) was purchased from Kokusan Chemicals (Japan). Hexane, ethyl acetate (EtOAc), tetrahydrofuran (THF), *tert*-butyl alcohol (*t*-BuOH), diethyl ether (Et_2O), triethylamine (Et_3N), calcium hydride (CaH_2), dichloromethane (CH_2Cl_2), ethanol (EtOH) and molecular sieves 3A were purchased from Nacalai Tesque (Japan). Ninhydrin and poly(ethylene glycol) methyl ether (average M_n 5000) were purchased from Sigma-Aldrich (Japan). All chemicals were used as received except for Et_3N which was distilled over ninhydrin and CaH_2 and placed over molecular sieves. Molecular sieves were dried by heating at 180 °C for 5 h. TLC silica gel 60 F254 plates were from Merck (Japan). Sephadex LH20 was from GE Healthcare (Japan). Deuterated solvents for ${}^1H$ NMR (CD_3OD, $CDCl_3$ and *d6*-DMSO) were from Cambridge Isotope Laboratories, Inc. (USA). Dialysis tubing (MWCO 2 kDa) and 0.45 μm syringe filters were purchased from Spectrum Laboratories Inc. (Japan). Dulbecco's phosphate buffered saline (10×, PBS), fetal bovine serum (FBS) and DMEM GlutaMAX were from Life Technologies (USA).

Preparation of cell lysate. RAW 264.7 macrophages were cultured in DMEM GlutaMAX supplemented with 10% heatinactivated FBS and 50 U/mL-50 µg/mL penicillin-streptomycin in a CO_2 incubator at 37 °C. Cells were scraped off when reaching 70–80% confluency. The cell suspension (3.20×10^6 cells/mL) was centrifuged at 500 rpm for 5 min and the cell pellet was washed with cold Dulbecco's phosphate buffered saline (PBS) three times. The cell suspension was centrifuged at 500 rpm for 5 min and resuspended in 1 mL passive lysis buffer at 1.28×10^7 cells/mL, and vortexed at RT for 10 min. The suspension was centrifuged, and the clear supernatant was collected and stored at -20 °C.

Synthesis

3-(Hydroxyl-methyl)-4-phenyl-1,2,5-oxadiazole 2-oxide (1). was prepared as reported.[35]

3-(Hydroxyl-methyl)-4-(4-nitrophenyl)-1,2,5-oxadiazole 2-oxide (2). was prepared as reported.[35]

3-(Azidomethyl)-4-phenyl-1,2,5-oxadiazole 2-oxide (3). 50.8 mg (0.26 mmol) of (**1**) was dissolved in 2 mL of toluene and cooled to 0 °C in an ice

bath. To the solution was added 56.8 μL (0.26 mmol, 1.0 eq.) of DPPA and 39.9 μL (0.26 mmol, 1.0 eq.) of DBU. The flask was evacuated/purged with argon (3 ×) and the mixture was stirred in the dark. After TLC indicated the disappearance of (**1**), 10 mL of water and 20 mL of EtOAc were added to the reaction mixture. The layers were separated and the aqueous phase was extracted with EtOAc (2 × 20 mL). The extracts were combined and washed with water (3 × 20 mL), 5% KHCO$_3$ (aq.) (2 × 20 mL) and brine (20 mL). The organic phase was dried over Na$_2$SO$_4$, filtered and concentrated under reduced pressure. The residue was purified by SiO$_2$ column chromatography (EtOAc/hexane = 1 : 10, R$_f$ = 0.3) to yield 35.1 mg (0.16 mmol, 61%) of a white solid. ^{1}H NMR (CDCl$_3$) δ = 7.72 (m, 2H, 2 × CH$_{aromat}$), 7.58 (m, 3H, 3 × CH$_{aromat}$), 4.47 (s, 2H, CH$_2$). The ^{1}H NMR data were in agreement with those previously reported.[35] The ^{1}H NMR spectrum is shown in **Figure 6**. FT-IR: ν (cm^{-1}) 2101 (N$_3$) and 1602, 1578 (furoxan ring). The IR spectrum is shown in **Figure 7**. HRMS (m/z,M + H$^+$, ESI-TOF-MS, FAB$^+$): calculated for C$_9$H$_7$N$_5$O$_2$ 218.0678, found 218.0680.

3-(Azidomethyl)-4-(4-nitrophenyl)-1,2,5-oxadiazole 2-oxide (4). 111.1 mg (0.47 mmol) of (**2**) was dissolved in 3 mL of toluene and cooled to 0 °C

in an ice bath. To the solution was added 100.7 µL (0.47 mmol, 1.0 eq.) of

DPPA and 69.9 µL (0.47 mmol, 1.0 eq.) of DBU. The flask was

evacuated/purged with argon (3 ×) and the mixture was stirred in the dark.

After TLC indicated the disappearance of (**2**), the reaction mixture was

concentrated under reduced pressure and the residue was purified by SiO_2

column chromatography (EtOAc/hexane = 1 : 7, R_f = 0.27) to yield 91.6

mg (0.35 mmol, 74%) of a yellow solid. ^{1}H NMR (CDCl$_3$) δ = 8.42 (m, 2H,

2 × CH$_{aromat}$), 7.98 (m, 2H, 2 × CH$_{aromat}$), 4.51 (s, 2H, CH$_2$). The ^{1}H NMR

data were in agreement with those previously reported.[35] The ^{1}H NMR

spectrum is shown in **Figure 8**. FT-IR: ν (cm^{-1}) 2112 (N$_3$), 1610, 1596

(furoxan ring) and 1526 (NO$_2$). The IR spectrum is shown in **Figure 9**

HRMS (m/z, M, ESI-TOF-MS, FAB$^-$): calculated for C$_9$H$_6$N$_6$O$_4$ 262.0451,

found 262.0452.

3-((4-(Aminomethyl)-1*H*-1,2,3-triazol-1-yl)methyl)-4-phenyl-1,2,5-

oxadiazole 2-oxide HCl salt (5). 104.0 mg (0.48 mmol) of (**3**), 43.8 mg

(0.48 mmol) of propargylamine hydrochloride, 2.4 mg (9.6 µmol) of

CuSO$_4$·5H$_2$O and 9.5 mg (48 µmol) of sodium ascorbate were dissolved in

a mixture of 3 mL of *t*-BuOH and 1.5 mL of H$_2$O. The solution was

degassed with argon by five freeze–thaw cycles and the mixture was stirred

for 24 h at 35 °C. After cooling down to room temperature, the mixture was diluted with 5% w/v $KHCO_3$ (aq.) (10 mL) and extracted with CH_2Cl_2 (3 × 60 ml). The combined extracts were dried over $NaSO_4$, filtered and concentrated under reduced pressure. The resulting oil was dissolved in 200 μL 2 M HCl/i-PrOH and diluted with 10 mL Et_2O to give a white solid. The solid was dried under reduced pressure, dissolved in 5 mL of H_2O and lyophilized to yield 117.3 mg (0.38 mmol, 79%) of a white solid. ^{1}H NMR ($d6$-DMSO) δ = 8.50 (bs, 3H, NH_3^+), 8.36 (s, 1H, CH triazole), 7.82 (m, 2H, 2 × CH_{aromat} furoxan), 7.63 (m, 2H, 2 × CH_{aromat} furoxan), 5.83 (s, 2H, CH_2-furoxan), 4.09 (s, 2H, $C\underline{H}_2$-NH_3^+). ^{13}C NMR (CD_3OD) δ = 156.85, 140.19, 131.24, 129.16, 127.71, 125.77, 125.28, 111.52, 42.03, 33.99. The ^{1}H NMR and ^{13}C NMR spectra are shown in **Figure 10**, **11** and FT-IR: ν (cm^{-1}) 3241 (N–H), 1595, 1577 (furoxan ring). The azide band of (**3**) at 2102 cm^{-1} was not observed anymore. The IR spectrum is shown in **Figure 12**. HRMS (m/z, M+H$^+$, ESI-TOF-MS, FAB$^+$): calculated for $C_{12}H_{12}N_6O_2$ 273.1100, found 273.1098.

3-((4-(Aminomethyl)-1H-1,2,3-triazol-1-yl)methyl)-4-(4-nitrophenyl)-1,2,5-oxadiazole 2-oxide HCl salt (6). 197.4 mg (0.75 mmol) of (**4**), 68.9 mg (0.75 mmol) of propargylamine hydrochloride, 3.8 mg (15.2 μmol) of

CuSO$_4$·5H$_2$O and 14.9 mg (75 μmol) of sodium ascorbate were dissolved in a mixture of 2 mL of *t*-BuOH, 1 mL of EtOH, 1 mL of THF and 2 mL of H$_2$O. The solution was degassed with argon by five freeze–thaw cycles and the mixture was stirred for 24 h at 35 °C. After cooling down to room temperature, the mixture was diluted with 5% w/v KHCO$_3$ (aq.) until the solution reacted basic by pH paper and extracted with CH$_2$Cl$_2$ (3 × 50 mL). The extracts were dried over NaSO$_4$, filtered and concentrated under reduced pressure to yield 192.6 mg (81%) of a yellow solid. ^{1}H NMR (CDCl$_3$) δ = 8.45 (d, 2H, 2 × CH$_{aromat}$ furoxan), 8.21 (d, 2H, 2 × CH$_{aromat}$ furoxan), 7.79 (s, 1H, CH triazole), 5.57 (s, 2H, CH$_2$-furoxan), 4.01 (s, 2H, CH$_2$-NH$_2$). ^{13}C NMR (CD$_3$OD) δ = 155.36, 149.57, 148.91, 131.69, 129.17, 124.02, 123.13, 111.43, 41.72, 36.09. The ^{1}H NMR and ^{13}C NMR spectra are shown in **Figure 13**, **14**. HRMS (m/z, M+H$^+$, ESI-TOF-MS, FAB$^+$): calculated for C$_{12}$H$_{11}$N$_6$O$_4$ 318.0951, found 318.0948.

The HCl salt of 3-((4-(aminomethyl)-1*H*-1,2,3-triazol-1-yl)- methyl)-4-(4-nitrophenyl)-1,2,5-oxadiazole 2-oxide was prepared by dissolving the solid (28.0 mg, 0.091 mmol) in 0.91 mL 1 M HCl (aq.). The solution was filtered through a 0.45 μm hydrophilic filter to remove small particles and lyophilized to yield 29.8 mg (0.084 mmol, 92%) of a pale yellow solid. ^{1}H

NMR (*d6*-DMSO) δ = 8.42 (m, 5H, NH_3^+ and 2 × CH_{aromat} furoxan), 8.35 (s, 1H, CH triazole), 8.10 (m, 2H, 2 × CH_{aromat} furoxan), 5.89 (s, 2H, CH_2-furoxan), 4.08 (s, 2H, C$\underline{H}_2$-NH_3^+). The ^1H NMR spectrum is shown in **Figure 15**. FT-IR: ν (cm^{-1}) 3405 (N–H), 1609, 1595 (furoxan ring) and 1520 (NO_2). The IR spectrum is shown in **Figure 16**. HRMS (m/z, M+H^+, ESI-TOF-MS, FAB^+): calculated for $C_{12}H_{11}N_6O_4$ 318.0951, found 318.0956.

PEG-NHS (8). 3 g (0.6 mmol) of **PEG-OH (7)** was dissolved in 100 mL of toluene and dried by azeotropic distillation using a Dean-Stark trap under argon. After all toluene had been distilled off the dried **(7)** was dissolved in 25 mL DMF. To the clear solution was then added under argon 768.5 mg (3 mmol, 5 eq.) of DSC and 422 μL (3 mmol, 5 eq.) of Et_3N. The reaction mixture was placed in an oil bath at 40 °C and stirred for 24 h. After cooling down to room temperature the reaction mixture was diluted with 150 mL of Et_2O to precipitate the polymer. The suspension was filtered and the residue was washed with Et_2O (3 × 20 mL). The residue was dried under vacuum to yield 2.9 g (97%) of a white solid. ^1H NMR (*d6*-DMSO) δ = 4.44 (bs, $CH_2OC(O)$), 3.80–3.30 (bs, CH_2CH_2O PEG), 3.23 (s, CH_3O PEG), 2.81 (s, 2 × CH_2 NHS). The degree of modification

was calculated to be 97% by comparing the integral values of the NHS signal and the OCH$_3$ signal of PEG. The ^{1}H NMR spectrum is shown in **Figure 17** FT-IR: ν (cm^{-1}) 1812 and 1789 (C=O imide), 1742 (C=O carbonate).

PEG-alkyne (9). 617 mg (0.12 mmol) of **(8)**, 79 μL (1.2 mmol, 10 eq.) of propargylamine and 172 μL (1.2 mmol, 10 equiv.) of Et$_3$N were dissolved in 6 mL DMF. The solution was evacuated/ purged with N$_2$ (3 ×) and stirred for 24 h at RT. The mixture was acidified with 2 mL of 1 M NaHSO$_4$ (aq.) and the solution was transferred to a dialysis tube (MWCO 2 kDa) and dialyzed against 1 L of water for 48 h by replacing water every 12 h. The solution was lyophilized to yield 600 mg (97%) of a white solid. ^{1}H NMR (CDCl$_3$) δ = 5.20 (bs, NH), 4.20 (bs, CH$_2$OC(O)), 3.96 (bs, CH$_2$NH), 3.90–3.40 (bs, CH$_2$CH$_2$O PEG), 3.37 (s, CH$_3$O PEG), 2.24 (s, CH alkyne). The degree of modification was calculated to be about 97% by comparing the integral ratio of the alkyne proton signal and the OCH$_3$ signal of PEG. The ^{1}H NMR spectrum is shown in **Figure 18**. FT-IR: ν (cm^{-1}), 1724 (C=O carbamate). No clear vibration band due to the alkyne was observed.

PEG-furoxan conjugate (PEG-F, 10).

Method A: prepared by nucleophilic substitution of (**5**) with (**8**). 20.6 mg (4.1 μmol) of (**8**), 6.35 mg (20.5 μmol, 5 eq.) of (**5**) and 5.76 μL (0.205 mmol, 10 eq.) of Et_3N were dissolved in 1 mL DMSO. The flask was evacuated/purged with N_2 (3 ×) and the mixture was stirred for 24 h. The mixture was acidified with 1 mL of 1 M $NaHSO_4$ (aq.) and the solution transferred to a dialysis tube (MWCO 2 kDa) and dialyzed against 1 L of water for 24 h by replacing water every 12 h. The solution was lyophilized to yield 19.7 mg (95%) of a white solid. The degree of modification was calculated to be about 95% by comparing the integral ratio of the phenyl signals of furoxan and the OCH_3 signal of PEG.

Method B: prepared by the copper(I)-catalyzed 1,3-Huisgen cycloaddition reaction between (**3**) and (**9**). 106.6 mg (21.3 μmol) of (**9**), 11.6 mg (53.4 μmol, 2.5 eq.) of (**3**), 0.11 mg (0.43 μmol) of $CuSO_4 \cdot 5H_2O$ and 4.3 mg (21.3 μmol) of sodium ascorbate were dissolved in a mixture of 1 mL of *t*-BuOH and 1.7 mL of H_2O. The solution was degassed with argon by three freeze-thaw cycles and the mixture was stirred for 24 h at 35 °C. After cooling down to room temperature, the solution was transferred to a dialysis tube (MWCO 2 kDa) and dialyzed against 1 L of water for 48 h and replacing water every 24 h. The solution was lyophilized

to yield 99.7 mg (94%) of a white solid. The degree of modification was calculated to be about 88% by comparing the integral ratio of the phenyl signals of furoxan and the OCH_3 signal of PEG.

The ^{1}H NMR spectrum is shown in **Figure 19**. ^{1}H NMR (CDCl$_3$) δ = 7.86 (bs, CH triazole + 2 × CH$_{aromat}$ furoxan), 7.58 (bs, 3 × CH$_{aromat}$ furoxan), 5.55 (bs, CH$_2$-furoxan + NH), 4.45 (bs, C$\underline{H}_2$-NH), 4.22 (bs, CH$_2$OC(O)), 3.90-3.40 (bs, CH$_2$CH$_2$O PEG), 3.37 (s, CH$_3$O PEG). FT-IR: ν (cm^{-1}), 1721 (C=O carbamate), 1600 and 1578 (furoxan ring).

PEG-furoxan conjugate (PEG-NF, 11).

Method A: prepared by nucleophilic substitution of (**6**) with (**8**). 100.7 mg (20.1 μmol) of (**8**), 32 mg (100.5 μmol, 5 eq.) of the free amine of (**6**) and 14 μL (100.5 μmol, 5 eq.) of Et$_3$N were dissolved in 4 mL DMF. The flask was evacuated/purged with argon (3 ×) and the mixture was stirred for 24 h. The mixture was acidified with 1 mL of 1 M NaHSO$_4$ (aq.) and the solution transferred to a dialysis tube (MWCO 2 kDa) and dialyzed against 1 L of water for 24 h by replacing water every 12 h. The solution was lyophilized to yield 100 mg (99%) of a white solid. The degree of modification was calculated to be about 50% by comparing the integral

ratio of the phenyl signals of furoxan and the OCH_3 signal of PEG.

Method B: prepared by copper(I)-catalyzed 1,3-Huisgen cycloaddition reaction between (4) and (9). 33.2 mg (6.6 μmol) of (9), 4.4 mg (16.8 μmol, 2.5 eq.) of (4), 0.03 mg (0.12 μmol) of $CuSO_4 \cdot 5H_2O$ and 1.32 mg (6.6 μmol) of sodium ascorbate were dissolved in a mixture of 1.0 mL of t-BuOH and 1.7 mL of H_2O. The solution was degassed with argon by three freeze–thaw cycles and the mixture was stirred for 24 h at 35 °C. After cooling down to room temperature, the solution was transferred to a dialysis tube (MWCO 2 kDa) and dialyzed against 1 L of water for 48 h by replacing water every 24 h. The solution was lyophilized to yield 30.3 mg (91%) of a white solid. The degree of modification was calculated to be about 84% by comparing the integral ratio of the phenyl signals of furoxan and the OCH_3 signal of PEG.

The ^1H NMR spectrum is shown in Figure 20. ^1H NMR ($CDCl_3$) δ = 8.45 (d, $2 \times CH_{aromat}$ furoxan), 8.19 (d, $2 \times CH_{aromat}$ furoxan), 7.89 (s, CH triazole), 5.57 (bs, CH_2-furoxan + NH), 4.46 (bs, $C\underline{H}_2$-NH), 4.23 (bs, $C\underline{H}_2O(CO)$), 3.90-3.40 (bs, CH_2CH_2O PEG), 3.37 (s, CH_3O PEG). FT-IR: ν (cm^{-1}), 1720 (C=O carbamate), 1611 and 1600 (furoxan ring), 1518

(NO_2).

Griess assay

To quantify NO release the concentration of NO_2^- was measured by the Griess assay in transparent 96 well polystyrene plates. The samples were reacted with 50 µL of 2% (w/v) SA in 5% HCl (aq.) for 5 min before adding 50 µL 0.1% (w/v) NED (aq.).[91] After 5 min the absorbance at 550 nm was measured and the NO_2^- concentrations were calculated from the standard curves of 0-100 µM NO_2^- in either 2.5 mM cysteine, 2.5 mM glutathione, 45% FBS or 0.58×10^7 cells/mL cell lysate in 50 mM PBS (pH 7.1) containing 2.5 mM DTPA. All samples were corrected for absorbance of polystyrene, reaction medium and the SA/NED reagent mixture by subtraction of the absorbance of wells containing water only

Preparation of the NO donor stock solutions

Stock solutions of the different donors were prepared by dissolving in milliQ water. For the PEG conjugates the amounts to be dissolved were based on the molecular weight as determined from the ^{1}H NMR spectrum and the degree of functionalization. Before preparing the PEG-conjugate

stock solutions, **(10)** and **(11)** (10 mg) were dissolved in 100 μL DMF. To the colorless solutions was added 100 μL of a diethylammonium diethyldithiocarbamate solution in DMF (14.8 mg/mL) resulting in a brown solution. This solution was then loaded on a Sephadex LH20 size exclusion column (1.5 cm diameter × 26 cm height) and eluted with DMF. Fractions were collected in 1.5 mL Eppendorf tubes and the solutions were measured by UV/Vis. The fractions that contained PEG were pooled and concentrated under reduced pressure. The solid was dissolved in $CDCl_3$ and measured by ^{1}H NMR to confirm the presence of PEG. After removal of $CDCl_3$ under reduced pressure the conjugates were dissolved in water and lyophilized. The lyophilized solid was used to prepare stock solutions.

NO release experiments in the presence of cysteine or glutathione

50 μL of the NO-donor (500 μM) in water was mixed with 50 μL of 5 mM cysteine/glutathione in 100 mM PBS containing 5 mM DTPA in a 96 well plate (pH 7.1). NO_2^- standard curves were prepared on the same plate by mixing 50 μL of $NaNO_2$ solution at different concentrations with 5 mM cysteine/glutathione in 50 mM PBS containing 5 mM DTPA. All samples were run in triplicate. The plates were placed in a humidified incubator at

37 °C and taken out at the indicated time points.

NO release under deoxygenated conditions

300 μL of (**5**) in water (500 μM) and 2 mL of 5 mM cysteine in 50 mM phosphate buffer containing 5.0 mM DTPA were degassed by bubbling with water vapor saturated nitrogen gas through the solution using a needle inserted through the septum in a glass tube. A second needle was inserted in the septum for N_2 to escape. The solutions were degassed for at least 30 min at RT. After degassing the pressure, the relieve needle was taken out and under a positive nitrogen pressure, 300 μL of cysteine solution was withdrawn through the septum with a gastight syringe. This was then rapidly injected through the septum of the tube containing the solution (**5**) under a positive nitrogen pressure. Parallel to this experiment air saturated donors and cysteine solutions were mixed as well. After 3 h at RT the SA (150 μL) and NED (150 μL) solutions were added. The solutions were transferred (150 μL) to a well plate and the absorbance at 550 nm was read. The concentrations were calculated from a standard curve prepared at the same time. The NO_2^- concentrations were 5.4 ± 0.96 μM and 11.6 ± 0.37 μM ($n = 3$) in the absence and presence of oxygen

respectively.

Electrochemical detection NO release from (10)

Because the electrode responded to cysteine the concentration of 2.5 mM saturated the electrode signal. I therefore adjusted by trial-and-error the cysteine concentration to 25 μM. At this concentration the sensor could be operated in the range specified for NO detection. A volume of 1 mL of 10 mM phosphate buffer at pH 7.4 was degassed by bubbling N_2 for at least 30 min and transferred to the measuring chamber. Then 10 μL of a solution of 2.5 mM cysteine in 50 mM PBS containing 2.5 mM DTPA was added giving a final cysteine and DTPA concentration of 25 μM. The solution was maintained at 37 °C and after the current became stable, 10 μL of a 2.5 mM solution of **(10)** in milliQ water was added giving a final concentration of 25 μM. The change in current in pA was then measured as a function of time.

Effect of chemical decomposition on NO release

A stock solution of the donors at 500 μM donor solution in water was prepared. 50 μL of each donor was mixed with 50 μL 100 mM PBS

containing 5 mM DTPA and placed in a humidified incubator at 37 °C. The rest of the solution was immediately frozen and stored at -20 °C. After 24 h the stock solution was warmed to room temperature and 50 µL was mixed with 50 µL of 100 mM PBS containing 5 mM DTPA on the same plate. Immediately 100 µL of a 5 mM cysteine solution in 50 mM PBS containing 5 mM DTPA was added to all samples and placed in a humidified incubator at 37 °C. A NO_2^- standard was prepared in the same way by mixing 50 µL NO_2^- (aq.) with 50 µL of 50 mM PBS containing 5 mM DTPA followed by the addition of 100 µL of 5 mM cysteine in 100 mM PBS containing 5 mM DTPA. After 24 h the plate was taken out for the Griess assay.

NO release in the cell lysate and fetal bovine serum

The cell lysate and the FBS were diluted 9:1 with 10× PBS giving 1.16×10^7 cells/mL cell lysate or 90% FBS solutions. Then, 50 µL of these solutions were added to 50 µL of the sample solutions. A NO_2^- standard was prepared in a similar way by mixing 50 µL NO_2^- (aq.) at different concentrations with 50 µL 1.16×10^7 cells/mL cell lysate or 90% FBS. After 24 h the plate was taken out and the NO_2^- concentration was determined by the Griess assay.

Furoxan stability

UV/Vis: The different donors at 500 μM in water were mixed (80 μl) with an equal volume of 100 mM PBS containing 5 mM DTPA in 600 μL microfuge tubes and placed inside an incubator at 37 °C. At different time points the tubes were taken out, and cooled to RT before recording the UV/Vis spectrum.

^{1}H NMR: Solutions of **(10)** and **(11)** were prepared by mixing a solution at 4.5 mg/mL in 2 mL of water with 2 mL of 100 mM PBS containing 5 mM DTPA. The solutions were incubated at 24 h at 37 °C, before being frozen and lyophilized. To the residue was added 700 μL *d6-*DMSO and the ^{1}H NMR spectrum was recorded.

HT-29 cell culture

Cells were cultured in McCoy's 5A medium containing 10% fetal bovine serum and 50 U/mL-50 μg/mL penicillin-streptomycin in a CO_2 incubator at 37 °C. The cells were trypsinized and passaged when reaching 70–80% confluency.

Effect of conjugates (10) and (11) on the antiproliferative effect of

37

ibuprofen (IBU) in HT-29 cells

Cells were seeded at 1.5×10^4 cells per well in a 96 well polystyrene plate. To the different wells were added in triplicate solutions of **(10)/(11)**, IBU or a mixture of **(10)/(11)** and IBU (IBU/furoxan molar ratio = 1/1) at different concentrations in 100 μL medium containing 10% water and 1% DMSO. After culturing for 2 d, the supernatant was removed and the cell viability was measured by the MTT assay.

MTT assay

After 2 d the supernatant was removed and replaced with 100 μL medium and 10 μL MTT solution in PBS (5 mg/mL). After 2 h at 37 °C, the formed formazan crystals were dissolved in 100 μL of 0.1 g/mL SDS in 0.01 M HCl (aq.) and the absorbance at 570 nm was measured. The cell viability is expressed as the percentage of cells that had not been treated.

NO_2^- quantification in cell supernatants

Since the photometric Griess assay for assessing NO release is not sensitive enough for quantifying NO_2^- in cell culture supernatants, by using a fluorescence Griess assay.[92] After culturing the HT-29 cells for 2 d 80 μL

of the cell supernatant was transferred to a black polystyrene plate and diluted to 100 μL with milliQ water. To the solution was then added 10 μL of a solution of 2,3-diaminonaphthalene (0.05 mg/mL) in 0.62 M HCl (aq.). After reacting for 10 min in the dark 5 μL of 3 M NaOH (aq.) was added and the fluorescence was measured ($\lambda_{ex} = 365$ nm, $\lambda_{em} = 450$ nm). The NO_2^- concentration was calculated from a standard in the range 0–10 μM prepared in 80 μL culture medium and 20 μL water.

Results and Discussion

Synthesis of azide- and amine-containing furoxan derivatives

Azide-containing furoxan derivatives (**3**) and (**4**) by were first synthesized *via* a single step conversion of the alcohol using the diphenyl phosphorylazide/1,8-diazabicyclo[5.4.0]-7-undecene (DPPA/DBU) Merck method as shown in **Scheme 2**.[93] The IR spectra of (**3**) and (**4**) showed peaks at 2102 and 2112 cm^{-1} that can be assigned to the asymmetric N_3 stretching vibration (**Figure 7** and **Figure 9**).[94] Furthermore, the C=N stretching vibrations of the furoxan ring of (**3**) and (**4**) were found at 1595, 1577 and 1609, 1594 cm^{-1} , respectively.[95] Compound (**4**) also showed the characteristic N–O stretching vibration of the NO_2 group at 1520 cm^{-1}.[96] Although both azides (**3**) and (**4**) have been reported, these compounds were prepared in a two-step synthesis from the corresponding alcohol by tosylation with tosyl chloride followed by nucleophilic displacement with sodium azide.[35] Compound (**3**) was also prepared in two steps from the methyl derivative by bromination with *N*-bromosuccinimide and reaction with sodium azide.[97] Compared to these methods, this method has the advantage in synthesizing azide-containing furoxans in a single step and

good yields. To prepare amine-containing furoxan derivatives (**5**) and (**6**), azide derivatives (**3**) and (**4**) were reacted with propargylamine·HCl salt by the copper-catalyzed Huisgen cycloaddition reaction.[98] Both compounds were characterized by ^{1}H and ^{13}C NMR, IR as well as HRMS (**Figure 6-16**). The formation of the triazole ring for (**5**) and (**6**) was confirmed by ^{1}H NMR showing the CH protons of the triazole ring at 8.36 and 7.79 ppm, respectively. IR showed the absence of the bands at 2101 and 2112 cm^{-1} due to the N_3 of (**5**) and (**6**), respectively.
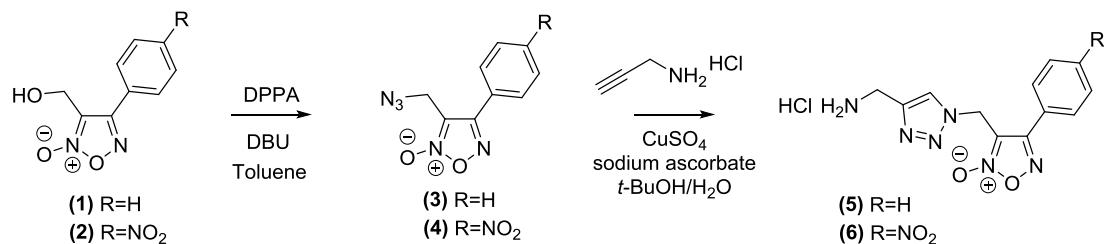
Scheme 2. Synthesis scheme of low molecular weight furoxans.
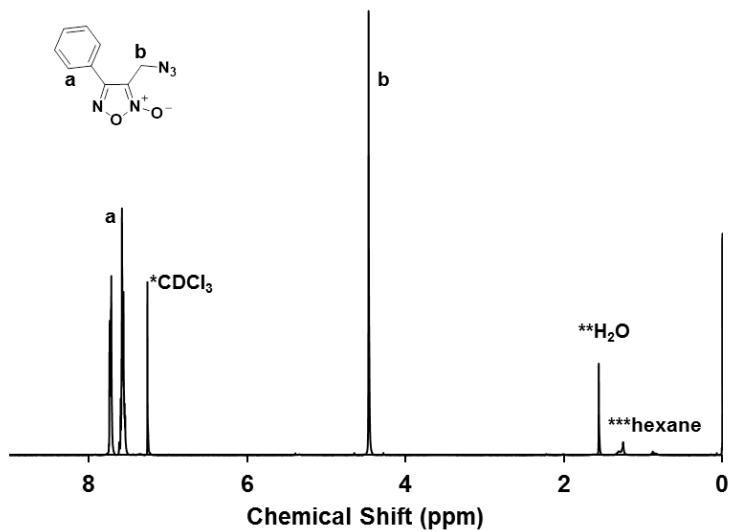
Figure 6 ^{1}H NMR spectrum of 3-(azidomethyl)-4-phenyl-1,2,5-oxadiazole 2-oxide (3).
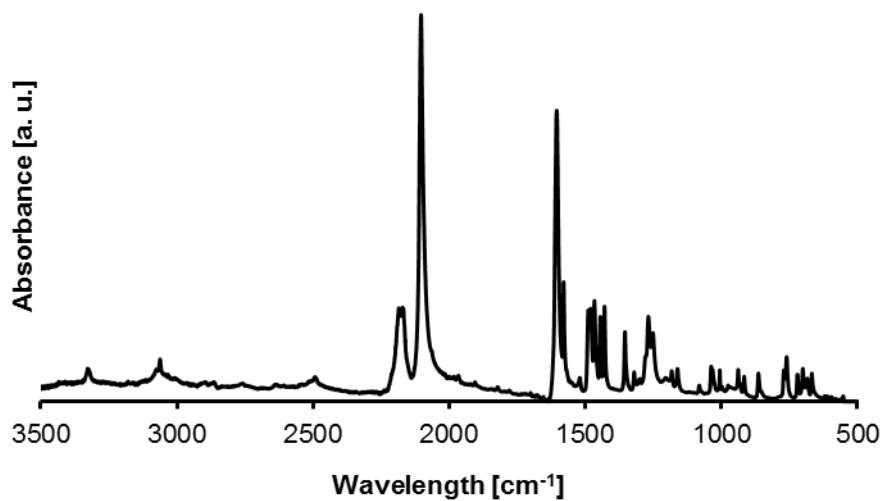
Figure 7. Infrared spectrum of 3-(azidomethyl)-4-phenyl-1,2,5-oxadiazole 2-oxide (3) in the region of 3500-500 cm⁻¹.
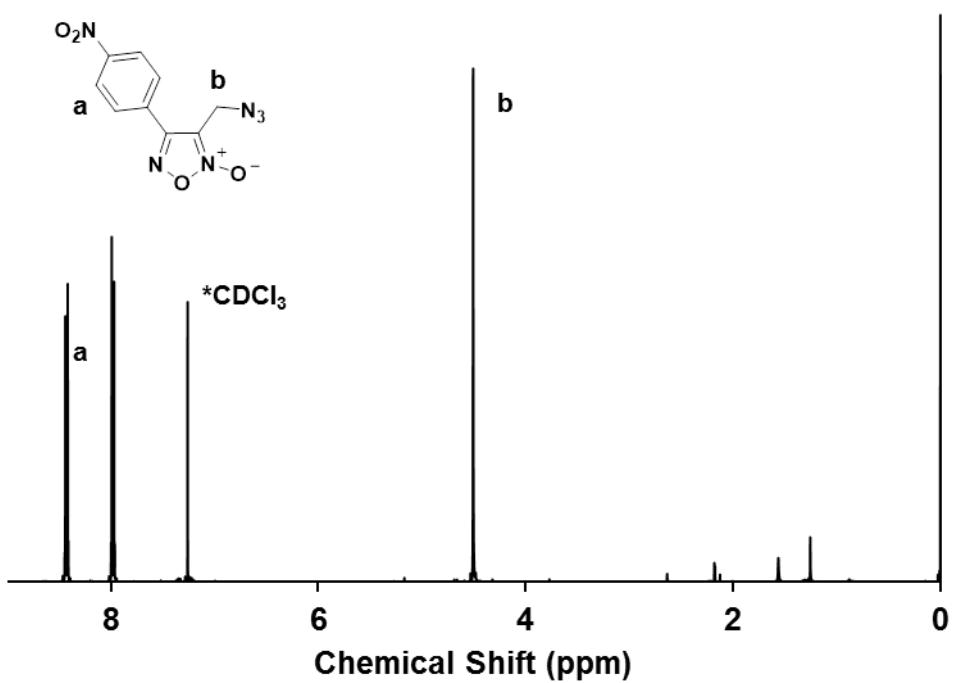
**Figure 8. ¹H NMR spectrum of 3-(azidomethyl)-4-(4-nitrophenyl)-1,2,5-oxadiazole 2-oxide (4) in CDCl₃.**
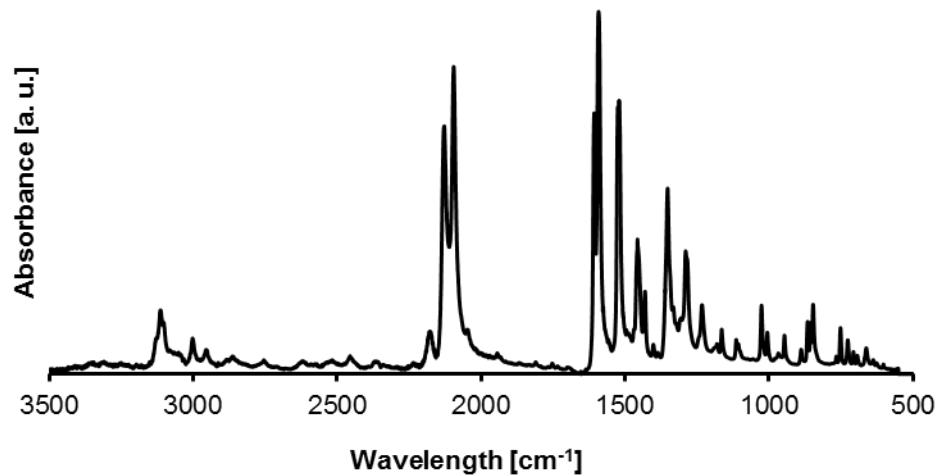
Figure 9. Infrared spectrum of 3-(azidomethyl)-4-(4-nitrophenyl)-1,2,5-oxadiazole 2-oxide (4) in the region of 3500-500 cm^{-1}.
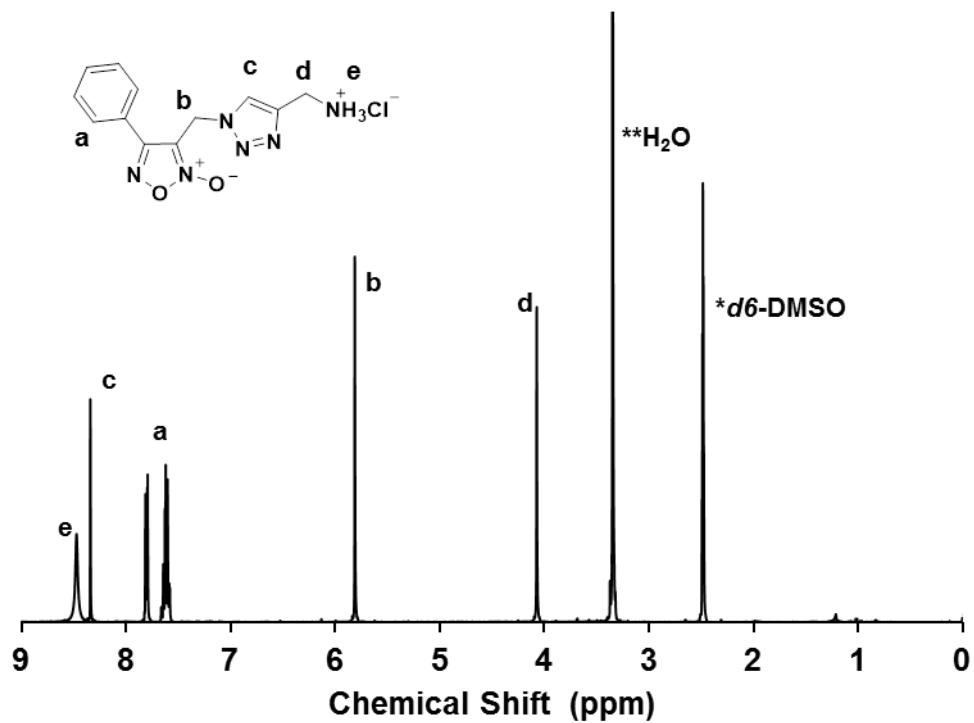
**Figure 10. ^{1}H NMR spectrum of 3-((4-(aminomethyl)-1H-1,2,3-triazol-1-yl)methyl)-4-phenyl-1,2,5-oxadiazole 2-oxide HCl salt (5) in $d6$-DMSO.**
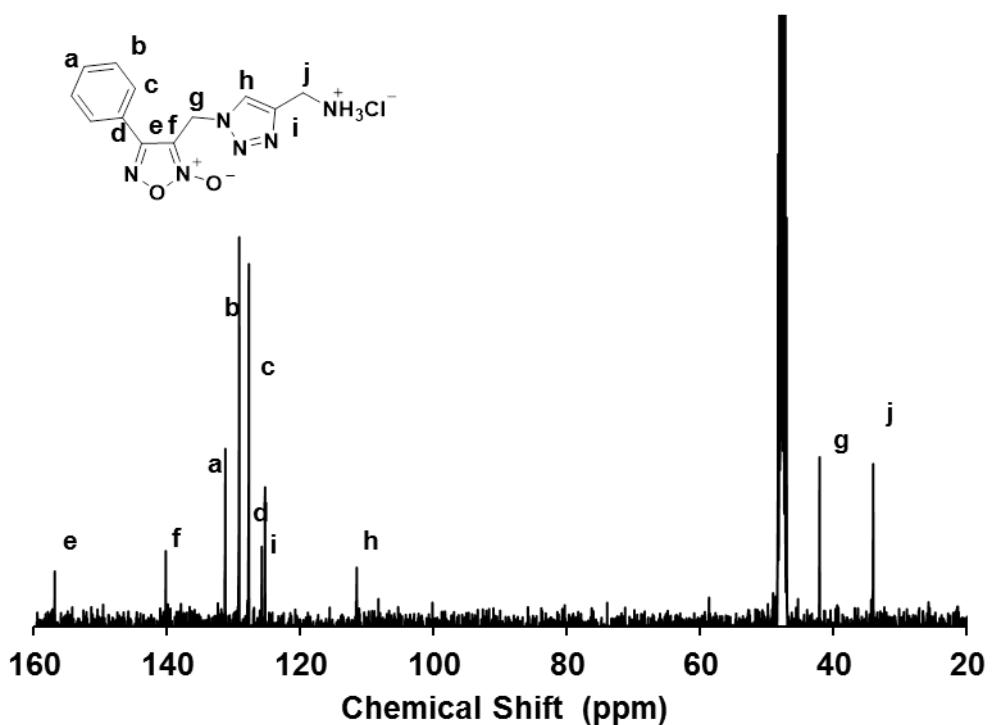
Figure 11. ^{13}C NMR spectrum of 3-((4-(aminomethyl)-1*H*-1,2,3-triazol-1-yl) methyl)-4-phenyl-1,2,5-oxadiazole 2-oxide HCl salt (5) in CD$_3$OD.
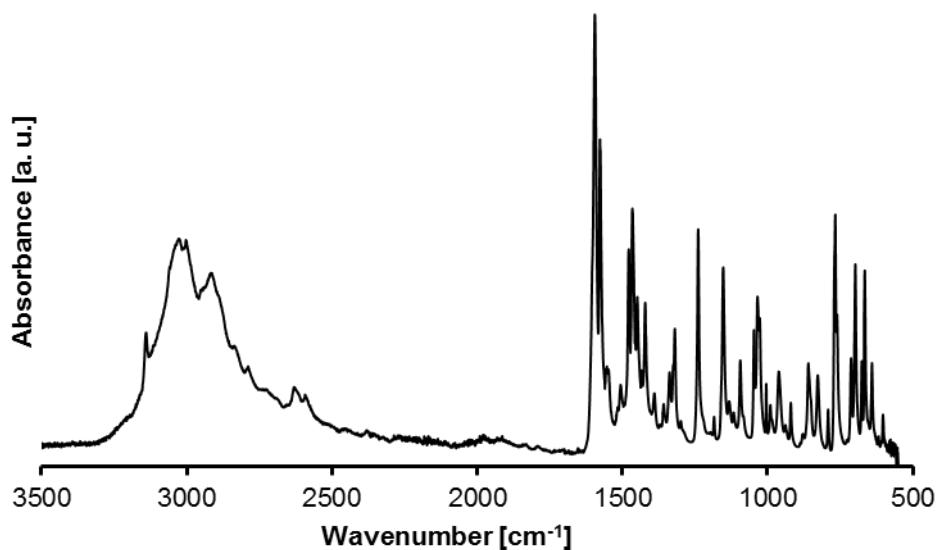

Figure 12. Infrared spectrum of 3-((4-(aminomethyl)-1*H*-1,2,3-triazol-1-yl) methyl)-4-phenyl-1,2,5- oxadiazole 2-oxide HCl salt (5) in the region of 3500-500 cm^{-1}.
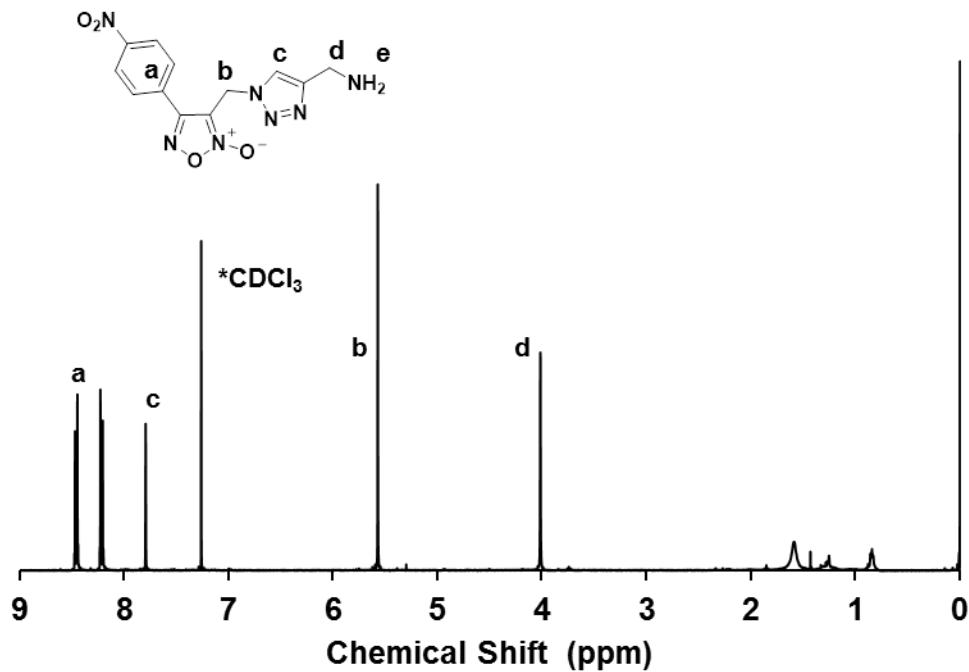
Figure 13. ^{1}H NMR spectrum of free amine of 3-((4-(aminomethyl)-1*H*-1,2,3-triazol-1-yl)methyl)-4-(4-nitrophenyl)-1,2,5-oxadiazole 2-oxide HCl salt (6) in CDCl₃.
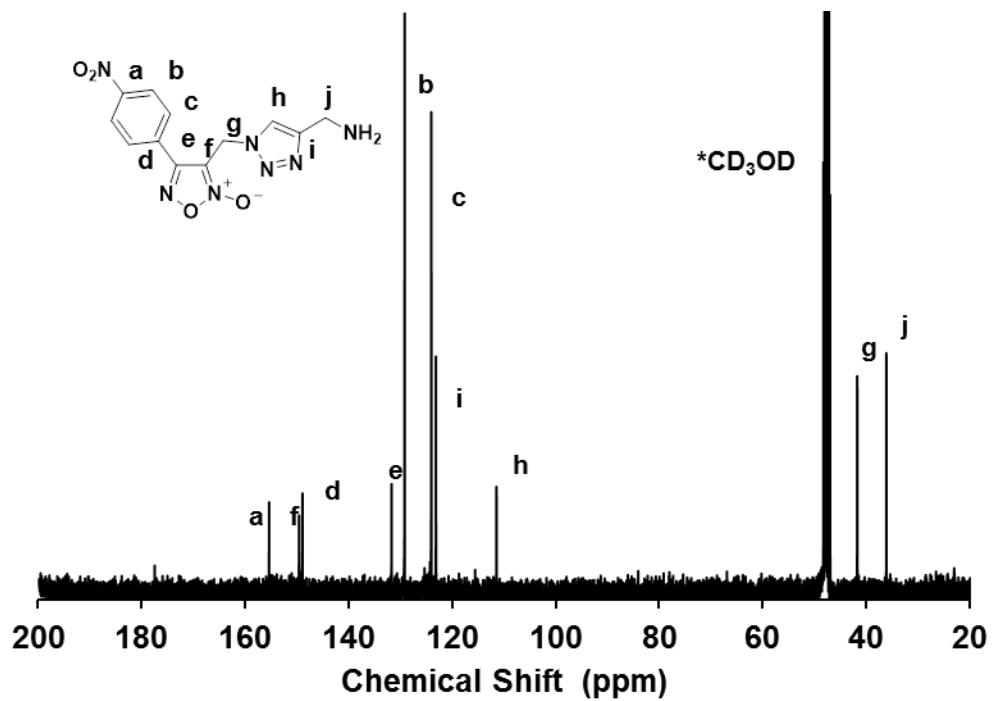

Figure 14. ^{13}C NMR spectrum of free amine of 3-((4-(aminomethyl)-1*H*-1,2,3-triazol-1-yl)methyl)-4-(4-nitrophenyl)-1,2,5-oxadiazole 2-oxide HCl salt (6) in CD₃OD.
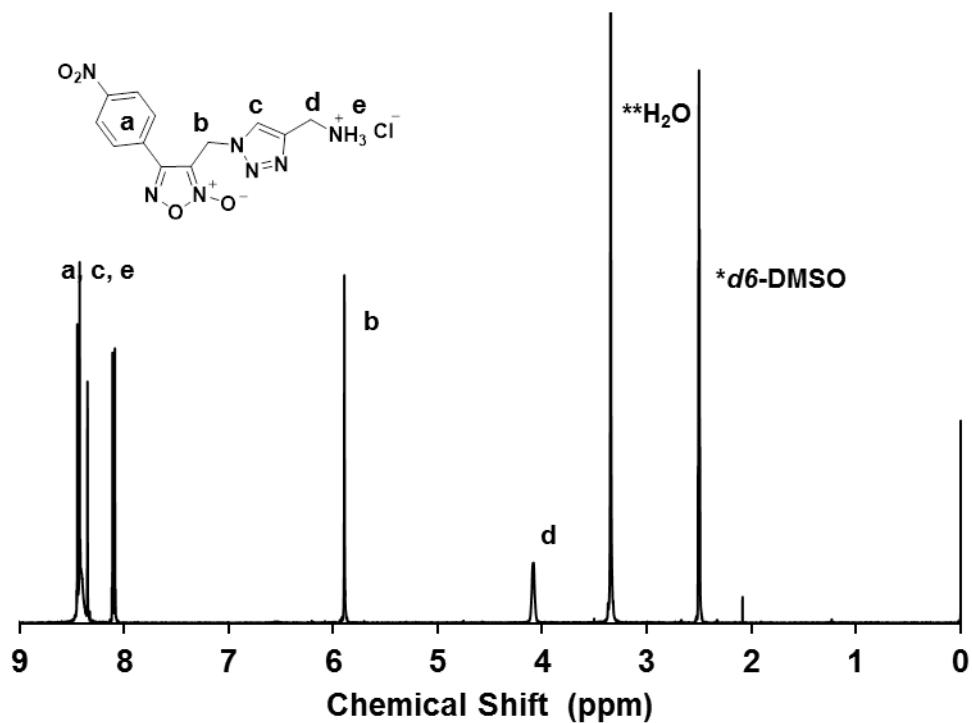
**Figure 15.** ^{1}H NMR spectrum of 3-((4-(aminomethyl)-1*H*-1,2,3-triazol-1-yl) methyl)-4-(4-nitrophenyl)-1,2,5-oxadiazole 2-oxide HCl salt (6) in *d6*-DMSO.
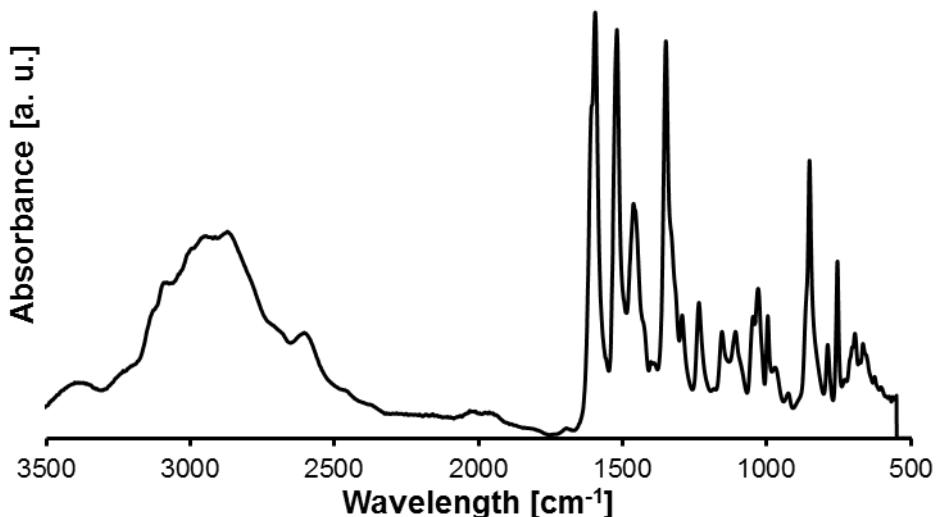

Figure 16. Infrared spectrum of 3-((4-(aminomethyl)-1*H*-1,2,3-triazol-1-yl) methyl)-4-(4-nitrophenyl)-1,2,5-oxadiazole 2-oxide HCl salt (6) in the region of 3500-500 cm^{-1}.

## Synthesis of the PEG–furoxan conjugates by nucleophilic substitution

The first approach in preparing the PEG–furoxan conjugates was nucleophilic substitution of *N*-hydroxysuccinimide carbonate activated PEG (PEG-NHS, **8**) with the amine-containing furoxan derivatives (**5**) and (**6**) as outlined in **Scheme 3**. Firstly, hydroxyl-terminated PEG (PEG-OH, **7**) was reacted with *N,N'*-disuccinimidyl carbonate (DSC) to yield PEG-NHS (**8**). Successful modification was confirmed by ^{1}H NMR which showed the presence of a new signal at 4.44 ppm of the CH_2 next to the carbonate and the singlet at 2.81 ppm of the four succinimide protons. IR showed two bands of the $\nu(C=O)$ stretching vibrations at 1812 and 1789 cm^{-1} of the cyclic imide and a band at 1742 cm^{-1} of the carbonate (**Figure 21**). The amine-containing furoxan derivatives (**5**) and (**6**) were then reacted with PEG-NHS (**8**) yielding the conjugates (**10**) and (**11**). The reaction was almost quantitative for (**10**) (degree of functionalization: 95%) when adding 5 eq. of (**5**) relative to the NHS carbonate. However, the extent of the reaction was only 50% for (**11**) under the same conditions indicating the low reactivity of amine derivative (**6**).

Synthesis of the PEG–furoxan conjugates by the copper-catalyzed Huisgen cycloaddition reaction

Preparation of the PEG–furoxan conjugates by the Huisgen cycloaddition of PEG-alkyne (**9**) with (**3**) and (**4**). PEG-alkyne (**9**) was prepared from PEG-NHS (**8**) by nucleophilic substitution with propargylamine. Successful reaction was confirmed by ^{1}H NMR and IR. **Figure 17-21**. ^{1}H NMR showed that the CH_2 bound to the carbonate shifted from 4.44 to 4.20 indicating the formation of the carbamate. This was further supported by the appearance of a broad signal at around 5.20 ppm due to the NH carbamate proton. IR also showed a shift of the $\nu(C=O)$ stretching vibration from 1742 to 1724 cm^{-1} further supporting the formation of the carbamate. The CH alkyne proton appeared at 2.24 ppm in the ^{1}H NMR spectrum, but no clear band could be observed in the IR spectrum. PEG-alkyne (**9**) was reacted with 2.5 eq. of (**3**) and (**4**) to yield the conjugates (**10**) and (**11**) with a degree of functionalization of 88 and 84% as evidenced from the appearance of the CH triazole proton and the disappearance of the alkyne proton in the ^{1}H NMR spectra. IR further showed the presence of the signals due to the furoxan ring and the NO_2 band in the case of (**11**) (**Figure 21**). For further study, the conjugates (**10**)

and **(11)** prepared by this method were used.
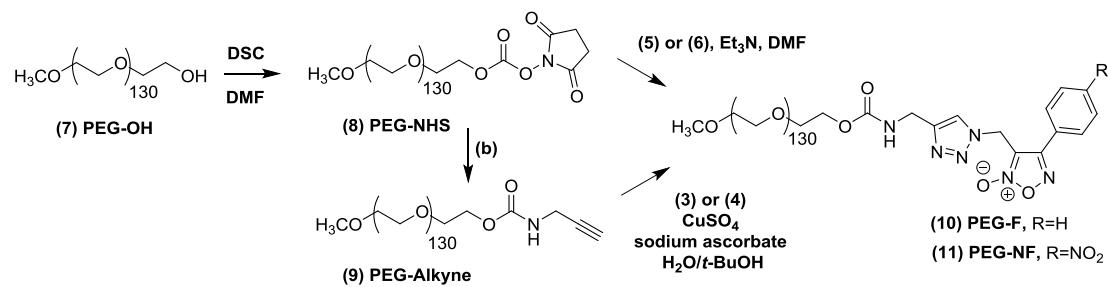
**Scheme 3. Synthesis scheme of PEG-furoxan conjugates.**
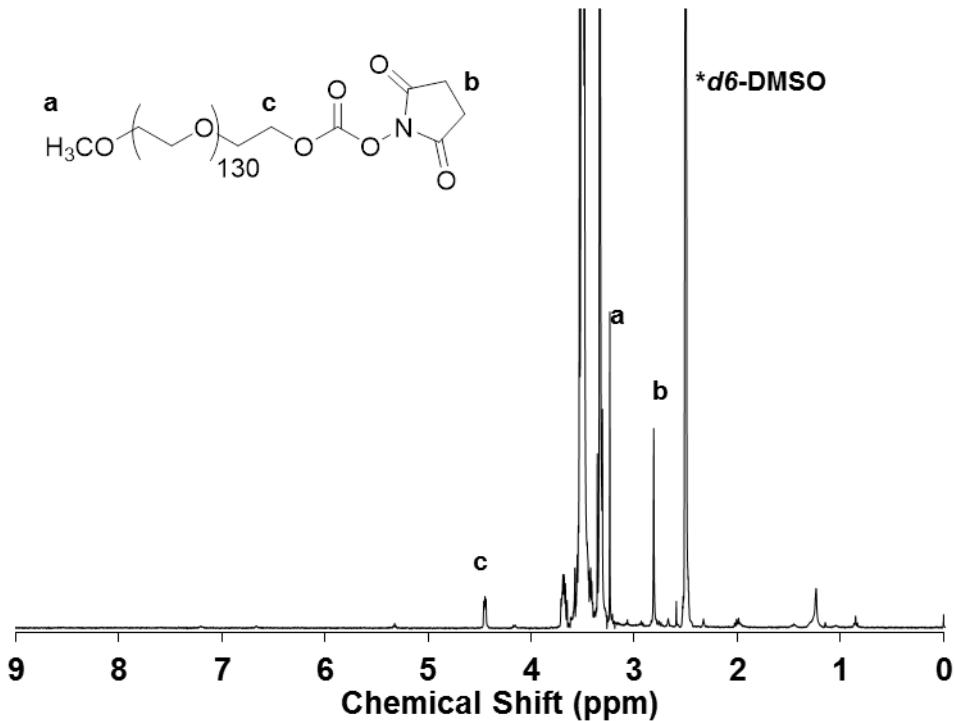
Figure 17. ^{1}H NMR spectrum of PEG-NHS (8) in $d6$-DMSO.
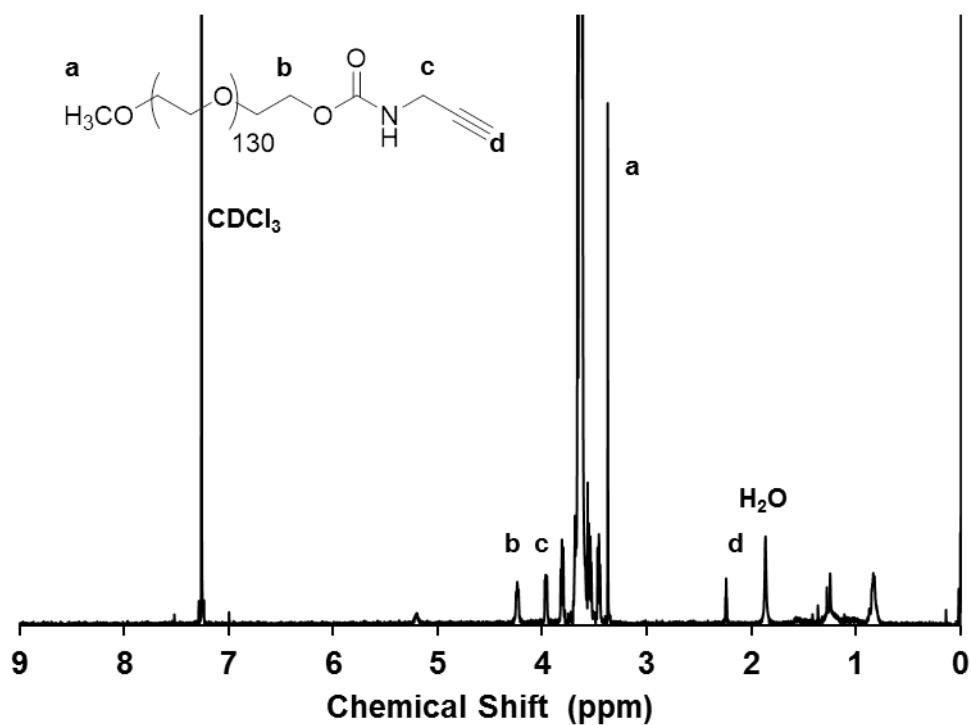
**Figure 18. ^{1}H NMR spectrum of PEG-alkyne (9) in CDCl$_3$.**
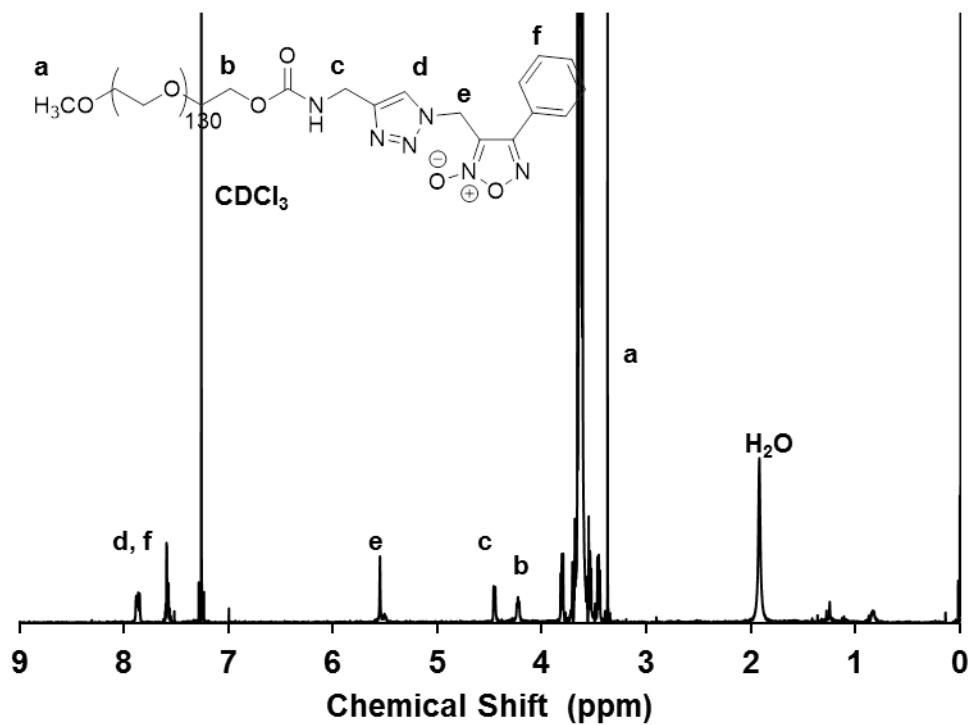
Figure 19. ^{1}H NMR spectrum of PEG-F (10) in CDCl$_3$.
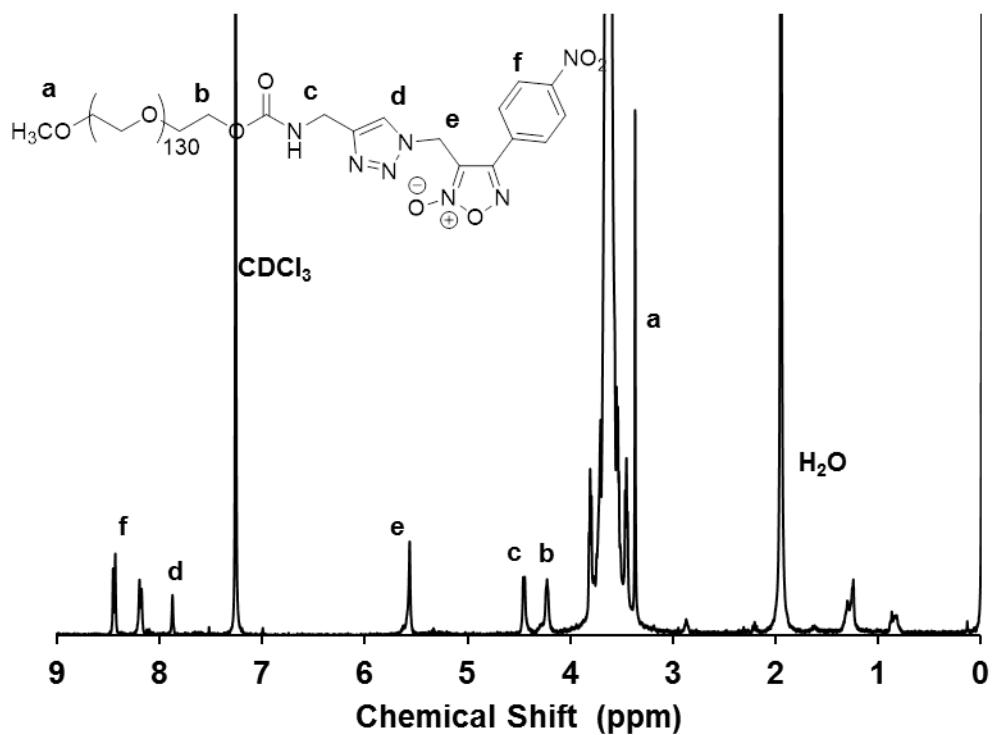
**Figure 20. ¹H NMR spectrum of PEG-NF (11) in CDCl₃.**
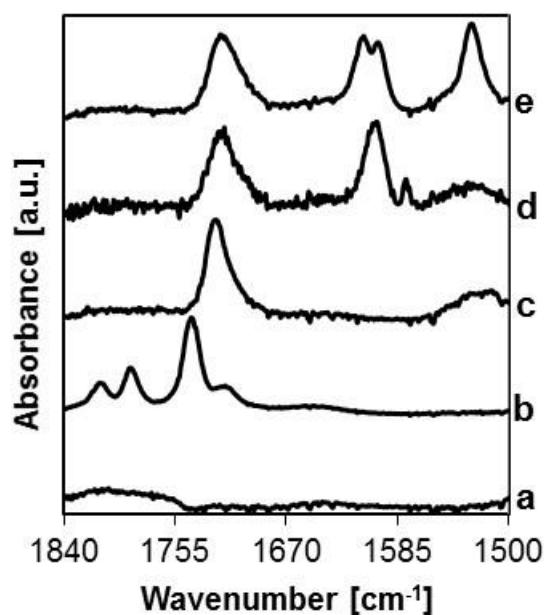
Figure 21. Infrared spectra of PEG-F and PEG-NF and the different intermediates used to prepare them in the region 1840-1500 cm⁻¹. (a) PEG-OH (7), (b) PEG-NHS (8), (c) PEG-alkyne (9), (d) PEG-F (10) and (e) PEG-NF (11).

NO release from the PEG–furoxan conjugates in the presence of cysteine

Furoxans are known to release NO in response to compounds containing thiol groups. Thus, NO release in the presence of cysteine was studied. For comparison, the amine-containing furoxan derivatives (**5** and **6**) were also included. The amount of released NO was quantified by measuring the nitrite (NO_2^-) concentration using the Griess assay.[99] As can be seen from **Figure 22 A**, the furoxans (**5** and **6**) released NO in the presence of cysteine, with the nitrophenyl derivative (**6**) giving slightly faster NO release. This faster release may be due to the electron-withdrawing nature of the NO_2 group at the *para* position which increases the furoxan reactivity towards thiols.[35] Compared to the furoxans (**5** and **6**), the PEG–furoxan conjugates (**10** and **11**) showed slower NO release as shown in **Figure 22 B**. This seems to be due to an electronic effect as indicated by a difference in the chemical shift of the CH_2 protons between the furoxan and triazole rings in *d6*-DMSO. For (**5**) and (**6**), this signal appeared at 5.83 and 5.89 ppm, whereas it shifted to 5.71 and 5.76 ppm for (**10**) and (**11**), respectively. (**Figure 23**) This increased electron density for this CH_2 protons indicates that the carbamate is affecting the electron

density of the furoxan ring and its reactivity with cysteine, and therefore NO release. Furthermore, the release of NO was also tested in the presence of glutathione, another abundant thiol-containing molecule in the body, and observed a similar trend with cysteine as shown in **Figure 22 C** and **D.**
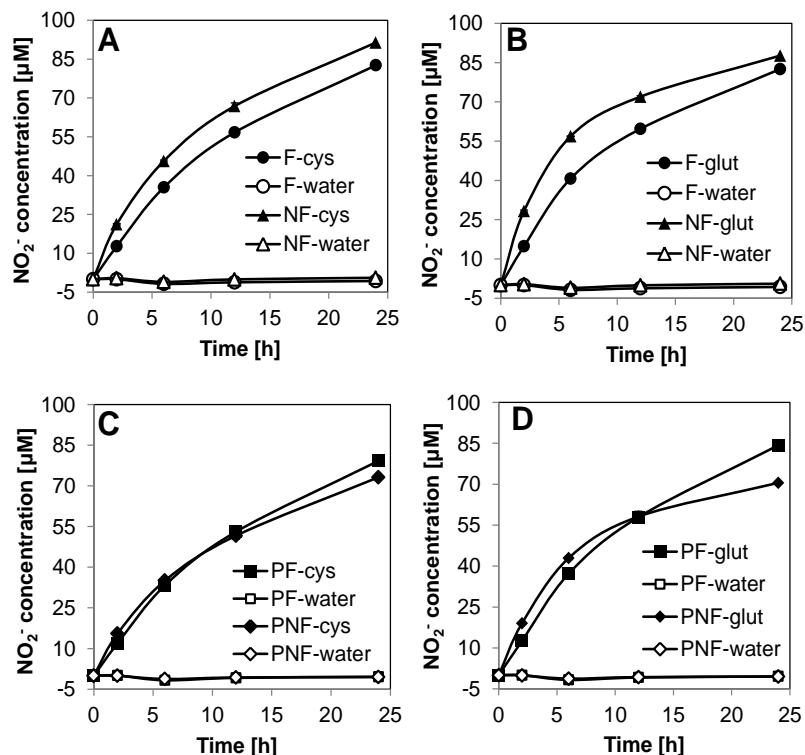
Figure 22. NO release from (5), (6), (A and B), PEG-F (10) and PEG-NF (11) (C and D) at 250 μM in the absence or presence of cysteine and glutathione as measured by the Griess assay. (n=3).
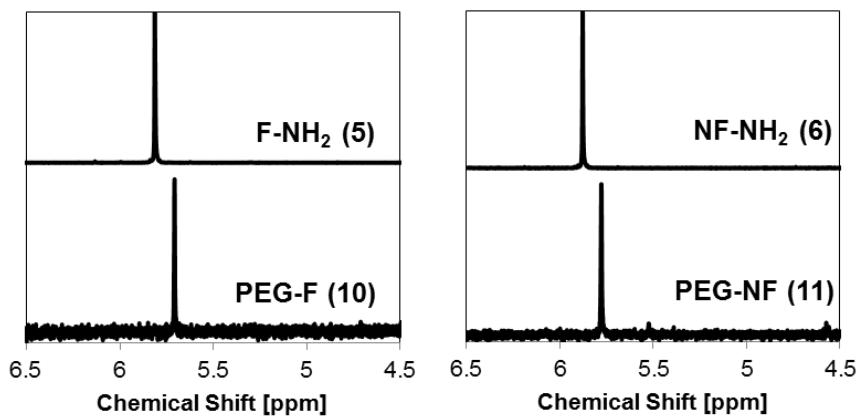
Figure 23. ^{1}H NMR spectra of amine-containing furoxan derivatives F-NH$_2$ (5) and NF-NH$_2$ (6) and PEG-F (10), PEG-NF (11) in the region 4.5-6.5 ppm in *d6-DMSO*.

Griess assay under deoxygenated conditions and electrochemical detection of NO

The release of NO from furoxans is complex and several mechanisms have been suggested including the formation of nitroxyl anion (NO$^-$) as an intermediate that is oxidized to NO.[8] Although the Griess assay has been widely used for assessing NO release from furoxans, it is possible that the measured NO$_2^-$ arises from a different reaction pathway and is not formed directly by oxidation of NO. One such pathway would involve the direct reaction of NO$^-$ with molecular oxygen to form peroxynitrite that could also eventually yield NO$_2^-$.[100,101] To exclude this possibility, i.e., that the measured NO$_2^-$ in the Griess assay is not formed by the oxidation of NO, experiments were carried in the absence of oxygen. The reaction mixtures

54

of furoxan (**5**) (250 μM) in the presence of 2.5 mM cysteine in 50 mM PBS were reacted under N_2 for 3 h and analyzed by the Griess assay. In the absence of oxygen, the concentration was 5.4 ± 0.96 μM showing that the NO_2^- concentrations in Figure **22** partially arise from the oxidation of NO. On the other hand, the NO_2^- concentration was 11.6 ± 0.37 μM for the reaction carried out in the presence of oxygen. This higher NO_2^- concentration could indeed be due to peroxynitrite formation under aerobic conditions. In addition, there are two possible side reactions that can lower the NO_2^- concentration: the reaction of cysteine with HNO (protonated form of NO^-) to form disulfides and sulfenamides and HNO dimerization to hyponitrous acid ($H_2N_2O_2$) and dehydration to nitrous oxide (N_2O).[102] Both reactions may become more pronounced in the absence of oxygen which is possibly responsible for the oxidation of NO^- to NO under oxygenated conditions. To further confirm the release of NO directly, a NO-specific electrode sensor was applied. As shown in **Figure 24**, NO release can be detected from conjugate (**10**) in the presence of cysteine. This result shows qualitatively that NO can be released thereby further supporting that the Griess assay is indeed a measure of NO production.
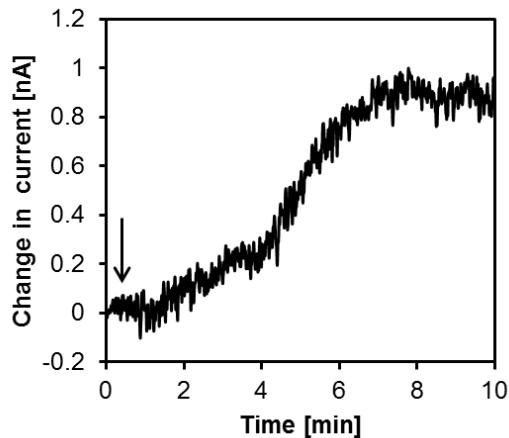
Figure 24. NO release from PEG-F (10) as detected by a NO-specific electrode. A solution of 25 μM cysteine in 10 mM PBS was maintained at 37 °C and after the current stabilized, 10 μL of a solution of PEG-F (10) in water was added (the final concentration was 25 μM) as indicated by the arrow.

NO release from the PEG–furoxan conjugates in the presence of fetal bovine serum and macrophage cell lysate

The NO release from the furoxans and the PEG–furoxan conjugates was investigated in the presence of fetal bovine serum (FBS) and cell lysate from murine macrophages. The furoxans (**5** and **6**), and PEG–furoxan conjugates (**10** and **11**) were incubated at 37 °C in the presence of 45% FBS or 5.8×10^6 cells per mL cell lysate for 24 h and NO_2^- levels were measured by the Griess assay. For the samples incubated with FBS, the NO_2^- concentrations were below the detection limit of the assay indicating that FBS did not induce NO release from these furoxans (**Figure 25**). On the other hand, the addition of cell lysate resulted in the increase of the

NO_2^- concentration showing that NO release can be induced by the intracellular components. The difference between FBS and cell lysate may be due to the difference in the concentration of thiol-containing compounds. It has been reported that compounds containing thiol groups such as cysteine, glutathione and proteins with free cysteine residues are abundant inside cells (e.g. in the millimolar level for glutathione), while the concentrations of these compounds are much lower in human serum (8 μM for cysteine and 2 μM for glutathione).[103,104]
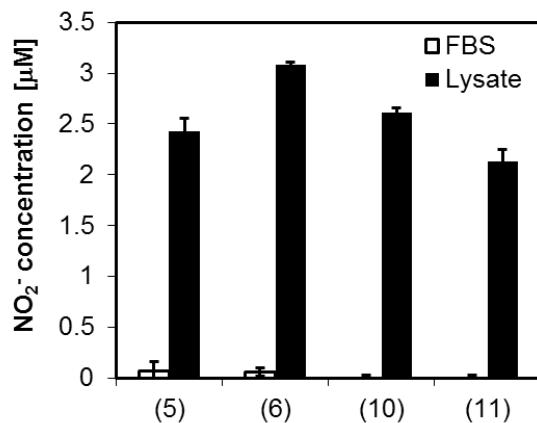
Figure 25. NO release from the amine-containing furoxans (5 and 6) and the PEG-furoxan conjugates (10 and 11) in the presence of 45% fetal bovine serum (FBS) (white columns) or 5.8×10^6 cells per mL cell lysate (black columns) from 264.7 murine macrophages in 50 mM PBS (pH 7.1) at 37 °C after 24 h as measured by the Griess assay. Furoxan concentration: 250 μM. $n = 3$.

Hydrolytic stability of the PEG–furoxan conjugates

The stability of the PEG–furoxan conjugates was evaluated under

physiological conditions. I first followed the changes in the UV/Vis spectra of the conjugates in PBS at pH 7.1 over the course of 3 days. As shown in **Figure 26**, both the furoxans and PEG–furoxan conjugates showed a decrease in the absorbance at around 260 nm and an increase in the absorbance at wavelengths above 300 nm over time. The observed spectral changes appeared more pronounced for the furoxan with a nitrophenyl group (**6** and **11**) than that with a phenyl group (**5** and **10**), but these spectral changes were not observed in water, which suggests that the changes in PBS were related to a hydrolysis reaction taking the slightly basic pH into consideration.
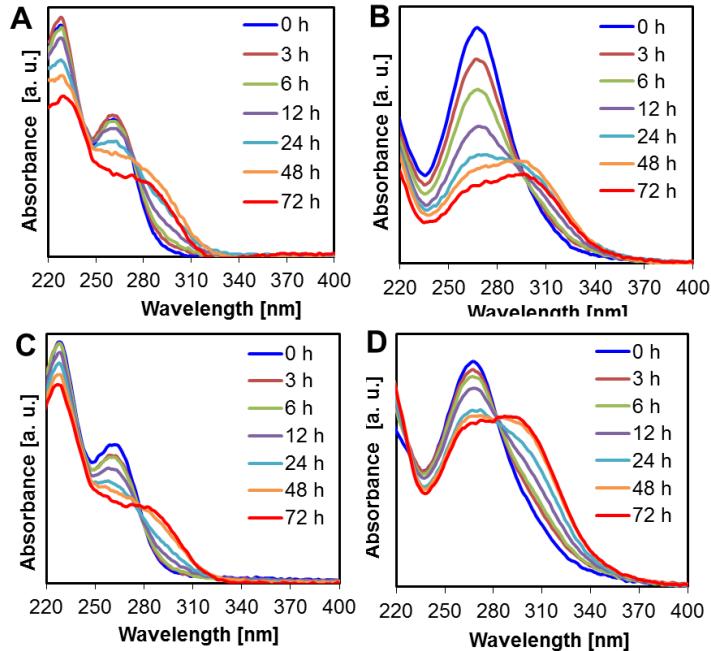
Figure 26. Change in the UV/Vis spectra of amine-containing furoxan (5) and (6) (A and B), and PEG-furoxan conjugates (10) and (11) (C and D) in 50 mM PBS (pH 7.1) at 37 °C.
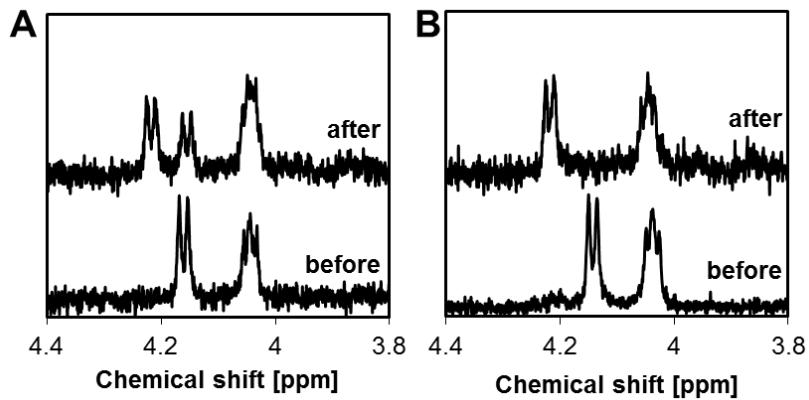
Figure 27. ^{1}H NMR spectra showing the region 4.4–3.8 ppm of PEG-F (10) (A) and PEG-NF (11) (B) after incubation in 50 mM PBS (pH 7.1) for 24 h at 37 °C. **Solvent:** *d6*-DMSO

To understand these spectral changes, ^{1}H NMR spectra after incubation of the conjugates in PBS was recorded. As can be seen in **Figure 27A**, the CH_2 in between the triazole and carbamate ($C\underline{H}_2$-NH), showing up at around 4.15 ppm, decreases in intensity and a new signal at 4.22 ppm was observed. In the case of **(11)**, the peak at around 4.15 ppm disappeared completely and a new peak appeared at 4.22 ppm in a 1: 1 ratio with the CH_2 next to the carbamate. On the other hand, no significant change in the peak at 4.04 ppm due to the CH_2 protons next to the carbamate bond ($CH_2O(CO)$) was observed for both **(10)** and **(11)**. This result indicates that some chemical reaction took place in the triazole–furoxan part of the molecule. Since it was not clear whether the triazole–furoxan structure was still conjugated to PEG, after 24 h of incubation in PBS, the product was

dialyzed against water to remove small compounds below 2 kDa. Surprisingly, the ^{1}H NMR spectrum showed the absence of the *para* substituted phenyl group indicating that the furoxan ring was no longer attached to PEG (**Figure 28A**). This was also supported by IR showing the absence of the furoxan ring vibration and the NO_2 vibration bands (**Figure 29A**). The presence of the carbamate bond and triazole ring was confirmed by ^{1}H NMR and IR. The aromatic region showed a broad
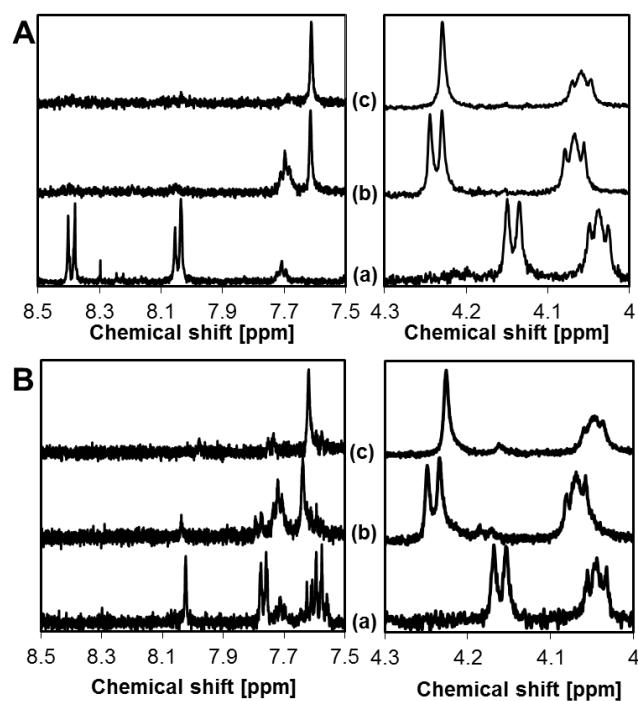
Figure 28. ^{1}**H NMR spectra of the (A) PEG-NF (11) (a) before and (b, c) after incubation in 50 mM PBS (pH 7.1) for 24 h at 37 °C. (B) PEG-F (10) (a) before and (b, c) after incubation in 50 mM PBS (pH 7.1) for 96 h at 37 °C. The spectra for (c) were recorded in the presence of D$_2$O. The conjugates were dialyzed and lyophilized before recording ^{1}H NMR in *d6*-DMSO.**

triplet as well as a singlet (**Figure 28A** (**b**)). This triplet was assigned to the NH of the carbamate as it could be exchanged with D_2O (**Figure 28A** (**c**)). Further support for this comes from the doublet at 4.22 ppm, assigned to the CH_2 next to the NH of the carbamate, which becomes a singlet after D_2O exchange. The singlet at 7.62 ppm was assigned to the proton of the triazole ring suggesting that the triazole ring was still intact. Therefore, it seems that the loss of the signals due to the nitrophenyl group was due to the cleavage of the bond between the triazole and furoxan rings. Furthermore, the PEG conjugate (**10**) also showed similar ^{1}H NMR and IR spectral changes but the reaction was much slower compared to (**11**) requiring more than 4 days at pH 7.1 to reach completion (**Figure 28B** and **29B**).
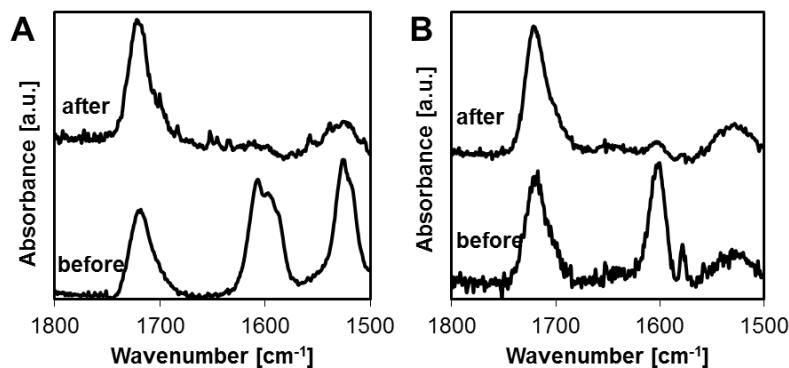

Figure 29. IR spectra of PEG-NF (11) incubated in 50 mM PBS (pH 7.1) for 24 h at 37 °C (A) and PEG-F (10) incubated in 50 mM PBS (pH 7.1) for 96 h at 37 °C
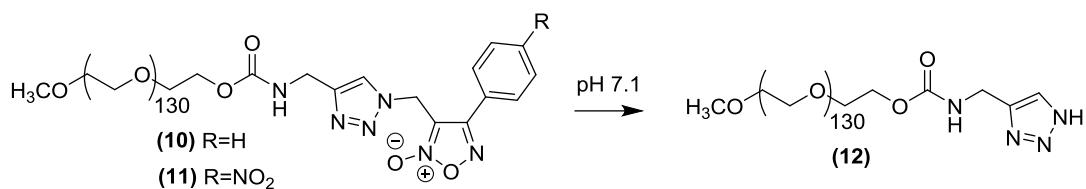
Scheme 4. Suggested decomposition reaction of the PEG-furoxan conjugates.

Based on these results, I propose the formation of PEG– triazole (**12**) as shown in **Scheme 4**. Several reports showed that the triazole group can behave as a leaving group, which has been used to prepare NH-1,2,3-triazoles under basic conditions by the retro-Michael addition reaction of β-tosylethyl[105] and cleavage of *N*-hydroxymethyl,[106] pivaloylmethyl[107] and carbamate[108] derivatives. In addition, the formation of this triazole structure was suggested from a nitrophenyl-substituted furoxan linked to the peptidomimetic scaffold in the presence of cysteine solely based on HPLC and mass data.[35] To gain support for the formation of (**12**) from (**10**) and (**11**), the ^{1}H NMR spectrum was recorded in CDCl$_3$. The triazole proton and the protons next to the NH of the carbamate appeared at 7.63 and 4.47 ppm, respectively (**Figure 30**). These chemical shifts are very similar to that reported for *tert*-butyl ((1,2,3-triazol-4-yl)methyl)carbamate: 7.62 and 4.40 ppm respectively.[109] At this point, the mechanism of how (**12**) forms from (**10**) and (**11**) is not clear.
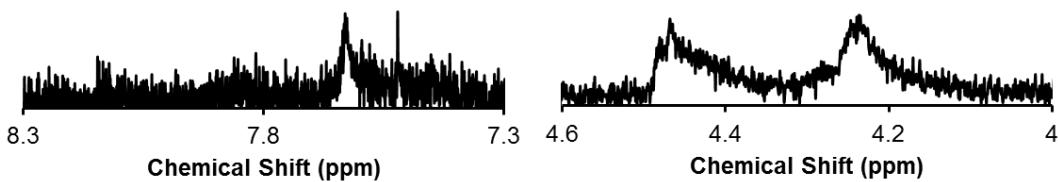
Figure 30. ^{1}H NMR spectrum of PEG-triazole (12) in CDCl$_3$.

To evaluate the effect of this structural change on the NO release behavior, the furoxans (**5** and **6**) and PEG–furoxan conjugates (**10** and **11**) were pre-incubated in PBS for 24 h and reacted with cysteine to induce NO release. As can be seen in **Figure 31**, lower levels of NO$_2^-$ were observed for all compounds after 24 h of pre-incubation. This data suggests that the decomposition of the furoxans and PEG–furoxan conjugates give products which have no or less NO release ability. Interestingly, both the PEG–furoxan conjugates showed significantly higher NO release compared to the corresponding furoxans, indicating that the PEG conjugation improved the stability of furoxans. Furthermore, the nitrophenyl derivatives (**6** and **11**) appeared to be more susceptible towards degradation than the phenyl derivatives (**5** and **10**) as these compounds showed a stronger decrease in the measured NO$_2^-$ concentrations. This observation is also supported by the UV/Vis spectra in **Figure 26**, which show that the nitrophenyl derivatives undergo more drastic spectral changes compared to the phenyl

derivatives. It seems that furoxan with electron-withdrawing groups (i.e., the nitrophenyl derivatives) accelerated both NO release and furoxan decomposition, which also explains the observed difference between **(10)** and **(11)** in release profiles at longer time points (**Figure 22A** and **B**).
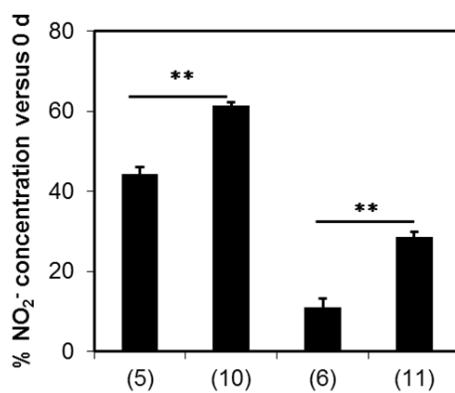
Figure 31. The amount of NO released from the furoxan and PEG-furoxan conjugates (250 μM) pre-incubated in PBS for 24 h. The samples were pre-incubated in 50 mM PBS (pH 7.1) for 24 h, reacted with 2.5 mM cysteine in 50 mM PBS (pH 7.1) for 24 h and the NO_2^- concentration was determined by the Griess assay. **$p < 0.01$, $n = 3$

Effect of (10) and (11) on the anti-proliferative effect of ibuprofen in colon cancer cells

Several studies reported that NO enhances the chemopreventive effect of non-steroidal anti-inflammatory drugs. For example, NSAIDs having a NO-releasing moiety showed stronger anti-proliferative and pro-apoptotic effects in different cancer cells compared to the NSAID alone.[110] Thus, I

investigated whether the combination of ibuprofen (IBU), a commonly used NSAID, and conjugates **(10)** and **(11)** show enhanced anti-proliferative effects in HT-29 colon cancer cells
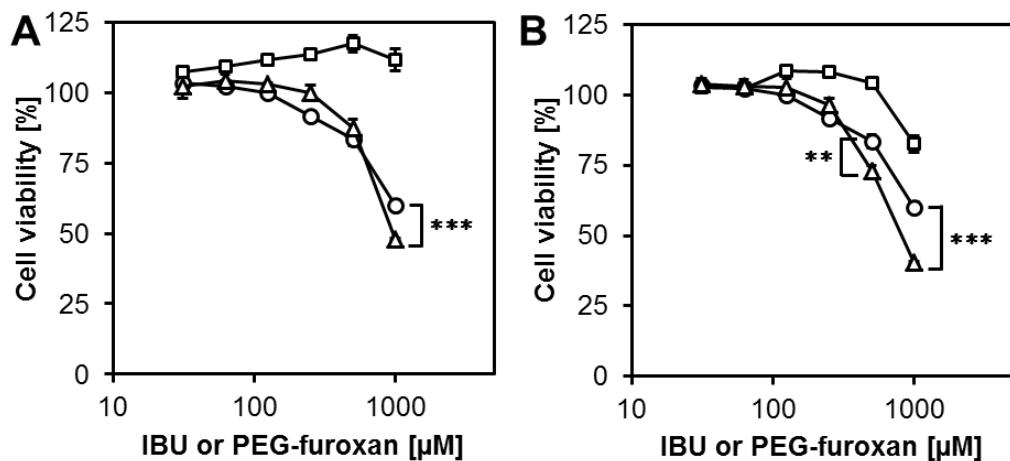
Figure 32. Anti-proliferative effect of IBU in the presence of PEG-furoxan conjugates (10) and (11) (A and B). HT29 cells were cultured for 2 d in the presence of IBU (circle), PEG–furoxan conjugates (square) and IBU and PEG–furoxan conjugates (triangle). **$p < 0.01$, ***$p < 0.001$, $n = 3$.

As can be seen in **Figure 32**, IBU showed a weak anti-proliferative effect with a LD_{50} value above 1000 μM. Combination of IBU and the conjugates (IBU/furoxan molar ratio = 1/1) significantly reduced the cell viability at higher doses compared to IBU alone. In particular, conjugate **(11)** (LD_{50} = 810 μM) showed a stronger effect than conjugate **(10)** (LD_{50} = 960 μM). Interestingly, conjugate **(10)** alone increased the cell viability

showing its weak proliferative effect. Conjugate **(11)** also showed a similar increase in the cell viability below 500 μM, but showed significant toxicity at 1000 μM. These observations may relate to the role of NO in cancer biology. It has been reported that NO exhibits both tumoricidal and tumor promoting properties, depending on the NO concentration and duration of action.[111] Continuous NO release is known to stimulate cell proliferation at lower concentrations. Therefore, the proliferative effect of conjugates **(10)** and **(11)** may be due to the slow NO release that stimulates proliferation of HT-29 cells. The observed toxicity of conjugate **(11)** at a high concentration could be due to the decomposition products. Due to its low hydrolytic stability compared to conjugate **(10)**, conjugate **(11)** decomposed to release larger amounts of the decomposition products which may be toxic to the cells.

To further confirm that the observed synergetic effect on the anti-proliferative effect of IBU was due to NO released from the conjugate, the NO_2^- concentration was measured in culture medium by a fluorescence Griess assay. As shown in **Figure 33**, the addition of conjugate **(10)** increased the NO_2^- concentration in a dose-dependent manner. This result indicates that the enhanced anti-proliferative effect in HT-29 cells treated

with both IBU and conjugate **(10)** can be attributed to NO release from the conjugate. On the other hand, for conjugate **(11)** the NO_2^- concentration was not increased significantly. Although enhanced reduction in the cell viability for cells treated with conjugate **(11)** was observed, this effect may be caused by the decomposition byproducts and not due to NO release.
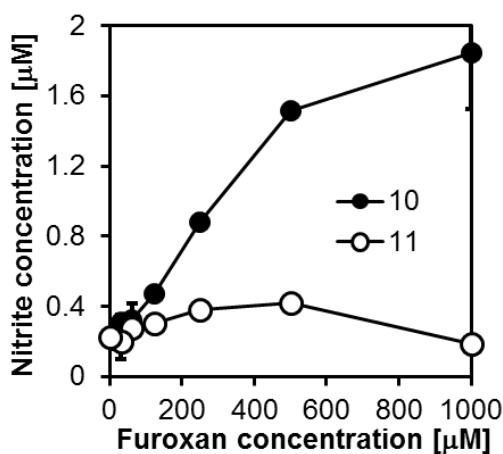
Figure 33. Release of NO as detected by the concentration of NO_2^- in the medium after culturing for 2 d using the fluorescence Griess assay. HT-29 cells (1.5×10^4 cells/well) were treated with PEG-furoxan (10) or (11) at the indicated concentrations for 2 d before measuring the NO_2^- concentration.

Conclusion

Polymeric NO donors were prepared by linking furoxan derivatives to poly(ethylene glycol) (PEG) using the copper-catalyzed Huisgen cycloaddition reaction. The conjugates were prepared using two different furoxan derivatives having phenyl or nitrophenyl substituent groups attached to the furoxan ring. The conjugates released NO in the presence of cysteine, glutathione and the cell lysate of murine macrophages, but not FBS. Both the furoxans and PEG–furoxan conjugates decomposed in PBS to yield products with no or less NO release activity. The PEG conjugation slowed down the decomposition and released a significantly higher amount of NO compared to the corresponding furoxans after 24 h of incubation in PBS at 37 °C. Furthermore, the PEG conjugate of furoxan with a phenyl substituent released NO and enhanced the anti-proliferative effect of ibuprofen in HT-29 colon cancer cells.

Chapter 3

Furoxan-bearing micelles for nitric oxide delivery

Introduction

As described in chapter 2, PEG-furoxan conjugates slowly underwent decomposition under physiological conditions, which may limit its therapeutic application. In this chapter, to solve this problem, a polymeric micelle having a hydrophobic core bearing furoxan moieties was prepared. In this approach, it is expected that the hydrolytic decomposition of furoxan can be slowed down by placing the furoxan moieties within the hydrophobic core.

Amphiphilic block copolymer containing furoxan was prepared by using a combination of the reversible addition-fragmentation chain transfer (RAFT) polymerization[112,113] and CuAAC. RAFT polymerization is one of the controlled living radical polymerization. RAFT polymerization can be used to design polymers with complex architectures, such as linear, comb-like, star and brush polymers, dendrimers and cross-linked networks.[114] The self-assembling behavior of the furoxan-containing block copolymer was characterized by dynamic light scattering (DLS), transmission electron

microscopy (TEM) and atomic force microscopy (AFM). The NO release property as well as stability against hydrolytic decomposition of the micelles was also evaluated. Furthermore, the effect of the micelles on the IBU-induced anti-proliferative effect was assessed in human colon cancer HT-29 cells.
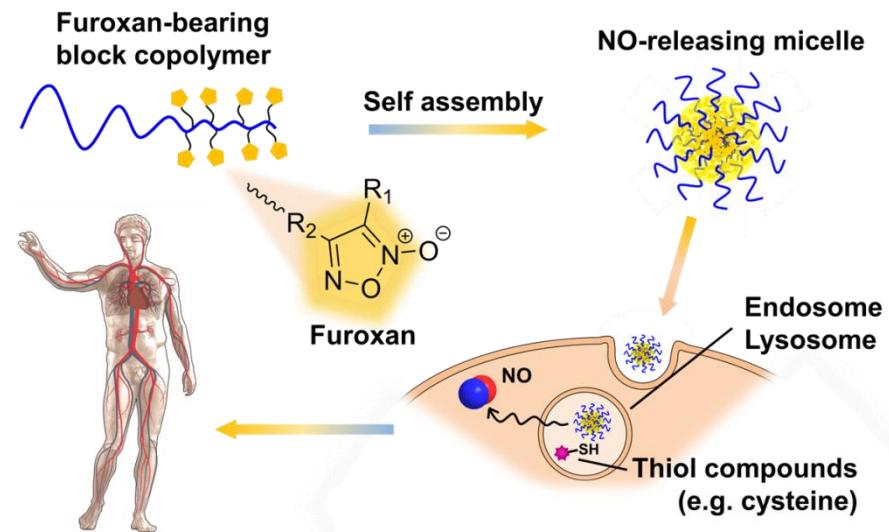
Figure 34. Furoxan-bearing micelles for nitric oxide delivery.

Experimental

Instrumentation

NMR spectroscopy. ^{1}H NMR and were measured with a Bruker DPX400 NMR spectrometer. For ^{1}H NMR spectra a total of 32 scans were collected and the D1 was set to 10 s for the polymers and 1 s for the low molecular weight compounds. Chemical shifts are referenced to the residual undeuterated NMR solvent signal at 2.50 (d_6-DMSO), 7.26 ppm (CDCl$_3$), and 4.79 (D$_2$O).

UV/Vis spectroscopy. The absorbance was measured with a Tecan infinite M200 plate reader in transparent polystyrene 96 well plates and UV/Vis spectra were recorded on either a HITACHI U-2810 spectrophotometer or Thermo Scientific NanoDrop 2000c spectrophotometer using 2 μL of sample volume.

Attenuated total reflection infrared spectroscopy (ATR-IR). Attenuated total reflection infrared (ATR-IR) spectra were obtained on a Thermo Scientific Nicolet iS5 equipped with an iD5 universal ATR sampling accessory

Gel permeation chromatography (GPC). Elution charts were collected with a Tosoh GPC-8020 instrument equipped with refractive index (RI) detector. The KD-803 (Shodex) column was operated at 50 ℃ while flowing 100 mM LiCl in DMF at 1.0 mL/min. Polydispersity index (M_w/M_n) values were calculated based on the elution time of polyethylene glycol standard polymers.

Dynamic light scattering (DLS). Hydrodynamic diameter was measurements with an Otsuka ELSZ machine using 4.5 mL disposable polystyrene cuvettes. Micelle solutions were filtered through 0.45 μm syringe filter prior to analysis. The mean diameter (Z-average) and polydispersity index (PDI=μ_2/Γ^2) were calculated by the cumulant method.

Contact angle measurement. Contact angles of the samples were determined using a Kyowa Interface Science Drop Master DM 300.

Atomic force microscopy (AFM). The micelle solution in water was dropped onto a fresh mica surface and then dried by blowing off the solution by a hand blower. Images were acquired on a Seiko Instruments SPA400 in dynamic force mode (DFM) using a Si probe with Al coating (SI-DF20, Seiko).

Transmission electron microscopy (TEM). The micelle solution was placed onto a carbon coated 250 mesh copper grids and then dried by blotting the side of the grid with filter paper. The grids were negatively stained with 0.5 wt% Preyssler-type potassium phosphotungstate solution. Images were acquired on a Hitachi H-7650 TEM operating at 100 kV.

Materials

N-(2-hydroxyethyl)acrylamide, 4-acryloylmorpholine (AM), tris(trimethylsilyl)silane, carbonyldiimidazole (CDI), propargylamine, 2-acetamidoethanol, 3-(4,5-dimethylthiazol-2-yl)-2,5-diphenyltetrazolium bromide (MTT), *N*-1-naphthylethylenediamine dihydrochloride (NED) and sulfanilamide (SA) were purchased from Tokyo Chemical Industry Co., Ltd. (Osaka, Japan). 2,2'-Azobis(isobutyronitrile) (AIBN), super dehydrated dimethyl sulfoxide (DMSO), super dehydrated dimethylformamide (DMF), diethyl ether (Et_2O), copper(II) sulfate pentahydrate ($CuSO_4 \cdot 5H_2O$), sodium ascorbate, L-cysteine, sodium nitrite ($NaNO_2$), potassium bicarbonate ($KHCO_3$), sodium hydrogen sulfate ($NaHSO_4$), sodium sulfate (Na_2SO_4), ibuprofen (IBU), 36% (w/v) hydrochloric acid (HCl (aq)), silica (SiO_2) were purchased from Wako

(Japan). 2-(((dodecylthio)carbonthioyl)thio)-2-methylpropanoic acid, ninhydrin, aluminum oxide (Al_2O_3) were purchased from Sigma-Aldrich (Japan). Hexane, ethyl acetate (EtOAc), tetrahydrofuran (THF), *tert*-butyl alcohol (*t*-BuOH), triethylamine (Et_3N), calcium hydride (CaH_2), dichloromethane (CH_2Cl_2), methanol (MeOH), and molecular sieves 3A were purchased from Nacalai Tesque (Kyoto, Japan). Deuterated solvents for ^1H NMR (D_2O, $CDCl_3$ and d_6-DMSO) were from Cambridge Isotope Laboratories, Inc. (USA). Dialysis tubing (MWCO 2 kDa) was purchased from Spectrum Laboratories (USA). 10× PBS was from Invitrogen. AIBN was recrystallized from MeOH. *N*-(2-hydroxyethyl)acrylamide and 4-acryloylmorpholine were passed through an Al_2O_3 column to remove inhibitor. Et_3N was distilled over ninhydrin and CaH_2 and kept over molecular sieves. All other chemicals were used as received. McCoy's culture 5A, fetal bovine serum and penicillin−streptomycin were purchased from Invitrogen (USA).

Synthesis

PHEA-CTA (15). *N*-(2-hydroxyethyl)acrylamide (HEA, **13**) was polymerized using AIBN as the initiator and 2-(((dodecylthio)carbon thioyl)thio)-2-methylpropanoic acid (**14**) as the chain transfer agent (CTA). The [HEA]/[CTA]/[AIBN] molar ratio was 25/1/0.1 and the monomer concentration was 1 M. 575.5 mg (5 mmol) of (**13**), 72.9 mg (0.2 mmol) of (**14**) and 3.28 mg (0.02 mmol) of AIBN were dissolved in 5 mL of DMSO. The solution was degassed with argon by five freeze-thaw cycles and heated at 60°C for 24 h. The polymerization was stopped by placing the Schlenk tube in liquid nitrogen. After thawing, the solution was transferred to a dialysis tube (MWCO 2 kDa) and dialyzed against 3 L water for 24 h with replacing the water every 12 h. The solution was lyophilized to yield 609 mg (94%) of a yellow solid. ^{1}H NMR (D$_2$O) δ = 8.35-7.90 (bs, NH-C(O) PHEA), 3.85-3.55 (bs, C$\underline{H}_2$-OH PHEA), 3.53-3.05 (bs, NH-C$\underline{H}_2$ PHEA and CH$_2$-S-C(S) CTA), 2.50-1.00 (m, CH$_2$-CH PHEA, and 2 × CH$_2$ CTA), 1.19 (8 × CH$_2$ CTA), 1.11 and 1.08 (bs, C(CH$_3$)$_2$ CTA), 0.80 (bs, CH$_2$-C$\underline{H}_3$ CTA). Whereas the NH protons could be still observed the OH of PHEA and CO$_2$H of the CTA were completely exchanged with D$_2$O and not observed. The ^{1}H NMR spectrum is shown in **Figure 35**. The degree

75

of polymerization was 25 as calculated from the integral ratio of the -CH$_2$-signal between 3.85-3.55 ppm of PHEA and the -CH$_3$ signal at 0.80 ppm of the CTA.

PHEA-PAM-CTA (17). 4-Acryloylmorpholine (**AM**, **16**) was polymerized using AIBN as the initiator and (**15**) as the macro CTA. The [AM]/[macro CTA]/[AIBN] molar ratio was 100/1/0.2 and the monomer concentration was 1 M. 705.9 mg (5 mmol) of (**16**), 162.1 mg (0.05 mmol) of (**15**) and 1.64 mg (0.01 mmol) of AIBN were dissolved in 5 mL DMSO. The solution was degassed with argon by five freeze-thaw cycles and heated at 60°C for 24 h. The polymerization was stopped by placing the Schlenk tube in liquid nitrogen. After thawing, the solution was transferred to a dialysis tube (MWCO 2 kDa) and dialyzed against 3 L water for 24 h and replacing water every 12 h. The solution was lyophilized to yield 845 mg (97%) of a pale yellow solid. ^{1}H NMR (D$_2$O) δ = 8.25-8.00 (bs, NH-C(O)), 4.25-3.05 (m, NH-C$\underline{H}_2$-C$\underline{H}_2$-OH PHEA, N-CH$_2$-CH$_2$-O PAM and CH$_2$-S-C(S) CTA), 2.68 (bs, C$\underline{H}$-CH$_2$ PAM), 2.30-1.00 (m, CH$_2$-CH PHEA, C$\underline{H}_2$-CH PAM and 10 x CH$_2$ CTA), 1.06 and 1.03 (bs, C(CH$_3$)$_2$ CTA), 0.86 (bs, 3H, CH$_2$-C$\underline{H}_3$ CTA). Whereas the NH protons could be still observed the OH of PHEA and CO$_2$H of the CTA were completely exchanged with

D$_2$O and not observed. The ^{1}H NMR spectrum is shown in **Figure 36**. The degree of polymerization was calculated from the molar ratio of PAM/PHEA units using the integral values of the signals at 3.80-3.33 and 2.68 ppm and the number of HEA monomer units in the macro CTA (**15**). The degree of polymerization for PAM was 100.

PHEA-PAM (18). 824.5 mg (0.048 mmol) of (**17**), 59.1 µL (0.24 mmol) of tris(trimethylsilyl)silane and 15.8 mg (0.096 mmol) of AIBN were dissolved in 5 mL DMF. The solution was degassed with argon by five freeze-thaw cycles and heated at 80°C for 20 h. The reaction was stopped by placing the Schlenk tube in liquid nitrogen. After thawing, the solution was added drop wise to Et$_2$O (150 mL). The precipitate was filtered off, washed with Et$_2$O (2 × 10 mL) and dried under reduced pressure to yield 754.6 mg (93%) of a white powder. ^{1}H NMR (D$_2$O) δ = 4.25-3.05 (m, NH-C$\underline{H}_2$-C$\underline{H}_2$-OH PHEA, N-CH$_2$-CH$_2$-O PAM), 2.68 (bs, C$\underline{H}$-CH$_2$ PAM), 2.30-1.00 (m, CH$_2$-CH PHEA, C$\underline{H}_2$-CH PAM), 1.05 and 1.00 (bs, C(CH$_3$)$_2$ CTA). The NH, OH of PHEAA and CO$_2$H of the CTA were not observed due to exchange with D$_2$O. The spectrum is shown in **Figure 37**. The UV/Vis spectrum of the polymer in DMF showed the absence of the absorption at 310 nm confirming successful end group removal (**Figure**

41).

P(CDI)-PAM (19). 734.4 mg (43.0 μmol, 1.08 mmol OH groups) of (**18**) was dried at 60°C overnight under reduced pressure over KOH pellets. The polymer was dissolved in 18 mL DMF and 1.78 g (10.8 mmol, 10 equiv) of CDI was added. The flask was evacuated/purged with N_2 (3×) and the mixture stirred for 24 h. The polymer solution was added to diethyl ether (100 mL) and the precipitate was recovered by centrifugation to yield 766.6 mg (97%) of a white powder. ^{1}H NMR (CDCl$_3$) δ = 8.19 (bs, CH imidazole), 7.40 (bs, CH imidazole), 7.00 (bs, CH imidazole), 4.43 (bs, CH_2-O-C(O)), 4.00-3.00 (m, NH-C$\underline{H}_2$-C$\underline{H}_2$-O-C(O)-imidazole and N-CH$_2$-CH$_2$-O PAM), 2.63 (bs, C$\underline{H}$-CH$_2$ PAM), 2.20-0.84 (m, CH$_2$-CH PHEA, CH-C$\underline{H}_2$ PAM and C(CH$_3$)$_2$ CTA). The spectrum is shown in **Figure 38**. The degree of modification was 100% as calculated from the integral ratio of the imidazole signals and the CH PAM signal. This degree of functionalization was further supported by measuring ^{1}H NMR of the polymer in CDCl$_3$.

P(alkyne)-PAM (20). 754.2 mg (38.8 μmol, 0.97 mmol of imidazole groups) of (**19**), 1.36 mL (9.7 mmol) of Et$_3$N and 621.3 mg (9.7 mmol) of

propargylamine were dissolved in 20 mL DMF. The flask was evacuated/purged with N_2 (3 ×) and the mixture stirred for 48 h. The mixture was acidified with 10 mL of 1 M $NaHSO_4$ (aq) and the solution transferred to a dialysis tube (MWCO 2 kDa) and dialyzed against 3 L water for 24 h with replacing water every 12 h. The solution was lyophilized to yield 625.8 mg (84%) of a pale yellow solid. ^{1}H NMR ($CDCl_3$) δ = 7.80-6.40 (bs, NH amide and carbamate), 3.98 (bs, CH_2-O-C(O)-alkyne), 4.00-3.00 (bs, NH-C$\underline{H}_2$-C$\underline{H}_2$-O-C(O)-NH-C$\underline{H}_2$- alkyne and N-CH_2-CH_2-O PAM), 2.63 (bs, C$\underline{H}$-CH_2 PAM), 2.3-0.83 (m, CH alkyne, CH_2-CH PHEA CH-C$\underline{H}_2$ PAM and C(CH_3)$_2$ CTA). The spectrum is shown in **Figure 39**. Due to overlap of the alkyne proton with PAM and PHEA signals the degree of modification could not be calculated using integral ratios. Since ^{1}H NMR showed the absence of imidazole peaks and the ^{1}H NMR spectrum in d_6-DMSO did no show a signal between 4.5-5.0 ppm due to OH groups it was assumed that the reaction was quantitative.

P(furoxan)-PAM (21). 632.1 mg (3.3 µmol, 0.83 mmol alkyne groups) of (**8**), 179.6 mg (0.83 mmol, 1 equiv) of (**20**), 0.194 mg (16.5 µmol) of $CuSO_4$·$5H_2O$ and 16.3 mg (82.6 µmol) of sodium ascorbate were dissolved in a mixture of 15.5 mL of *t*-BuOH and 26.3 mL of H_2O. The solution was

degassed with argon by five freeze-thaw cycles and the mixture stirred for 24 h at 35°C. After cooling down to room temperature, the solution was first filtered through a 0.45 µm syringe filter and transferred to a dialysis tube (MWCO 2 kDa) and dialyzed against 3 L water for 48 h and replacing water every 12 h. The solution was lyophilized to yield 675.9 mg (83%) of a white solid. ^{1}H NMR (CDCl$_3$) δ = 7.91 (bs, CH triazole), 7.88 (bs, 2 x CH$_{aromat}$ furoxan), 7.52 (bs, 3 × CH$_{aromat}$ furoxan), 5.55 (bs, CH$_2$-furoxan), 4.35 (bs, CH$_2$-NH-C(O)-O), 3.95-3.20 (bs, NH-CH$_2$-CH$_2$-O-C(O)-NH and N-CH$_2$-CH$_2$-O PAM), 2.64 (bs, CH-CH$_2$ PAM), 1.93-0.83 (m, CH$_2$-CH PHEA, CH-CH$_2$ PAM and C(CH$_3$)$_2$ CTA). The NH protons of the amide and carbamate appeared as a broad signal between 7.8-6.4 ppm. The ^{1}H NMR spectrum is shown in **Figure 40**. The degree of modification was calculated to be 72% by comparing the integral ratio of the CH$_2$-furoxan protons and the CH signal of PAM. For NO release and cell culture experiment, the polymer was further purified as follows: The polymer was dissolved at 40 mg/mL in DMF and 125 µL of this solution mixed with 125 µL of 21.2 mg/mL of diethyl ammonium dithiocarbamate in DMF. This solution was then loaded onto a Sephadex LH20 size exclusion column and eluted with DMF. Fractions were analyzed by UV/Vis using a Nanodrop

and those fractions containing polymers were combined and concentrated under reduced pressure. After dissolving in 250 µL DMF and dilution with water the mixture was passed through a 0.45 um syringe filter and dialyzed. The polymer was recovered by lyophilization.

Micelle formation

The furoxan-bearing block copolymer (**21**) was dissolved in DMF (20 mg/mL) and 250 µL of this solution was added drop wise to 2250 µL of milliQ water under stirring. After 30 min, the clear solution was transferred to a dialysis tube (MWCO 2kDa) and dialyzed against 1 L water overnight.

Critical micelle concentration (CMC) measurement

The micelle solutions at different concentrations in milliQ water were dropped (2 µL) onto parafilm and the contact angle was measured. The CMC was calculated from the contact angle versus concentration curve as reported.[115]

Griess assay

The concentration of NO_2^- was measured by the Griess assay in transparent 96 well polystyrene plates. The samples were reacted with 50

μL of 2% (w/v) SA in 5% HCl (aq) for 5 min before adding 50 μL 0.1% (w/v) NED (aq)[91] After 5 min, the absorbance at 550 nm was measured and the NO_2^- concentrations calculated from standard curves of 0-100 μM NO_2^- in either 1.25, 2.5, 12.5 or 25 mM cysteine, or 25 mM cysteine in 5% (w/v) Triton X-100 in 50 mM PBS (pH7.1) containing 2.5 mM DTPA. All samples were corrected for absorbance of polystyrene, reaction medium and the SA/NED reagent mix by subtraction the absorbance of wells containing water only.

NO release from the micelles and model compound (22)

Aqueous solutions of micelles and the model compound (**Scheme 6**, **22,** synthesized by co-workers) at 500 μM (50 μL) were mixed with either 50 μL of 2.5, 5.0, 25 or 50 mM cysteine in 100 mM PBS containing 5 mM DTPA. NO_2^- standard curves were prepared on the same plate by mixing 50 μL of $NaNO_2$ solution at different concentrations with 2.5, 5.0, 25 or 50 mM cysteine in 100 mM PBS containing 5 mM DTPA. The plates were placed in a humidified incubator at 37°C and taken out at the indicated time points for Griess assay. The concentration of furoxan in the micelle and model compound solutions was calculated, after diluting 1:1 with DMF,

from the absorbance at 263 nm and a standard curve of the model compound in H_2O/DMF 1:1. The furoxan concentration of the aqueous micelle solution was in good agreement with that estimated from the initial polymer weight, degree of functionalization and the final volume of the solution after dialysis.

NO release from the micelles in the presence of Triton X-100

The micelle solution was diluted to a final furoxan concentration of 500 μM and 10% (w/v) Triton X-100. To 50 μL in a well plate was then added 50 μL of 50 mM cysteine in 100 mM PBS containing 5.0 mM DTPA (pH7.1). The plates were placed in a humidified incubator at 37°C and taken out after 3 d for Griess assay.

Stability of the micelles and model compound

The micelle and model compound (**22**) solutions were diluted with an equal volume of 100 mM PBS containing 5 mM DTPA to a final furoxan concentration of 250 μM (pH7.1). The samples were kept for 0, 1, 3 and 7 d at 37ºC before being measured by UV-Vis.

NO release from the micelles and model compound (22) after incubation in PBS

The micelle and model compound (**22**) solutions were diluted 9:1 with 100 mM PBS to a final of 500 μM furoxan concentration and 10 mM PBS (pH 7.4). The samples were kept for 0, 1, 3 and 7 d at 37°C before being mixed 1:1 with 50 mM cysteine in 100 mM PBS containing 5 mM DTPA. After 3 d at 37°C, the amount of NO released was quantified by the Griess assay.

Cell culture

HT-29 human colon cancer cells were cultured in McCoy's 5A medium containing 10% fetal bovine serum and 50 U/mL-50 μg/mL penicillin−streptomycin in a CO_2 incubator at 37 °C. Cells were trypsinized and passaged when reaching 70−80% confluence.

Effect of the micelles on ibuprofen (IBU)-induced anti-proliferative effect in HT-29 cells

HT-29 cells were seeded at 1.5×10^4 cells/well in 96 polystyrene well plate with 100 μL medium. After 1 d at 37°C, the medium was replaced

with 100 μL of fresh medium containing 10 μL of the sample solutions of the micelles, IBU and mixture of micelles and IBU (furoxan/IBU molar ratio is 1) in water/DMSO (99:1). As a control, cells were treated with 100 μL medium alone. The cells were cultured for 2 d at 37°C. The medium was removed and replaced with 100 μL medium and 10 μL MTT solution in PBS (5 mg/mL). After 2 h at 37°C, the formed formazan crystals were dissolved in 100 μL of 0.1 g/mL SDS in 0.01 M HCl (aq) and the absorbance at 570 nm was measured. The statistical difference between two groups was calculated using Student's t-test (*n*=3).

Results and Discussion

## *Synthesis of furoxan-bearing block copolymer (21)*
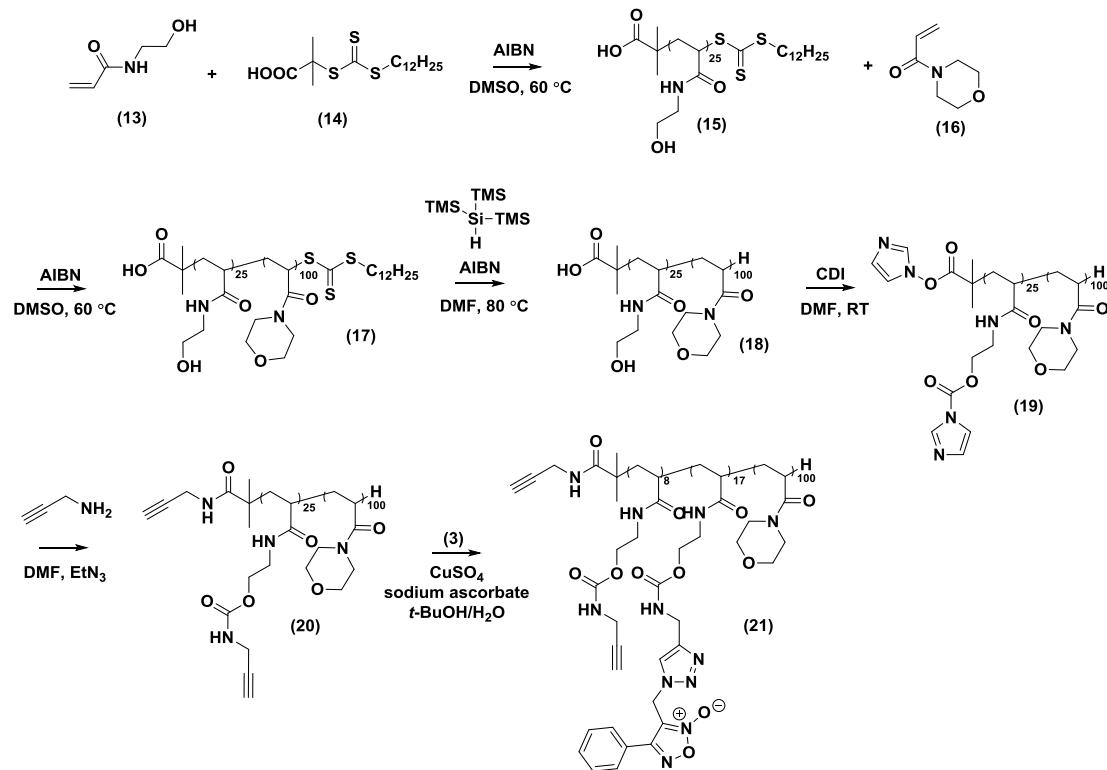
Scheme 5. Synthesis scheme to prepare diblock copolymer (21).

An amphiphilic block copolymer consisting of a hydrophilic PAM block and hydrophobic furoxan-bearing block was synthesized as shown in **Scheme 5**. Hydroxyl group-bearing block copolymer (**18**) was first synthesized by the RAFT polymerization technique. This polymer was modified with propargylamine to introduce alkyne groups, which were further reacted with an azide-containing furoxan derivative (**3**) using the

well-known copper-catalyzed Huisgen cycloaddition reaction between an azide and alkyne. Structures of each step of product were confirmed by ^{1}H NMR and IR. (**Figure 35-40** and **43**)
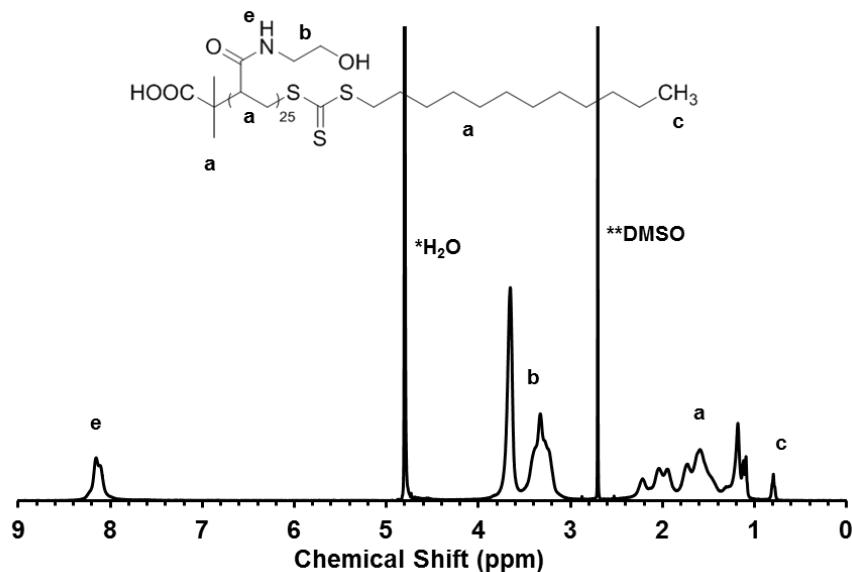
Figure 35. ^{1}H NMR spectrum of PHEA-CTA (15) in D$_2$O.
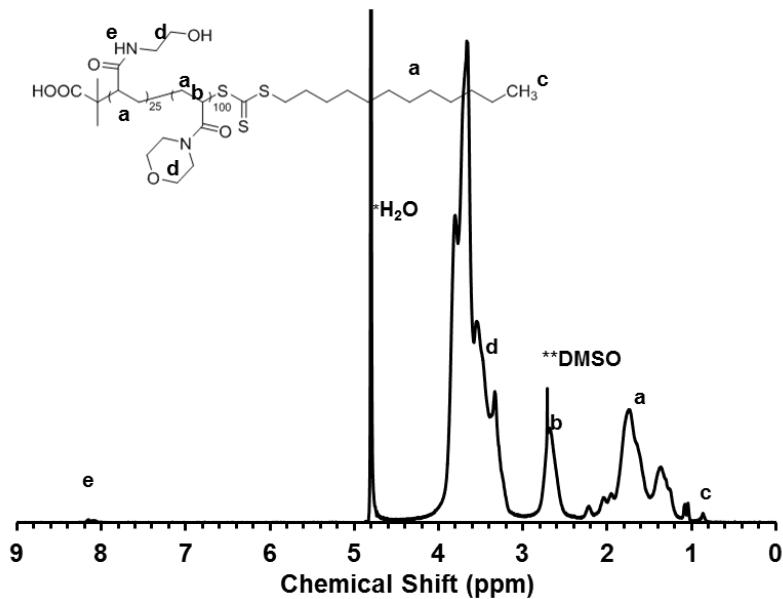
Figure 36. ^{1}H NMR spectrum of PHEA-PAM-CTA (17) in D$_2$O.
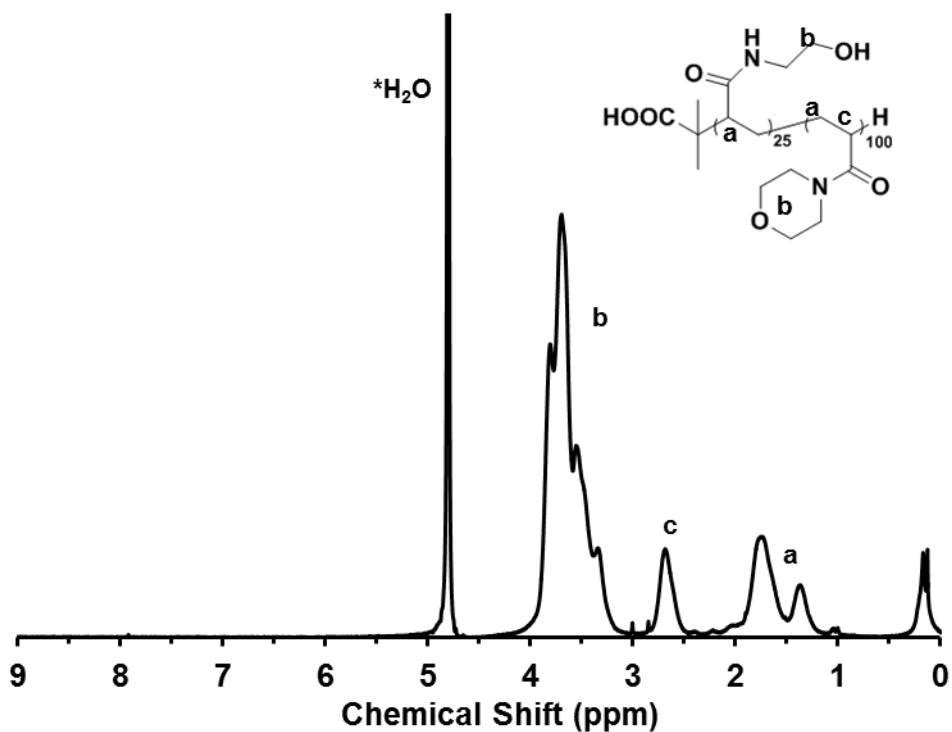
Figure 37. ^{1}H NMR spectrum of PHEA-PAM (18) in D$_2$O.
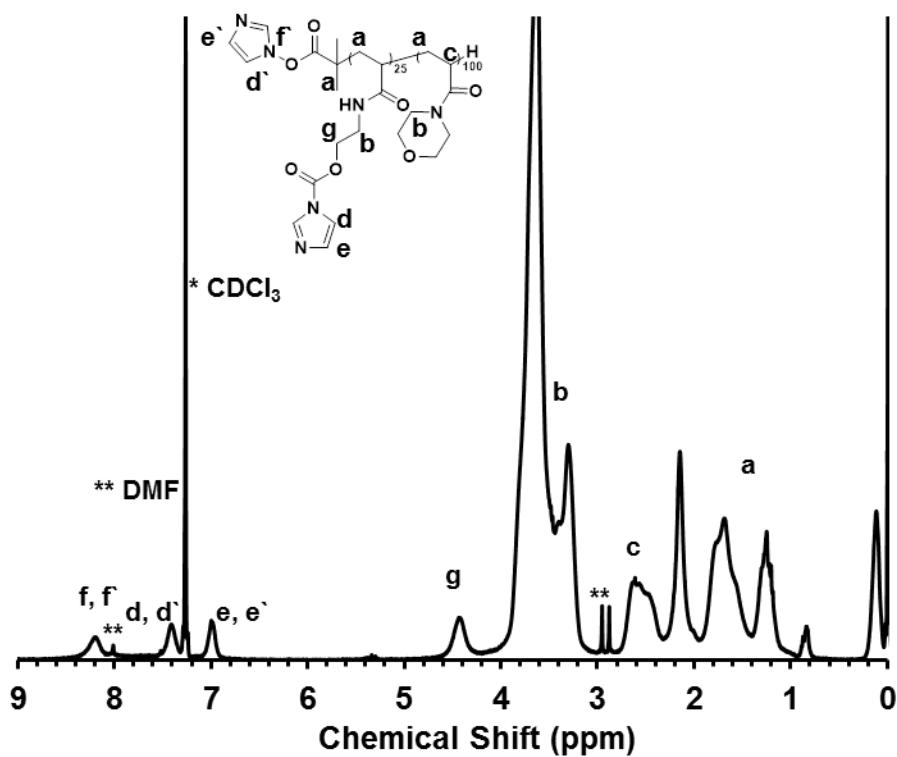
Figure 38. ^{1}H NMR spectrum of P(CDI)-PAM (19) in CDCl$_3$.
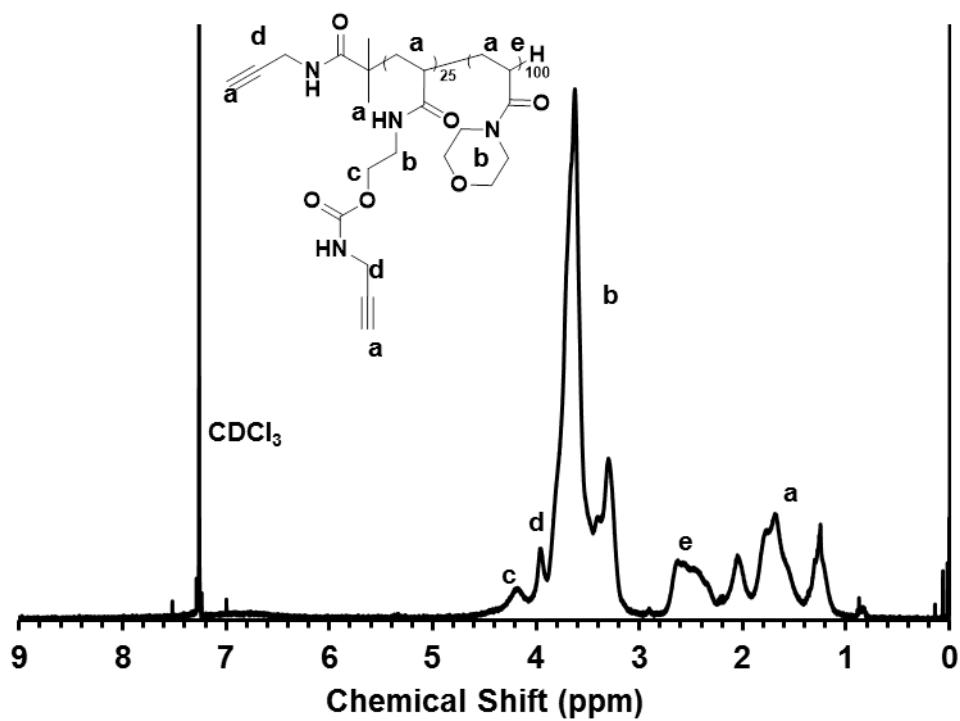
Figure 39. ¹H NMR spectrum of P(alkyne)-PAM (20) in CDCl₃.
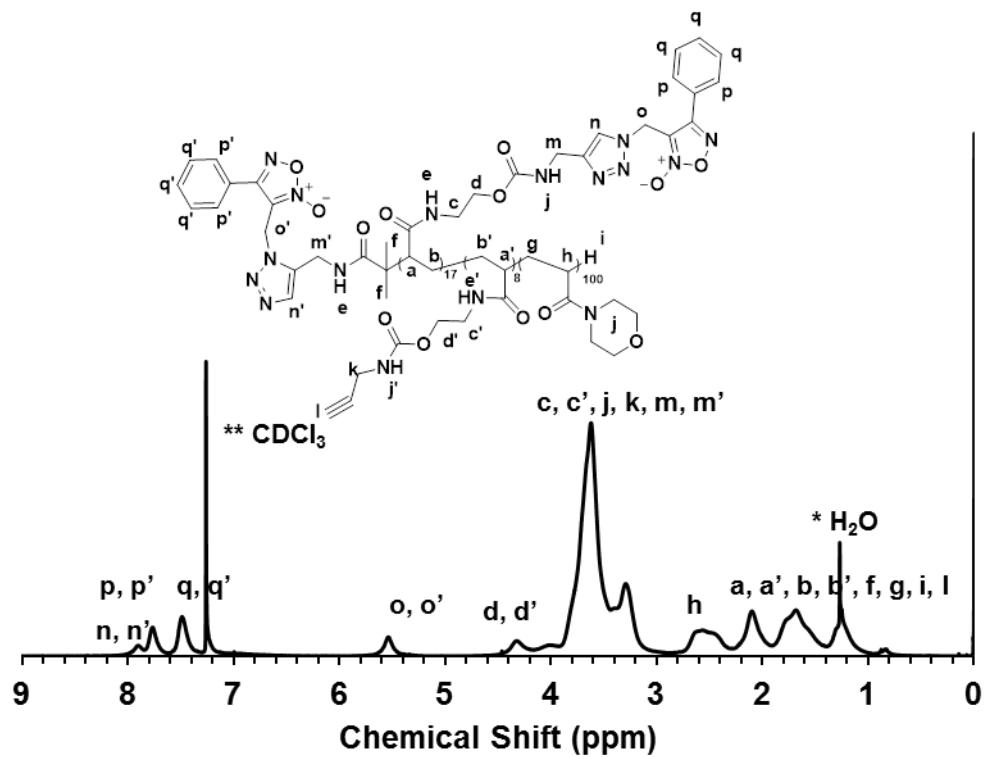
**Figure 40. ¹H NMR spectrum of P(furoxan)-PAM (21) in CDCl₃.**

N-(2-hydroxyethyl)acrylamide (HEA, **13**) was polymerized in DMSO at 60 °C for 24 h using 2-(((dodecylthio)carbonthioyl)thio)-2-methylpropanoic acid (**14**) as the chain transfer agent (CTA) and AIBN as the radical initiator. The HEA concentration was 1 M and the HEA/CTA/AIBN ratio was 25/1/0.1. The average degree of polymerization (DP) of the resulting polymer (**PHEA-CTA**, **15**) was 25 according to ^{1}H NMR. In addition, gel permeation chromatography (GPC) showed a unimodal peak with a low polydispersity index (M_w/M_n) of 1.05 showing a narrow size distribution (**Table 2**, **Figure 42**). Then, by using (**15**) as a macro-CTA, *N*-acryloylmorpholine (AM, **16**) was polymerized to yield PHEA-PAM-CTA block copolymer (**17**). The polymerization proceeded quantitatively when the AM concentration was 1 M and the AM/PHEA/AIBN ratio was 100/1/0.2. The block copolymer had a unimodal size distribution as confirmed by GPC (**Table 2** and **Figure 42**).

To avoid the formation of thiols by transamidation with the thiocarbonate group during post-modification of the block copolymer, that could potentially lead to dimerization, the CTA end-group was removed using radical-induced cleavage using tris(trimethylsilyl)silane as the hydrogen source[116]. The absence of the absorption at 310 nm due to the

trithiocarbonates group was confirmed by UV-Vis spectroscopy (**Figure 41**). Furthermore, GPC showed that no dimerization took place during the end group removal (**Figure 42**).
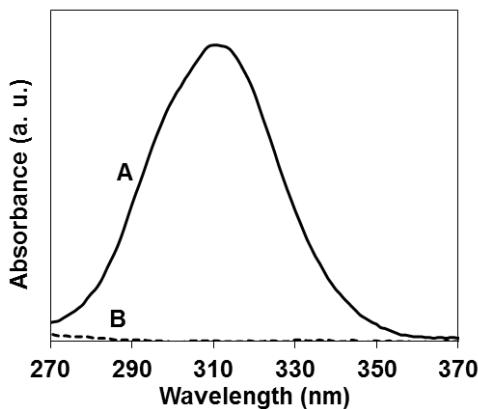
Figure 41. UV/Vis spectra of 17 (A) and 18 (B) in DMF (5 mg/mL) showing successful CTA group removal.

The hydroxyl groups of PHEA-PAM block copolymer (**18**) were activated by reacting with carbonyldiimidazole (CDI). The formation of the carbonyl imidazolide was confirmed by ^{1}H NMR showing peaks due to the imidazole group. Furthermore, IR showed, in addition to the broad band of the ν(C=O) stretching vibration of the amide of PHEA and PAM at around 1640 cm^{-1}, a weak new band at around 1764 cm^{-1} that can be assigned to the ν(C=O) stretching vibration of the imidazolide (**Figure 43**). The activated polymer (**19**) was then conjugated with propargylamine to yield the alkyne-bearing polymer (**20**). The shift of the ν(C=O) stretching

band at 1764 to 1722 cm^{-1} in the IR spectrum and the absence of imidazolide peaks in the ^{1}H NMR spectrum showed successful conjugation with propargylamine. Furthermore, GPC showed that the alkyne-bearing polymer (**20**) showed a unimodal peak indicating that crosslinking of the polymer chains did not occur during hydroxyl activation with CDI (**Figure 42**).

Table 2. **Molecular Weights of 15, 17, 18, 19, 20 and 21 by ^{1}H NMR and GPC**

Polymer	$M_{n,theo}$ (g/mol)[a]	$M_{n,NMR}$ (g/mol)[b]	M_w/M_n GPC[c]
15	3243	3243	1.05
17	17360	17360	1.05
18	17083	17083	1.04
19	19485	19485	n. m.[d]
20	19147	19147	1.04
21	24577	23057	1.08

[a] Theoretical molecular weight. [b] Molecular weight calculated by NMR. [c] Molecular weight and PDI determined by PEG standard GPC. [d] Not measured
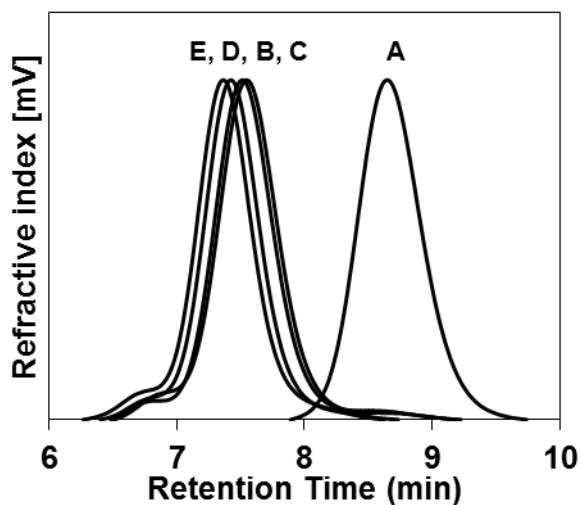
Figure 42. GPC elution profiles of 15 (A), 17 (B), 18 (C), 20 (D) and 21 (E) as measured by the change in refractive index (RI). The elution profiles have been normalized for comparison reasons.
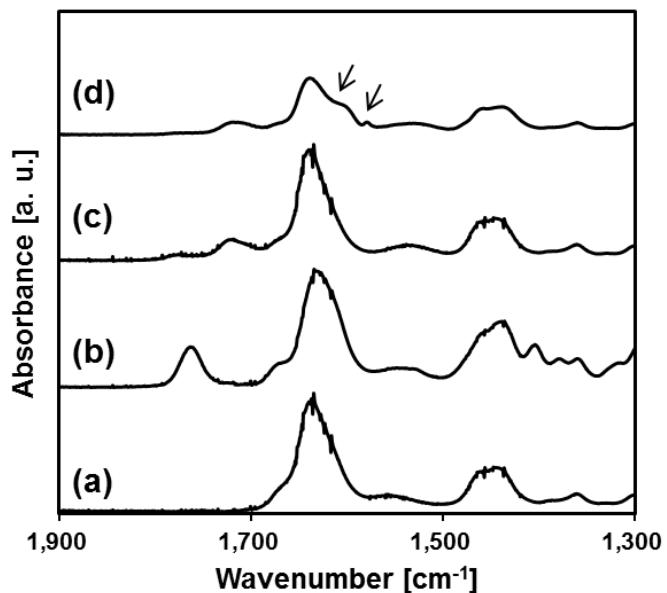

Figure 43. IR spectra of the different intermediates to prepare polymer 22. (a) 18, (b) 19, (c) 20 and (d) 21. The vibration bands of the furoxan ring are indicated by the arrows.

The alkyne-bearing polymer (**20**) was reacted with azide-containing

furoxan derivative (**3**) in *t*-BuOH/H$_2$O in the presence of a copper catalyst. The degree of functionalization was 72% as calculated from ^{1}H NMR using the integral values of the CH$_2$-furoxan protons at around 5.6 ppm and the CH of the PAM backbone at 2.6 ppm. In addition, the IR spectrum showed the shift of ν(C=O) stretching vibration from 1720 to 1715 cm^{-1} and the appearance of a shoulder and a weak absorption around 1600 cm^{-1} that can be assigned to the C=N stretching vibrations of the furoxan ring (**Figure 43**).

Preparation and characterization of the furoxan-bearing micelles

The furoxan-bearing micelles were prepared from block copolymer (**21**) by self-assembly in water. The micelles were about 50 nm in diameter with a narrow size distribution as determined by DLS (**Figure 44 A**). The spherical morphology of the micelles was confirmed by TEM and AFM (**Figure 44 B** and **C**). Furthermore, the micelles displayed a critical micelle concentration of 0.8 μM as determined by the contact angle measurement. [115] These results clearly show that the furoxan-bearing block of polymer (**21**) is hydrophobic enough to drive micellization.
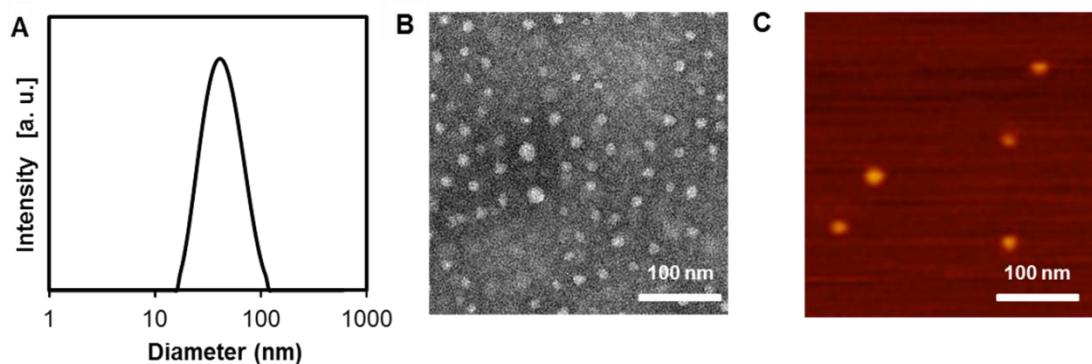
Figure 44. Structural characterization of the furoxan-bearing micelles. (A) Size distribution by DLS. (B) TEM image (negative staining with 0.5% Preyssler-type potassium phosphotungstate solution) (C) AFM image.

NO release from the micelles

It has been reported that NO release from furoxans can be induced by thiol-containing compounds such as cysteine. NO release from the micelles in the presence of cysteine at different concentrations was tested by Griess assay. As shown in **Figure 45A**, micelles release NO in the presence of cysteine and the amount of released NO increases with the increase of the cysteine concentration.

(22)
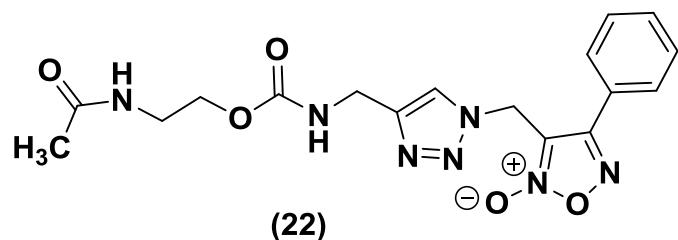
Scheme 6. Structure of model compound 22.
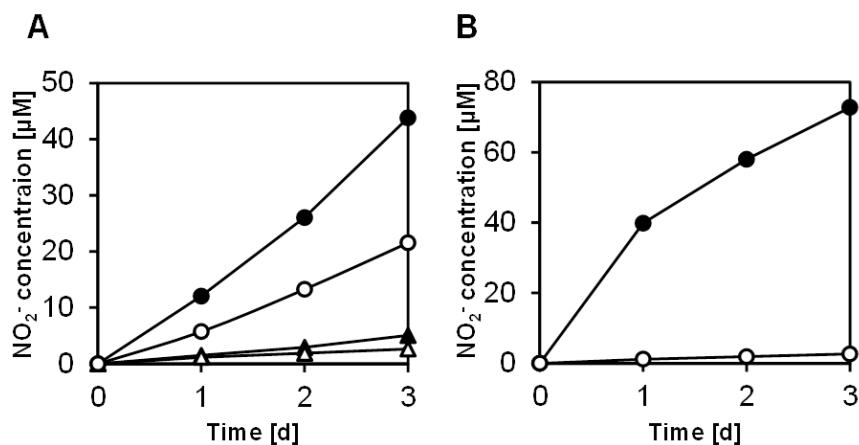
Figure 45. NO release from the micelles. (A) NO release from the furoxan-bearing micelles in the presence of cysteine at different concentrations. The micelles were reacted in 50 mM PBS (pH7.1) with 1.25 (open triangle), 2.5 (closed triangle), 12.5 (open circle) and 25 mM (closed circle) of cysteine (furoxan concentration: 250 μM) at 37°C. At the indicated time points, the nitrite (NO_2^-) concentration was measured by the Griess assay. (B) NO release from the micelles (open circles) and the model compound (22) (closed circles) in the presence of 1.25 mM cysteine. The micelles and compound (22) were reacted in 50 mM PBS (pH7.1) with 1.25 mM cysteine (furoxan concentration: 250 μM) at 37°C. At the indicated time points, the nitrite (NO_2^-) concentration was measured by the Griess assay.

The effect of the micelle structure on NO release was also studied. In this experiment, a furoxan derivative (**22, Scheme 6**) was prepared and used as a model compound by co-workers. As can be seen in **Figure 45B**, there is a dramatic difference in the amount of NO released between the micelles and compound (**22**) in the presence of 1.25 mM cysteine. Whereas the total amount of NO release after 3 d reached about 70 μM for compound (**22**), the micelles at the same furoxan concentration only released about 3 μM. This result may be due to the limited interaction

96

between cysteine and furoxan moieties located within the hydrophobic core of the micelles. To further support this hypothesis, NO release from the micelles was measured in the presence of Triton X-100, a surfactant that can disrupt the micelle structure. Upon the addition of Triton X-100, the micelles released 2.05 ± 0.08 times more NO compared to the micelles alone. This result clearly shows that the micelle structure is the critical factor affecting NO release.

Hydrolytic stability of the micelles

In chapter 2, the PEG-furoxan conjugate (**10** and **11**) slowly decomposed and lost its NO releasing ability in physiological buffer. Since the triazole group is known to behave as a leaving group, especially at basic condition, the formation of PEG-triazole (**12**) was suggested as a decomposition product. To evaluate the effect of micelle structure on decomposition of the furoxan moiety, the stability of the furoxan-bearing micelles and model compound (**22**) was investigated in PBS at 37°C. The furoxan decomposition was monitored by measuring UV/Vis spectroscopy since the previous work in chapter 2 had shown drastic spectral changes during decomposition of the PEG-furoxan conjugate. As can be seen in

Figure 46, model compound (**22**) underwent spectral changes over the course of 1 week, whereas the spectrum of the micelles was not affected significantly.
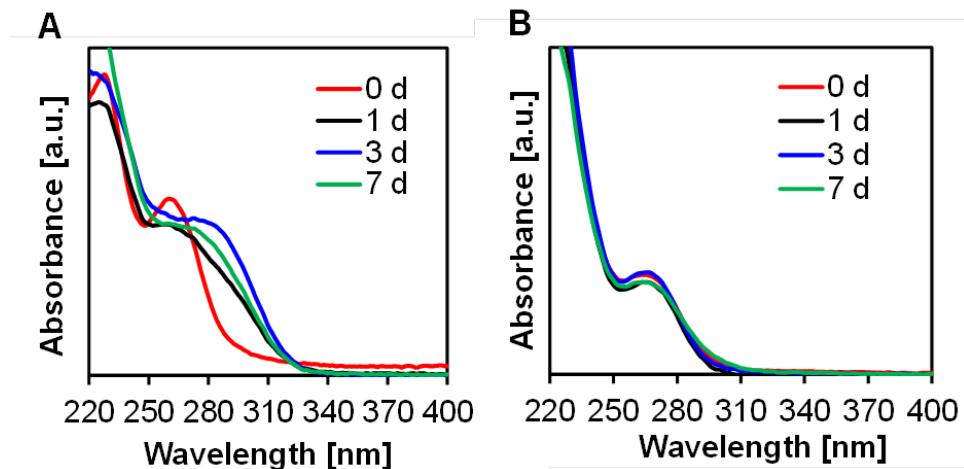
Figure 46. UV/Vis spectra of (A) model compound (22) and (B) furoxan-bearing micelles after incubation in PBS at 37°C. The model compound (22) and micelles (furoxan concentration: 250 μM) in 50 mM PBS (pH7.1) were kept at 37°C. The UV/Vis spectra were measured at the indicated time point.

The NO release ability of the micelles and model compound (**22**) were also evaluated after incubation for the indicated time in PBS at 37°C. As shown in **Figure 47**, the amount of released NO from the model compound (**22**) dropped to 40% after 1 d and to 0% after 1 week. In contrast, the NO releasing ability of the micelles was not affected significantly even after 1 week of incubation. This difference between the micelles and model compound can be explained by the hydrophobic core of the micelles

protecting the furoxan groups from hydrolysis.
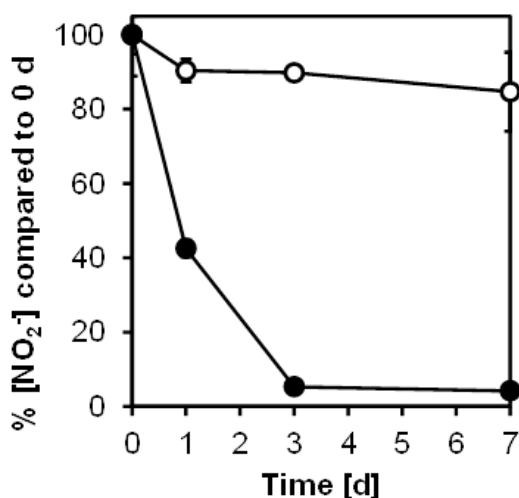
Figure 47. NO release form the furoxan-bearing micelles (open circle) and the model compound (closed circle) (22) after incubation in PBS at 37°C. The micelles and model compound (22) (furoxan concentration: 250 μM) were kept in 10 mM PBS (pH7.4) at 37°C. At the indicated time points, cysteine was added to a final concentration of 25 mM and kept for 3 d at 37°C. The NO$_2^-$ concentration was measured by the Griess assay.

Anti-proliferative effect of ibuprofen (IBU) and micelles in colon cancer cells

As mentioned in chapter 2, co-administration of NO donors and NSAIDs enhances the anti-proliferative effect of NSAIDs in cancer cells. PEG-furoxans have already exhibited the ability to enhance the anti-proliferative effect of ibuprofen in HT-29 colon cancer cells. In this chapter, the effect of the furoxan-bearing micelles on IBU-induced anti-

proliferative effect in human colon cancer HT-29 cells was also studied.
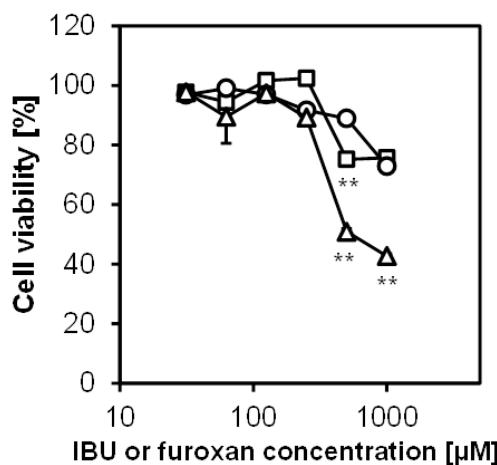
Figure 48. Anti-proliferative effect of IBU and furoxan-bearing micelles. HT-29 cells were cultured for 2 d in the presence of IBU (circle), micelles (square) and IBU with micells (triangle). Cell viability was assessed by the MTT assay. **p<0.01 versus IBU. *n*=3.**

As shown in **Figure 48**, IBU as well as the furoxan-bearing micelles alone showed a weak anti-proliferative effect in HT-29 cells (LD_{50}: >1000 μM). On the other hand, IBU with the furoxan-bearing micelles (IBU/furoxan molar ratio =1/1) showed significant reduction in the cell viability having a LD_{50} value of 500 μM. This result clearly shows that NO released from the micelles enhanced the anti-proliferative effect of IBU. Furthermore, in chapter 2, the LD_{50} for co-administration of IBU and the PEG-furoxan conjugate (**10**) was 960 μM which is much higher than that for IBU and micelles together. Therefore, the observed enhanced anti-

proliferative effect for the micelles may be due to the micelle structure that

enabled sustained release of NO.

Conclusion

The furoxan-bearing micelles were prepared from amphiphilic block copolymers consisting of a hydrophilic poly (*N*-acryloylmorpholine) (PAM) and a hydrophobic furoxan-bearing block. The micelle structure slowed down NO release in the presence of cysteine as well as hydrolytic decomposition of the furoxan moiety in physiological buffer solution. Furthermore, the micelles enhanced the IBU-induced anti-proliferative effect in human colon cancer HT-29 cells suggesting a potential use of the micelles in cancer chemotherapy.

Chapter 4

Copper removal from polymers by diethyldithiocarb-

amate complexation

Introduction

Copper-catalyzed reactions have become important synthetic tools for preparing polymeric materials with complex structures and functionality. Among the copper-catalyzed reactions used in polymer chemistry, the copper(I)-catalyzed 1,3-Huisgen cycloaddition reaction between an azide and alkyne to form the triazole has received increased interest in recent years. Another example is the copper-catalyzed atom transfer radical polymerization (ATRP) which has been used to prepare well-defined polymers.[117] However, one of the problems using these synthetic methodologies is the presence of trace amounts of copper in the final product. Apart from discoloring the polymer, the electrochemical properties of copper can also affect material performance. Furthermore, due to its toxicity, copper can be a problem for polymeric materials used in biomedical applications.[118] To avoid copper contamination problems, copper-free reactions have been developed including strain-promoted

azide-alkyne cycloaddition reactions[119] as well as metal-free ATRP using

an organic-based photoredox catalyst[120]. However, these methods have not

been widely used due to limited availability of alkyne substrates for the

copper-free 1,3-Huisgen cycloaddition reaction and requirement of a light

source for metal-free ATRP. Therefore, the majorities of studies use

copper-catalyzed reactions and remove the soluble copper catalysts after

polymer synthesis.

Several methods have been reported to remove copper catalysts

from polymeric materials. In general, alumina, silica, and clay are used to

adsorb copper catalyst from polymer solutions.[121] Another example is the

use of cation exchange resins which typically only work well for water-

soluble polymers.[122] Recently, an electrochemical method has also been

reported to remove copper from water-soluble polymer.[123] Despite the

many methods developed so far, there is no standard purification method

that is compatible with the wide range of the polymers typically prepared

by these copper-catalyzed reactions.

In chapter 2 and 3, I found that both PEG-furoxan conjugates and

furoxan micelles prepared by CuAAC contained trace amounts of copper

impurities after dialysis due to high affinity of copper towards the polymer, which seemed to affect NO release from the polymer.

In this chapter, development of new copper removal method for polymers which strongly bind to copper was described. A key component of this method is diethyldithiocarbamate (DTC) which serves as a ligand to dissociate copper from the polymer. It has been reported that DTC has a high affinity towards both Cu (I)[124] and Cu (II)[125]. The Cu (II) complex has been used for the photometric determination of copper.[126,127] In addition, this ligand has good solubility in many organic solvents. Therefore, it can be expected that the DTC complexation method could be applied for purification of polymers with different solubility parameters. After treated with DTC in *N,N*-dimethylformamide (DMF), the PEG-furoxan conjugates (**10**) and Pfuroxan-PAM (**21**) were isolated from the copper/DTC complex by size exclusion chromatography. This copper removal method was compared with other commonly used methods in terms of copper content and yield after purification. Furthermore, the NO release properties of the polymers after the different purification methods were also evaluated by the Griess assay.
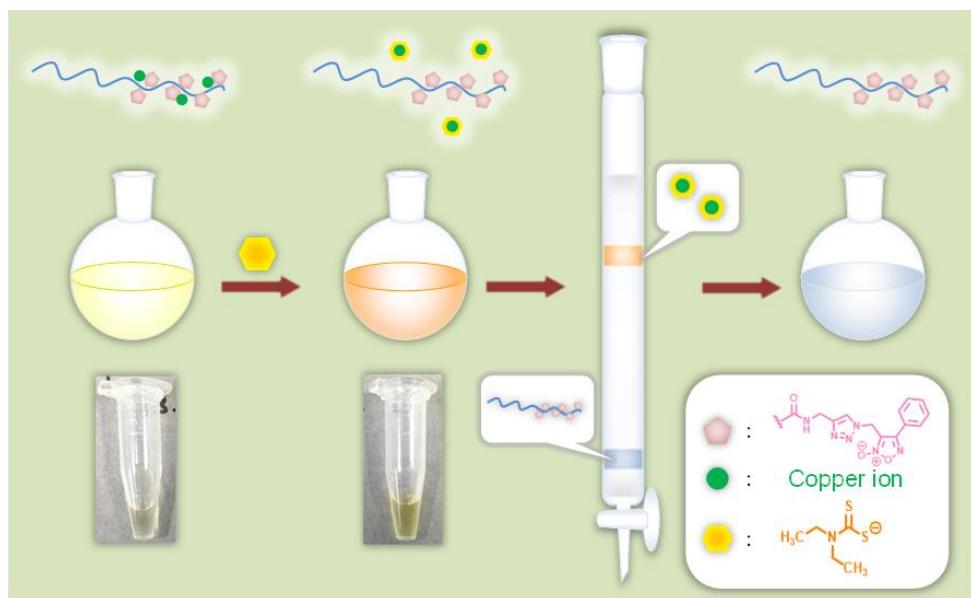
Figure 49. Copper removal from polymers by diethyldithiocarbamate complexation.

Experimental

Instrumentation

NMR spectroscopy. ^{1}H NMR spectra were measured with a Bruker DPX400 NMR spectrometer. A total of 32 scans were collected and the D1 was set to 10 s. Chemical shifts are referenced to the residual undeuterated NMR solvent signal at 7.26 ppm (CDCl$_3$).

UV/Vis spectroscopy. Absorbance and UV/Vis spectra were measured

on a Tecan infinite M200 in transparent polystyrene 96 well plates or a Thermo Scientific NanoDrop 2000c spectrophotometer.

Inductively coupled plasma atomic emission spectroscopy (ICP-AES). ICP-AES was done on a Shimadzu Sequential Plasma Emission Spectrometer ICPS-7510 instrument.

Materials

Diethylammonium diethyldithiocarbamate (DDTC), L-cysteine, sulfanilamide (SA), *N*-1-naphthylethylenediamine dihydrochloride (NED) and diethylenetriaminepentaacetic acid (DTPA), were purchased from Tokyo Chemical Industry (TCI) Japan. Tetrahydrofuran (THF) was from Nacalai Tesque. Super dehydrated dimethylformamide (DMF), copper (II) sulfate pentahydrate ($CuSO_4 \cdot 5H_2O$), Cu(I) bromide (CuBr), concentrated HCl (aq), sodium nitrite ($NaNO_2$), 5,5-dithio-bis-(2-nitrobenzoic acid (Ellman's reagent), ethylenediaminetetraacetic acid (EDTA), C-200 silica mesh size 75-150 μm (SiO_2) and the copper standard solution (1004 ppm) in 0.1 M HNO_3 (aq) were purchased from Wako Pure Chemical Industry (Japan). Activated neutral alumina   mesh size 58 Å (Al_2O_3) and Dowex Marathon MSC hydrogen form with a total exchange capacity of 4.5

mmol/g dry weight were purchased from Sigma-Aldrich (Japan). Sephadex LH-20 was from GE Healthcare (Japan). ICP grade nitric acid (HNO_3) was from Merck (Japan). TLC silica gel 60 F254 plates were from Merck (Japan). All chemicals were used as received except for THF which was distilled under atmospheric pressure prior to the copper removal experiments. Deuterated chloroform ($CDCl_3$) was from Cambridge Isotope Laboratories, Inc. (USA). Dialysis tubing (MWCO 2 kDa) was purchased from Spectrum Laboratories Inc. (Japan). 10X PBS was from Invitrogen.

Synthesis

The PEG-furoxan conjugate (**10**) and the block copolymer (**21**) were prepared by the copper catalyzed 1,3-Huisgen cycloaddition reaction between the azide-containing furoxan and the corresponding alkyne polymer as described previously (**Chapter 2** and **Chapter 3**). PEG-furoxan conjugate (**10**) and block copolymer (**21**) had a degree of functionalization of 81 and 72% respectively.

Preparation of the polymer samples for the copper removal experiments

To avoid sample inhomogeneity of the solid polymer that could affect the different copper removal methods, single stock solutions were prepared for (**10**) and (**21**). In case of P(furoxan)-PAM, 438 mg of (**21**) was dissolved in 8.8 mL DMF, added to 79 mL water and dialyzed against 2 L milliQ H_2O for 72 h with replacing the water 3 times. In case of PEG-furoxan (**10**) the stock solution was prepared by dissolving 238 mg in milliQ H_2O directly. To determine the polymer concentration of (**10**) and (**21**) a known volume was lyophilized and weighed. For the cation exchange resin the stock solutions were used directly. In case of the silica, alumina and DTC/Sephadex LH-20 a known volume of the stock solution was lyophilized and the solids used for the copper removal methods.

Copper removal using Al_2O_3 and SiO_2

Polymer solutions of (**10**) and (**21**) (300 μL, 100 mg/mL) in THF were added to a glass column (diameter 0.6 cm) containing 300 mg of adsorbent previously equilibrated with THF. The column was eluted with THF with and 5 fractions of 1 mL were collected. Fractions were spotted on TLC

silica plates by UV and those containing the polymer were combined. The solution was concentrated under reduced pressure to yield the polymer as a solid.

Copper removal using Dowex Marathon MSC cation exchange resin

8 mL of (**21**) (3.75 mg/mL) was mixed with 4 g of resin and 300 μL of (**10**) (100 mg/mL) was mixed with 1 g resin and shaken for 24 h at room temperature. The mixture was filtered and the resin washed with 1 mL water. After combining the washings with the filtrate the solution was lyophilized to yield the polymers as a solid.

Copper removal by the DTC complexation method

P(furoxan)-PAM (**21**) was dissolved at 80 mg/mL in DMF and 375 μL of this solution mixed with 375 μL of 42.4 mg/mL of DDTC in DMF resulting in a darkbrown solution. PEG-furoxan (**10**) (30 mg) was dissolved in 100 μL DMF. To the colorless solutions was added 100 μL of a DDTC solution in DMF (14.8 mg/mL) resulting in a brown solution. The brown solutions were loaded on a Sephadex LH-20 size exclusion column

(1.5 cm diameter x 26 cm height) previously washed with DMF and eluted with the same solvent. Collection of the fractions was done by gravity elution. A total of 25 fractions of 1.5 mL were collected in eppendorf tubes. Fractions were analyzed by measuring the UV/Vis spectra on a Nanodrop instrument. Fractions that contained (**10**) and (**21**) were pooled and concentrated under reduced pressure.

^{1}H NMR of the polymers after copper removal

The polymers after copper removal were dissolved in $CDCl_3$ and measured by ^{1}H NMR to confirm that no structural changes had taken place. The ^{1}H NMR samples were then concentrated under reduced pressure.

Recovery yields of the polymers after copper removal

The solids obtained after ^{1}H NMR were first dissolved in 0.5 mL DMF in case of P(furoxan)-PAM (**21**) and diluted with 1.5 mL H_2O. In case of PEG-furoxan (**10**) the polymer was dissolved in H_2O directly. The different solutions (8 total) were than dialyzed against 1 L milliQ for 48 h replacing the water 2 times. The polymer solutions were lyophilized to determine the recovery yields expressed as the weight$_{before}$/weight$_{after}$ ratio in %.

UV/Vis spectra mixtures DDTC and Cu (I) and Cu (II) salts

Solutions of Cu (I) and Cu (II) at 10 µM were prepared by dissolving $CuSO_4 \cdot 5H_2O$ (2.5 mg) and CuBr (1.4 mg) in 1 mL 100 mM DDTC/DMF solution. The brown solution was diluted to 10 µM Cu (I) or Cu (II) and 100 µM DDTC before measuring the UV/Vis spectra on a Nanodrop instrument.

Griess assay

To quantify NO release the concentration of NO_2^- was measured by the Griess assay. The samples were reacted with 50 µL of 2% (w/v) SA in 5% HCl (aq) for 5 min before adding 50 µL 0.1% (w/v) NED (aq).[91] On the same plate NO_2^- standard curves in the range 0-100 µM were prepared by mixing 50 µL of $NaNO_2$ (aq) solution at different concentrations with 50 µL 5 mM cysteine in 50 mM PBS with/without 5 mM DTPA. After 5 min the absorbance at 550 nm was measured and the NO_2^- concentrations calculated from a standard curve of NO_2^-. All samples were corrected for absorbance of polystyrene, reaction medium and the SA/NED reagent mix by subtraction the absorbance of wells containing water only.

Ellmann assay

Cysteine concentrations were measured by the Ellmann assay.[128] The samples (10 µL) were reacted with 10 µL Ellmann reagent (4.0 mg/mL) in Ellmann buffer (100 mM phosphate buffer containing 2.5 mM EDTA) for 10 min. The solution was then diluted with Ellmann buffer to 500 µL. A total volume of 300 µL was transferred to a transparent polystyrene plate. At the same time a standard of cysteine in the range 0 to 3.0 mM was prepared and measured in the same way. The absorbance at 412 nm was measured and the cysteine concentrations in the samples were calculated. All samples were corrected for absorbance of polystyrene, reaction medium and the Ellmann reagent by subtraction the absorbance of wells containing water only.

NO release from polymer (10) with/without DTPA

Solutions (60 µL) of PEG-furoxan (**10**) with a furoxan concentration of 500 µM were mixed with 60 µL 5.0 mM cysteine in 50 mM PBS pH7.1 with/without 5.0 mM DTPA. The tubes were placed in a bioshaker at 37°C and taken out at the indicated time point and frozen at -80°C. All samples were run in triplo. After collecting the last time point all samples were

thawed and 50 μL was transferred to a transparent well plate before adding the Griess reagents. The remaining 10 μL was used for measuring the cysteine concentrations.

Preparation of the polymer solutions for Griess assay

The solids obtained after determining polymer yield were dissolved in DMF and diluted with water in case of P(furoxan)-PAM (**21**). The solids for PEG-furoxan (**10**) were directly dissolved in water. The different solutions (8 in total) were than dialyzed against 1 L milliQ for 48 h replacing the water 2 times and used for the NO release experiments. The furoxan concentrations were calculated from the UV absorbance at 263 nm. The solutions were then diluted with milliQ water to a final furoxan concentration of 500 μM. This concentration was checked by measuring the UV/Vis spectra after dilution.

NO release from the polymer after copper removal

50 μL of polymer solution with a furoxan concentration (500 μM) in water was mixed with 50 μL 5 mM cysteine in 100 mM PBS in 600 μL eppendorf tubes (final pH: 7.1). To see the effect of DTPA on NO release

the 5 mM cysteine buffer contained 5 mM DTPA (final pH: 7.1). All samples were run in triplo. The tubes were placed in a bioshaker at 37°C and taken out after 1 d (PEG-furoxan (**10**)) or 3 d (P(furoxan)-PAM (**21**)). The samples (50 μL) were transferred to a transparent polystyrene plates and after adding the Griess reagents the absorbance was measured with a well plate reader the NO_2^- concentrations were calculated.

Preparation copper standard for ICP-AES measurements

The copper standard (1004 ppm) was diluted with 5% HNO_3 (aq) in glass vials to the different copper concentrations. The standard was linear in the range 0-50 ppm with a $R^2=1$.

Preparation of polymer samples for ICP-AES

After measuring NO release the stock solutions were lyophilized and the solids dried under vacuum at 60°C for 24 h. The polymers were dissolved in 65% HNO_3 at 40 mg/mL and heated at 90°C for 4 h. After cooling to room temperature the solutions were diluted for the ICP-AES measurements. The copper content is expressed as mg of copper/kg of polymer and given in ppm.

Results and Discussion

Copper quantification in the polymers

PEG with a terminal alkyne group and a block copolymer consisting of a PAM block and a alkyne group-bearing block were reacted with an azide-containing furoxan *via* the copper-catalyzed 1,3-Huisgen cycloaddition in a mixture of *tert*-butanol and water using the $CuSO_4$/sodium ascorbate catalytic system to yield PEG-furoxan conjugate (**10**) and P(furoxan)-PAM (**21**). After purification by dialysis against water, the copper content of the polymers was measured by inductively coupled atomic emission spectroscopy (ICP-AES). As shown in **Table 3**, both polymers contained copper and the amount of copper per triazole group was 3.6 times higher for (**21**). This higher level of copper contamination in (**21**) may be due to the presence of the neighboring triazole groups that link the furoxan groups to the polymer. There has been a report on polytriazoles as copper(I)-stabilizing ligands in the 1,3-Huisgen cycloaddition reaction,[129] suggesting that the high density of triazole groups on the polymer backbone is responsible for the high affinity for copper.

Table 3. Copper levels in the polymers after copper removal.

|	PEG-furoxan (**10**)		P(furoxan)-PAM (**21**)	
Purification method	Cu [ppm][a]	Removal [%][b]	Cu [ppm][a]	Removal [%][b]
No purification	23	n.a.[d]	374	n.a.[d]
Silica	< 3	100[c]	161	57
Alumina	< 3	100[c]	117	68
Cation exchange resin	< 3	100[c]	127	65
DTC/Sephadex LH-20	< 3	100[c]	14	96

[a] The amount of copper measured by ICP-AES and expressed as mg of copper/kg of polymer (ppm).

[b] The amount of copper removed as a percentage of that originally present in the polymer.

[c] Was below the detection limit and is therefore expressed as complete copper removal.

[d] Not applicable.

Copper removal from the polymers
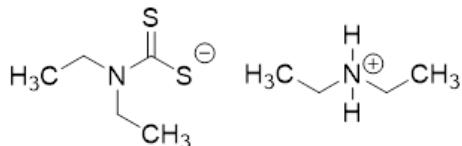
**Scheme 7. Structure of Diethylammonium diethyldithiocarbamate (DDTC)**

Since copper seemed to bind strongly to the polymers, it should be dissociated from the polymers before further purification to isolate the copper-free polymers. To dissociate copper form the polymers, DDTC compound was applied (**Scheme 7**) which has been shown to have high

affinity towards both Cu (I) and Cu (II). Whether DDTC can interact with copper in dimethylformamide (DMF) was tested in advanced, a solvent in which both PEG-furoxan conjugate (**10**) and P(furoxan)-PAM (**21**) are soluble. Upon mixing of DDTC with CuBr and $CuSO_4$, the UV/Vis spectra displayed an absorbance around 450 nm (**Figure 50**). Since this value is very similar to that reported for the bis(diethyldithiocarbamato)copper(II) $(Cu(DTC)_2)$ complex having an absorbance maximum at 437 nm in chloroform[125], it can be proclaimed that DTC interacts with Cu (II) and Cu (I) in DMF to form a complex displaying an absorbance maximum at 450 nm.
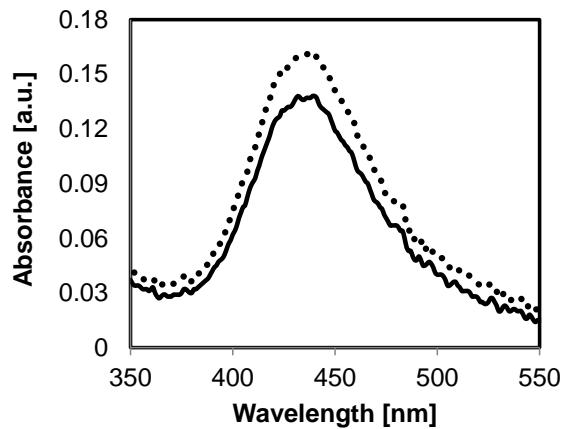

Figure 50. UV/Vis spectra in the region 350-550 nm showing the interaction between Cu (I) and Cu (II) with DDTC. Copper concentration: 10 μM and DDTC/Cu molar ratio: 10. Dotted line: $CuSO_4$, solid line: CuBr.

PEG-furoxan conjugate (**10**) was dissolved in DMF and mixed with a solution of DDTC in the same solvent. Upon mixing, the color of the PEG-furoxan conjugate solution changed from light yellow to brown (**Figure 51A**) and the UV/Vis spectrum displayed a new absorption maximum around 450 nm (**Figure 51B**) as was observed for DDTC and Cu (I)/Cu (II) solutions (**Figure 50**). The same absorbance at around 450 nm was also observed for a solution of P(furoxan)PAM (**21**) and DDTC in DMF (**Figure 52**). These results indicate that copper bound to the polymers also interacted with DDTC to form a Cu/DTC complex.
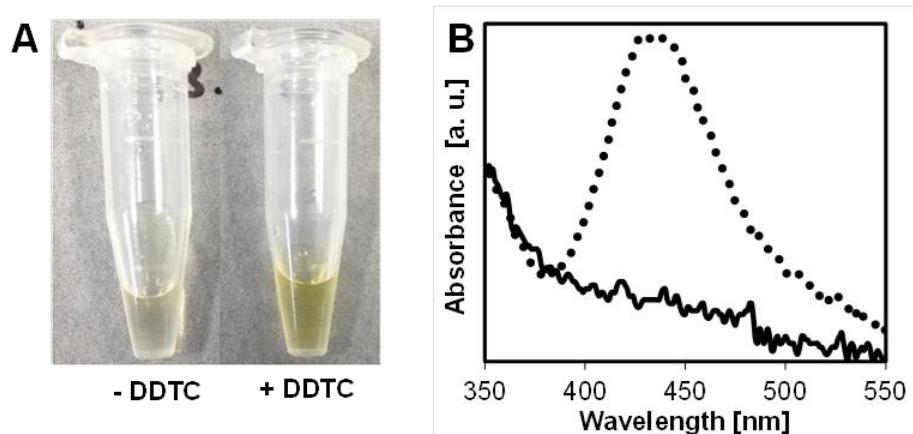

Figure 51. Complexation of DDTC with copper. (A) The presence of copper is readily detected by the change in color after mixing with DDTC. (B) UV/Vis spectra in the range 350-550 nm of PEG-furoxan (10) in the absence (solid line) and presence of DDTC (dotted line) in DMF.
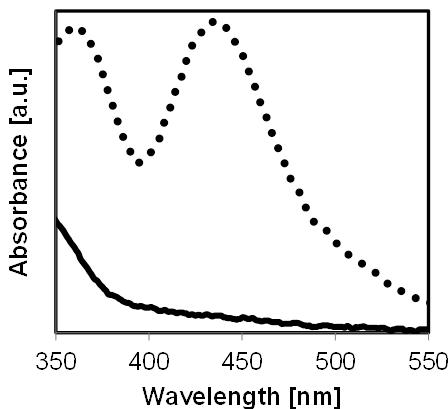
Figure 52. UV/Vis spectra in the range 350-550 nm of P(furoxan)-PAM (21) in the absence (solid line) or presence of DDTC (dotted line) in DMF. The absorbance band at 360 nm is due to free DDTC ligand.

To separate the polymer from the Cu/DTC complex, the mixture was purified by Sephadex LH-20 column chromatography using DMF as the eluent. In **Figure 53** a typical elution profile is shown. The fractions containing the polymers were collected and analyzed by ICP-AES. Compared to the original polymers, the amount of copper was below detection limit for the PEG-furoxan conjugate and reduced by 96% for the P(furoxan)-PAM. Furthermore, ^{1}H NMR did not show any obvious spectral changes before and after the DDTC treatment for both polymers showing that the polymers were not contaminated with DDTC.
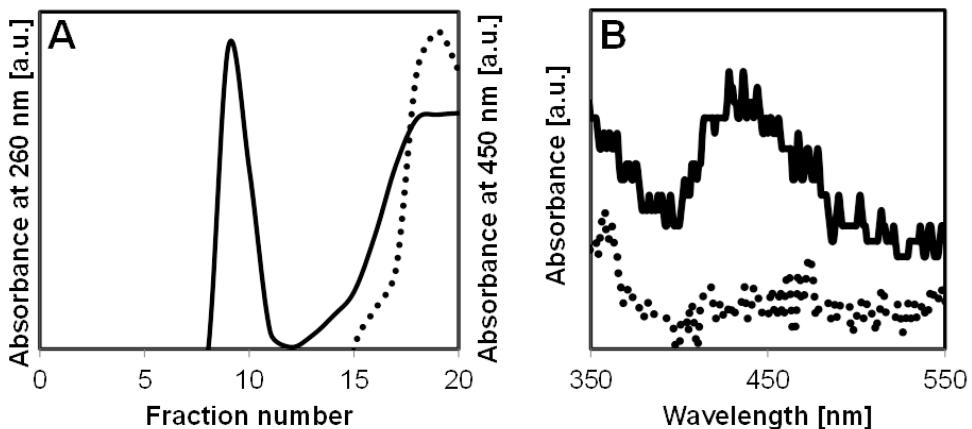
Figure 53. A typical elution profile showing that P(furoxan)-PAM (21) is well separated from the Cu/DTC complex. (A) Solid line: absorbance at 270 nm of the phenyl group of the polymer, dotted line: absorbance at 450 nm of the Cu/DTC complex. The increase in absorbance at 270 nm after fraction 12 is due to free DDTC which elutes faster than the Cu/DTC complex. (B) UV/Vis spectra of fraction 9 (dotted line) and fraction 19 (solid line).

Compared the DTC complexation method with the common methods using alumina, silica and cation exchange resin, for alumina and silica methods, the polymer solutions were passed over the adsorbents. For the cation exchange resin method, aqueous solutions of the PEG-furoxan conjugate (**10**) and the P(furoxan)-PAM (**21**) were mixed with the resin. As can be seen from **Table 3**, all methods efficiently removed copper from the PEG-furoxan conjugate (**10**) and the amount of copper was below the detection limit as determined by ICP-AES. On the other hand, the amount of copper in the P(furoxan)-PAM (**21**) was much higher after purification using the common methods compared to the DTC complexation method. Therefore, the DTC complexation method is especially useful for polymers

having high affinity towards copper.

Table 4. The recovery yields of the polymers after copper removal.

	Polymer yield [%][d]	
Purification method	PEG-furoxan (**10**)	P(furoxan)PAM (**21**)
Silica[a]	62	84
Alumina[a]	65	87
Cation exchange resin[b]	95	96
DDTC/Sephadex LH-20[c]	70	87

[a] The polymers were dissolved in THF and passed over silica or alumina.

[b] Polymer solutions in H_2O were left with cation exchange resin for 24 h.

[c] Polymer solutions in DMF were mixed with DDTC and eluted over Sephadex LH-20.

[d] Fractions containing polymer were concentrated under reduced pressure. After ^1H NMR analysis and solvent removal the polymer was dissolved in DMF and diluted with water in case of (**21**) or directly dissolved in water in case of (**10**) and dialyzed. After lyophilization the recovered polymer was quantified and expressed as the % of that original used. In case of the cation exchange resin the solution was lyophilized directly.

The recovery yields were determined after each copper removal treatment. As shown in **Table 4**, the DTC method resulted in comparable or slightly higher recovery yields for both polymers compared to the methods using the alumina and silica adsorbents. Higher polymer

recoveries were observed for the cation exchange resin method because the additional dialysis step, during which polymer loss mainly occurred in case of the other methods, was not required since the polymer solutions could be lyophilized directly after filtering off the resin.

Effect of the different copper removal methods on NO release

The effect of the different copper removal methods on NO release was evaluated by measuring the nitrite (NO_2^-) concentration, the oxidation product of NO, using the Griess assay. Polymers were reacted with 2.5 mM cysteine in PBS at 37°C for 1 d (**10**) or 3 d (**21**). Surprisingly, in the case of PEG-furoxan conjugate (**10**), the NO release experiment showed pronounced differences between the different copper removal methods although the amounts of remaining copper in all samples were below the detection limit of ICP-AES. The polymer purified by the DTC complexation method released the highest amount of NO and release from the polymers purified by the other methods was less than 25% (**Figure 54A**). This shows that even undetectable amounts of copper can have a significant effect on NO release. Interestingly when NO release was repeated in the presence of diethylenetriaminepentacetic acid (DTPA), a

chelating agent used for transition-metal ions like copper, NO release from the non-treated, silica, alumina and exchange resin-purified polymers was very similar but the DTC-purified polymer still showed highest release (**Figure 54A**). This result indicates that the remaining copper has a negative effect on NO release from the PEG-furoxan conjugate. Similar results were observed for the P(furoxan)-PAM (**21**) (**Figure 54B**). The NO release experiments clearly show that the DTC complexation method is powerful for removing copper from polymers that strongly bind to copper.
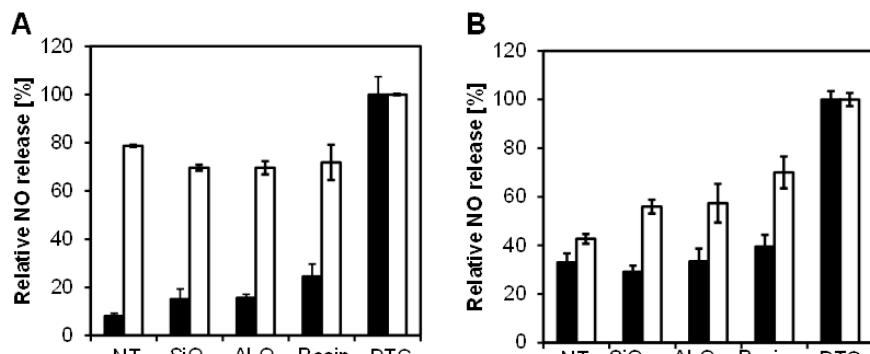
Figure 54. NO release from (A) (10) and (B) (21) before/after copper removal. The polymer solutions (furoxan concentration: 250 μM) were reacted with 2.5 mM cysteine in the absence (black columns) or presence of 2.5 mM DTPA (white columns) in PBS. After incubation at 37°C for 1 (10) or 3 d (21), the NO_2^- concentration was measured by the Griess assay. The results are expressed as the percentage of NO release from the polymer treated with DTC. NT: Non-treatment, SiO_2: silica, Al_2O_3: alumina, Resin: cation exchange resin, DTC: DTC complexation and size exclusion chromatography.

Effect of copper on cysteine concentration

Since it is known that NO release from furoxans is induced by the reaction with thiol-containing compounds like cysteine, it is unclear whether copper remaining in the polymers was affecting the cysteine concentration by catalyzing oxidation of cysteine to cystine.[130] Therefore the thiol concentrations was measured by Ellmann assay. As shown in **Figure 55A**, the cysteine concentration dropped from 2.5 to 0 mM already after 1 d in the presence of the PEG-furoxan conjugate (**10**) from which copper had not been removed. Since 10 times excess amount of cysteine was added compared to furoxan, this cysteine depletion seemed not to be only due to reaction with the furoxan. Interestingly, the decrease in cysteine concentration also correlated with the leveling off of the amount of NO released (**Figure 55B**). The hypothesis is that copper was responsible for the catalytic oxidation of cysteine to cystine by oxygen from the air. Therefore NO release experiment was repeated in the presence of DTPA. As can be seen from **Figure 55A**, the cysteine concentrations after 1-3 d of incubation were much higher compared to that in the absence of DTPA pointing to the involvement of copper ions. Also, the amount of NO released was increased in the presence of DTPA (**Figure 55B**).
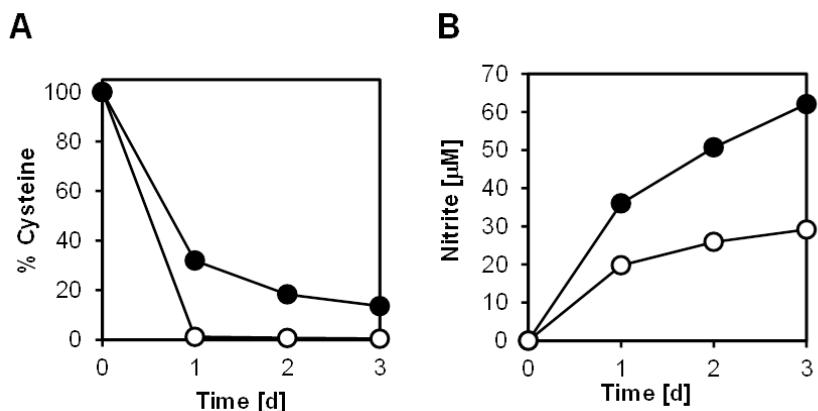
Figure 55. Effect of copper on the cysteine concentration and NO release from the PEG-furoxan (10). (A) Cysteine concentration as a function of time as determined by Ellmann assay. (B) NO release as a function of time as determined by the Griess assay. Non-treated PEG-furoxan (250 µM) was mixed with cysteine (2.5 mM) in PBS at 37°C in the presence (closed circle) or absence (open circle) of DTPA

To get proof for the copper-catalyzed oxidation reaction of cysteine to cystine by the copper contained in the polymers, I repeated the experiment at a higher cysteine concentration (25 mM). Both PEG-furoxan and PAM-PF with a furoxan concentration of 250 µM were reacted with 25 mM cysteine in PBS at 37°C. The reaction volume was 500 µM in order to collect a sufficient amount of solid for mass spectrometry (MS) analysis. After 3 d, a precipitate was observed for both PEG-furoxan conjugate (**10**) and P(furoxan)-PAM (**21**) solutions. This precipitate seems to be cystine which has a low aqueous solubility compared to cysteine. The formation of cystine was further supported by MALDI-TOF-MS which showed the cystine + H adduct at 241.04 (calculated value 241.03).

Conclusion

An efficient protocol for the removal of copper impurities from polymers by complexation with diethyldithiocarbamate (DTC) in dimethylformamide (DMF) followed by size exclusion chromatography using Sephadex LH-20 was developed. Both Cu (I) and Cu (II) can interact with DDTC forming a complex that absorbs at around 450 nm. The color change can be readily detected by eye and is also an easy test in the laboratory to confirm the presence of copper using UV/Vis spectroscopy. Furthermore, an advantage of the present method is that it is readily scalable to purify larger amounts of polymers by increasing the Sephadex LH-20 bed volume and amendable for automation using commercial available fraction collectors. Since DMF is a good solvent for a wide range of polymers, it is expected that this purification method could be an alternative for copper removal from polymers where current methods fail.

Chapter 5

NO-releasing micelles from amphiphilic furoxan-bearing block polymers by modification of poly(*N*-acryloylmorpholine)-*b*-poly(pentafluorophenyl acrylate) with amine-containing furoxan

Introduction

NO-releasing polymeric micelles were prepared form the furoxan-bearing block copolymer in chapter 3. However, the block copolymer prepared by using the copper-catalyzed reaction contained trace amount of copper impurities, which affects the NO release property and may induce a toxic side effect. Therefore, in this chapter, I aim to prepare the furoxan-bearing block copolymer without using the copper-catalyzed reaction.

Polymers containing pentafluophenyl ester groups are known to undergo the substitution reaction with various nucleophiles such as amines. Several reports appeared concerning preparation of functional (co)polymers *via* post-polymerization modification of this activated ester group to obtain polymeric materials with a complex structure and

functionality.[131-135] For example, Giles B. H. Chua et al. prepared a library of (meth)acrylamido (co)polymers by reacting poly(pentafluorophenyl (meth)acrylate) with α-amino, ω-methoxy functionalized di(ethylene glycol), and tri(ethylene glycol), as well as PEGs with different molecular weights. The resulting copolymers showed an improved solubility in water/alcohols and did not show toxicity in MRC5 fibroblast cells.[134] Wilaiporn G. reported that poly(pentafluorophenyl acrylate)-*b*-poly(*N*-isopropyl acrylamide) was synthesized by RAFT polymerization and the light-responsive moieties were introduced to this polymer by post-polymerization modification to yield amphiphilic block copolymers which self-assemble to form micelles in water.[131]

Inspired by these works, in this chapter, poly(*N*- acryloylmorpholine)-*b*-poly(pentafluorophenyl acrylate) diblock copolymer was prepared by RAFT polymerization and modified with amine-containing furoxan. The micelles were prepared by self-assembly in water and the morphology of the micelles was characterized by DLS and AFM. Furthermore, the NO release property of the micelles in the presence of cysteine was evaluated.

Experimental

Instrumentation

NMR spectroscopy. ^{1}H NMR and were measured with a Bruker DPX400 NMR spectrometer. For ^{1}H NMR spectra a total of 32 scans were collected and the D1 was set to 10 s for the polymers and 1 s for the low molecular weight compounds. Chemical shifts are referenced to the residual undeuterated NMR solvent signal at 2.50 (d_6-DMSO), 7.26 ppm (CDCl$_3$).

UV/Vis spectroscopy. The absorbance was measured with a Tecan infinite M200 plate reader in transparent polystyrene 96 well plates and UV/Vis spectra were recorded on either a HITACHI U-2810 spectrophotometer.

Attenuated total reflection infrared spectroscopy (ATR-IR). Attenuated total reflection infrared (ATR-IR) spectra were obtained on a Thermo Scientific Nicolet iS5 equipped with an iD5 universal ATR sampling accessory

Gel permeation chromatography (GPC). Elution charts were

collected with a Tosoh GPC-8020 instrument equipped with refractive index (RI) detector. The KD-803 (Shodex) column was operated at 50 ℃ while flowing 100 mM LiCl in DMF at 1.0 mL/min. Polydispersity index (M_w/M_n) values were calculated based on the elution time of polyethylene glycol standard polymers.

Dynamic light scattering (DLS). Hydrodynamic diameter was measurements with an Otsuka ELSZ machine using 4.5 mL disposable polystyrene cuvettes. Micelle solutions were filtered through 0.45 µm syringe filter prior to analysis. The mean diameter (Z-average) and polydispersity index (PDI=μ_2/Γ^2) were calculated by the cumulant method.

Atomic force microscopy (AFM). The micelle solution in water was dropped onto a fresh mica surface and then dried by blowing off the solution by a hand blower. Images were acquired on a Seiko Instruments SPA400 in dynamic force mode (DFM) using a Si probe with Al coating (SI-DF20, Seiko).

Materials

Pentafluorophenol, pentafluorophenyl acrylate, 4-

acryloylmorpholine (AM), *N*-1-naphthylethylenediamine dihydrochloride (NED) and sulfanilamide (SA) were purchased from Tokyo Chemical Industry Co., Ltd. (Osaka, Japan). 2,2'-Azobis(isobutyronitrile) (AIBN), super dehydrated dimethylformamide (DMF), diethyl ether (Et$_2$O), sodium nitrite (NaNO$_2$), propionyl chloride, sodium hydrogen sulfate (NaHSO$_4$), sodium sulfate (Na$_2$SO$_4$), 36% (w/v) hydrochloric acid (HCl (aq)), silica (SiO$_2$) were purchased from Wako (Japan). 2-(((dodecylthio)carbonthioyl)thio)-2- methylpropanoic acid, aluminum oxide (Al$_2$O$_3$) and lauroyl peroxide (LPO) were purchased from Sigma-Aldrich (Japan). Hexane, ethyl acetate (EtOAc), triethylamine (Et$_3$N), calcium hydride (CaH$_2$), 1,4-dioxane, dichloromethane (CH$_2$Cl$_2$), methanol (MeOH), and molecular sieves 3A were purchased from Nacalai Tesque (Kyoto, Japan). Deuterated solvents for ^{1}H NMR (CDCl$_3$ and d_6-DMSO) were from Cambridge Isotope Laboratories, Inc. (USA). Dialysis tubing (MWCO 2 kDa) was purchased from Spectrum Laboratories (USA). 10× PBS was from Invitrogen. AIBN was recrystallized from MeOH. pentafluorophenyl acrylate and 4-acryloylmorpholine were passed through an Al$_2$O$_3$ column to remove inhibitor. Et$_3$N was distilled over ninhydrin and CaH$_2$ and kept over

molecular sieves. 1,4-dioxane was distilled over CaH_2 under Ar and kept from light. All other chemicals were used as received.

Synthesis

PAM-CTA (23). 4-Acryloylmorpholine (AM, **16**) was polymerized using AIBN as the initiator and 2-(((dodecylthio)carbonthioyl)thio)-2-methylpropanoic acid (**14**) as the chain transfer agent (CTA). The [AM]/[CTA]/[AIBN] molar ratio was 70/1/0.2 and the monomer concentration was 1 M. 1.4117 g (10 mmol) of (**16**), 52.1 mg (0.14 mmol) of (**14**) and 4.69 mg (0.03 mmol) of AIBN were dissolved in 10 mL of DMF. The solution was degassed with argon by five freeze-thaw cycles and heated at 60°C for 24 h. The polymerization was stopped by placing the Schlenk tube in liquid nitrogen. After thawing, the solution was transferred to a dialysis tube (MWCO 2 kDa) and dialyzed against 3 L water for 24 h with replacing the water every 12 h. The solution was lyophilized to yield 1.3597 mg (93%) of a yellow solid. ^{1}H NMR (CDCl$_3$) δ =3.90-3.20 (bs, N-CH$_2$-CH$_2$-O PAM and CH$_2$-S-C(S) CTA), 3.53-3.05 (bs, NH-C$\underline{H}_2$ PHEA and CH$_2$-S-C(S) CTA), 2.68 (bs, C$\underline{H}$-CH$_2$ PAM), 2.30-1.00 (m, C$\underline{H}_2$-CH PAM and 10 x CH$_2$ CTA), 1.06 and 1.03 (bs, C(CH$_3$)$_2$

CTA), 0.86 (bs, 3H, CH$_2$-C$\underline{H}_3$ CTA). The ^{1}H NMR spectrum is shown in **Figure 56**. The degree of polymerization was 70 as calculated from the integral ratio of the -CH- signal at 2.68 ppm of PAM and the -CH$_3$ signal at 0.80 ppm of the CTA.

PAM-**PPA**-**CTA** (**25**). Pentafluorophenyl acrylate (**PA**, **24**) was polymerized using AIBN as the initiator and (**23**) as the macro CTA. The [PA]/[macro CTA]/[AIBN] molar ratio was 25/1/0.2 and the monomer concentration was 1 M. 119.1 mg (0.5 mmol) of (**24**), 205.5 mg (0.02 mmol) of (**23**) and 0.66 mg (0.004 mmol) of AIBN were dissolved in 1,4-dioxane to final volume of 0.5 mL. The solution was degassed with argon by five freeze-thaw cycles and heated at 70°C for 24 h. The polymerization was stopped by placing the Schlenk tube in liquid nitrogen. After thawing, the solution was precipitate in Et$_2$O (150 mL). The precipitate was filtered off, washed with Et$_2$O (2 × 10 mL) and dried under reduced pressure to yield 324.3 mg (99%) of a pale yellow solid. ^{1}H NMR (CDCl$_3$) δ = 3.95-3.20 (m, N-CH$_2$-CH$_2$-O PAM and CH$_2$-S-C(S) CTA), 3.20-2.70 (m, C$\underline{H}$-CH$_2$ PPA) 2.68 (bs, C$\underline{H}$-CH$_2$ PAM and CH$_2$-CH PPA), 2.30-1.00 (m, CH$_2$-CH PPA, C$\underline{H}_2$-CH PAM and 10 x CH$_2$ CTA, C(CH$_3$)$_2$ CTA), 0.87 (bs, 3H, CH$_2$-C$\underline{H}_3$ CTA). The ^{1}H NMR spectrum is shown in **Figure 57**. The degree of

polymerization was calculated from the molar ratio of PAM/PPA units using the integral values of the signals at 3.95-3.20 and 3.20-2.70 ppm and the number of AM monomer units in the macro CTA (**23**). The degree of polymerization for PPA was 21.

PAM-PPA (26). 204.2 mg (0.013 mmol) of (**25**), 129.3 mg (0.79 mmol) of AIBN were dissolved in 2 mL DMF. The solution was degassed with argon by five freeze-thaw cycles and heated at 80°C for 24 h. The reaction was stopped by placing the Schlenk tube in liquid nitrogen. After thawing, the solution was added drop wise to Et_2O (150 mL). The precipitate was filtered off, washed with Et_2O (2 × 10 mL) and dried under reduced pressure to yield 173.8 mg (86%) of a white powder. ^{1}H NMR (CDCl$_3$) δ = 3.95-3.20 (m, N-CH$_2$-CH$_2$-O PAM), 3.20-2.70 (m, C$\underline{H}$-CH$_2$ PPA) 2.68 (bs, C$\underline{H}$-CH$_2$ PAM and CH$_2$-CH PPA), 2.30-1.00 (m, CH$_2$-CH PPA, C$\underline{H}_2$-CH PAM, C(CH$_3$)$_2$ CTA and C(CH$_3$)$_2$ AIBN). The spectrum is shown in **Figure 58**. The UV/Vis spectrum of the polymer in DMF showed the 80% decrease of the absorption at 310 nm compare with untreated **PPA-PAM-CTA (25)** confirming the end group removal (**Figure 61**).

PAM-P(furoxan) (27). 50 mg (3.1 μmol) of (**26**), 54 mg (6.2 μmol, 2 eq.)

of the free amine of (5) and 48.9 μL (12.4 μmol, 4 eq.) of Et₃N were dissolved in 1 mL DMF. The flask was evacuated/purged with argon (3×) and the mixture was stirred for 48 h. The mixture was acidified with 1 mL of 1 M NaHSO₄ (aq.) and the solution transferred to a dialysis tube (MWCO 2 kDa) and dialyzed against 1 L of water for 48 h by replacing water every 12 h. The solution was lyophilized to yield 48 mg (90%) of a white solid. ^{1}H NMR (CDCl₃) δ = 7.95-7.30 (m, CH triazole, $5 \times$ CH$_{aromat}$), 5.55 (bs, CH₂-furoxan), 4.48 (bs, CH₂-NH-C(O)), 3.95-3.20 (bs, N-CH₂-CH₂-O PAM), 2.64 (bs, CH-CH₂ PAM), 2.35-0.83 (m, CH₂-CH PPA, CH₂-CH PAM, C(CH₃)₂ CTA and C(CH₃)₂ AIBN). The spectrum is shown in **Figure 59**. The degree of modification was calculated to be 95% by comparing the integral ratio of the CH₂-furoxan protons and the N-CH₂-CH₂-O signal of PAM.

Perfluorophenyl propionate (28). 250.7 mg (1.36 mmol) of pentafluorophenol dissolved in 5 mL of CH₂Cl₂ and cooled to 0 °C in an ice bath. To the solution propionyl chloride 130.8 μL (1.50 mmol, 1.1 eq.) in 5 mL of CH₂Cl₂ was added dropwise. The flask was evacuated/purged with argon (3 ×) and the mixture was stirred in the dark. After TLC indicated the disappearance of pentafluophenol, reaction mixture was

136

concentrated under reduced pressure. The residue was purified by SiO_2 column chromatography (EtOAc/hexane = 1 : 4, R_f = 0.8) to yield 301.1 mg (1.25 mmol, 92%) of a colorless oil. ^{1}H NMR (CDCl$_3$) δ = 2.70 (q, 2H, CH$_2$), 1.30 (m, 3H, CH$_3$). The ^{1}H NMR spectrum is shown in **Figure 60**. FT-IR: ν (cm^{-1}) 1790 (C=O) and 1516 (C-F). The IR spectrum is shown in **Figure 63**. HRMS (m/z, M, ESI-TOF-MS, EI$^+$): calculated for $C_9H_7N_5O_2$ 240. 0210, found 240. 0210.

Micelle formation

The furoxan-bearing block copolymer (**27**) was dissolved in DMF (20 mg/mL) and 250 μL of this solution was added drop wise to 2250 μL of milliQ water under stirring. After 30 min, the clear solution was transferred to a dialysis tube (MWCO 2kDa) and dialyzed against 1 L water overnight.

Griess assay

The concentration of NO_2^- was measured by the Griess assay in transparent 96 well polystyrene plates. The samples were reacted with 50 μL of 2% (w/v) SA in 5% HCl (aq) for 5 min before adding 50 μL 0.1% (w/v) NED (aq)[91] After 5 min, the absorbance at 550 nm was measured and

the NO_2^- concentrations calculated from standard curves of 0-100 μM NO_2^- in either 1.25, 2.5, 12.5 or 25 mM cysteine, 50 mM PBS (pH7.1). All samples were corrected for absorbance of polystyrene, reaction medium and the SA/NED reagent mix by subtraction the absorbance of wells containing water only.

NO release from the micelles and model compound (5)

Amine-containing furoxan (**5**) was selected as model compound for this experiment. Aqueous solutions of micelles and the model compound at 500 μM (50 μL) were mixed with either 50 μL of 2.5, 5.0, 25 or 50 mM cysteine in 100 mM PBS containing in 600 μL Eppendorf tubes. For each sample 3 tubes were prepared in parallel put at 37°C and each day samples was taken out and frozen at -80 °C. After the last time point was collected all samples were thawed and transfer to a 96 well plate. The NO_2^- levels were determined with the Griess assay. NO_2^- standard curves were prepared on the same plate by mixing 50 μL of $NaNO_2$ solution at different concentrations with 50 μL of 2.5, 5.0, 25 or 50 mM cysteine in 100 mM PBS. The concentration of furoxan in the micelle and model compound solutions was calculated, after diluting 1:1 with DMF, from the absorbance

at 263 nm and a standard curve of the model compound in H_2O/DMF 1:1. The furoxan concentration of the aqueous micelle solution was in good agreement with that estimated from the initial polymer weight, degree of functionalization and the final volume of the solution after dialysis.

Results and Discussion

Synthesis of furoxan-bearing block copolymer (27)
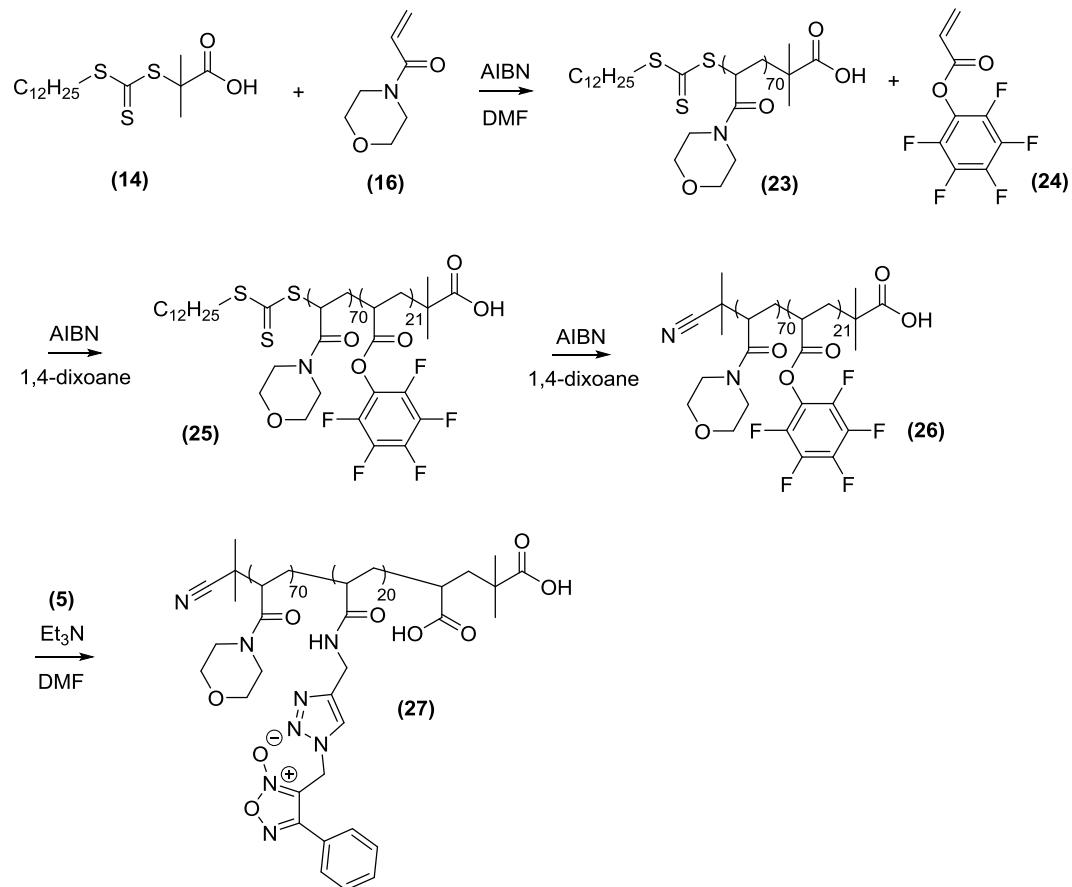
Scheme 8. Synthesis scheme to PAM-P(furoxan) (27).

The synthetic scheme to prepare amphiphilic block copolymer consisting of a hydrophilic poly (*N*-acryloylmorpholine) block and hydrophobic furoxan-bearing block is shown in **Scheme 8**. Pentafluorophenyl propionate was also synthesized to monitor the polymerization of pentafluophenyl acrylate as shown in **Scheme 9**.

Hydrophilic PAM-CTA (**23**) was first synthesized by the RAFT polymerization technique. This polymer was further copolymerized with pentafluophenyl acrylate to yield a diblock copolymer (**26**) which was modified with amine-containing furoxan (**5**) to obtain an amphiphilic block copolymer (**27**). The products were characterized by ^{1}H NMR and IR. (**Figure 56-60** and **62**)
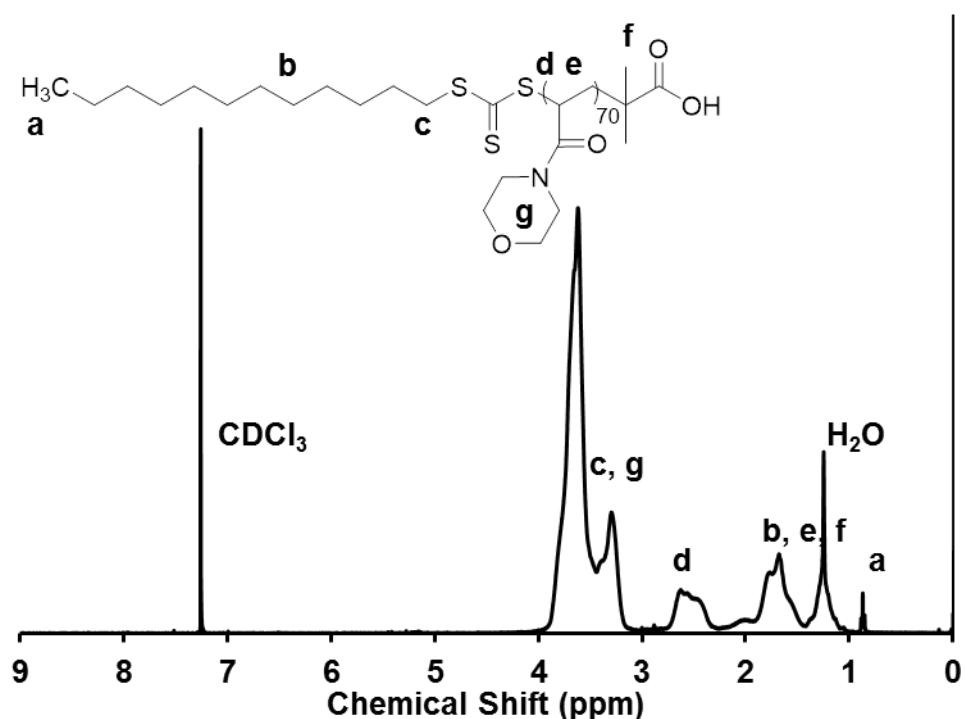
Figure 56. ^{1}H NMR spectrum of PAM-CTA (23) in CDCl₃.
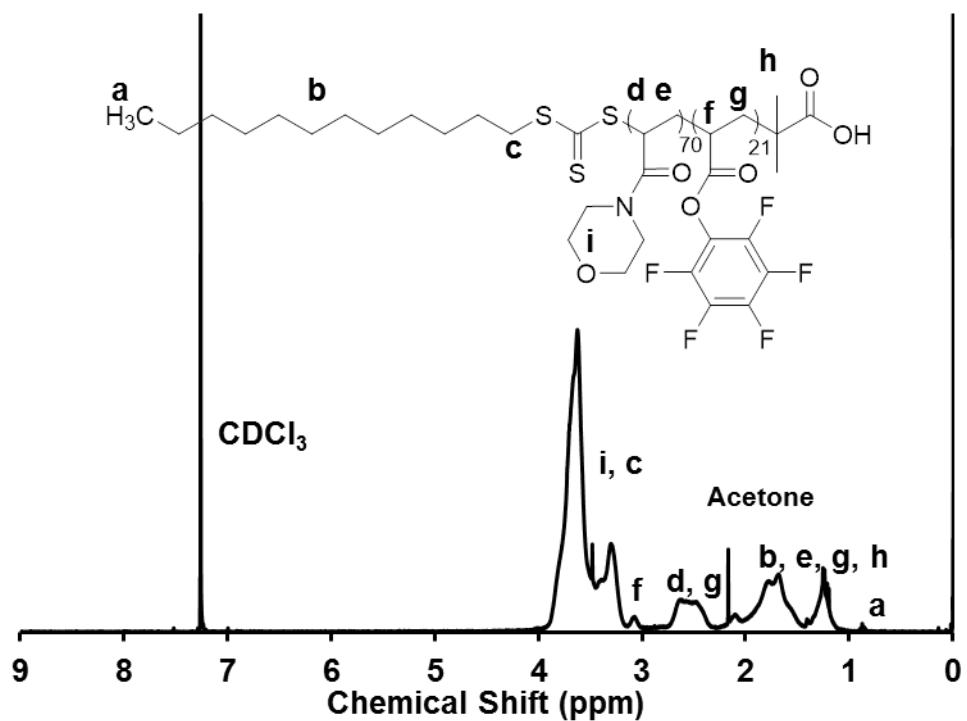
Figure 57. ^{1}H NMR spectrum of PAM-PPA-CTA (25) in CDCl$_3$,
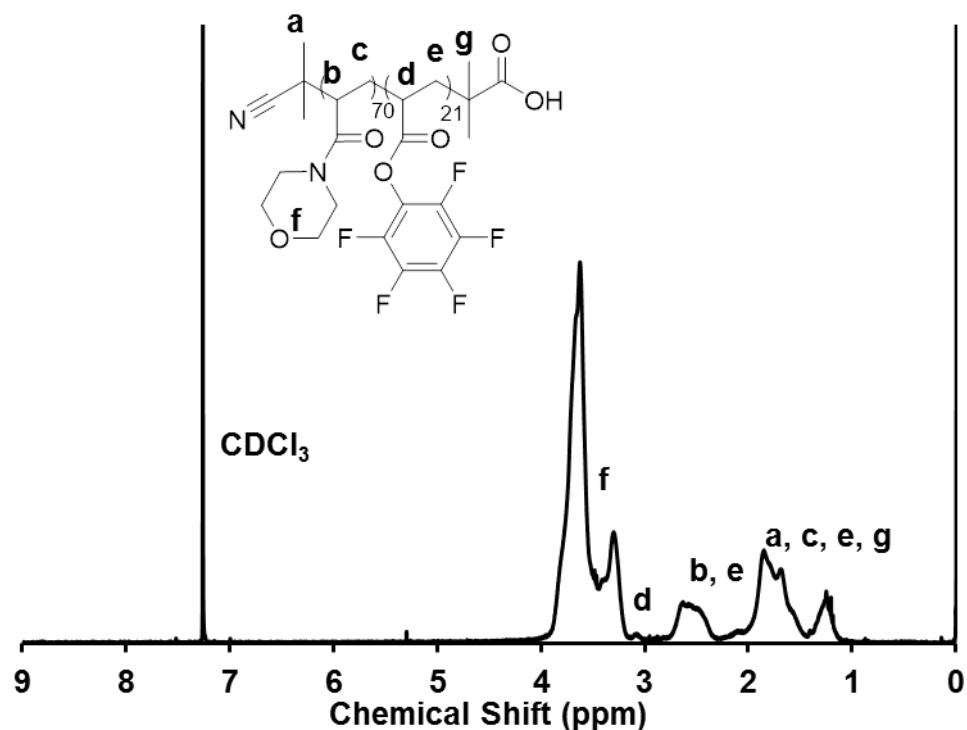
**Figure 58. ^{1}H NMR spectrum of PAM-PPA (26) in CDCl$_3$.**
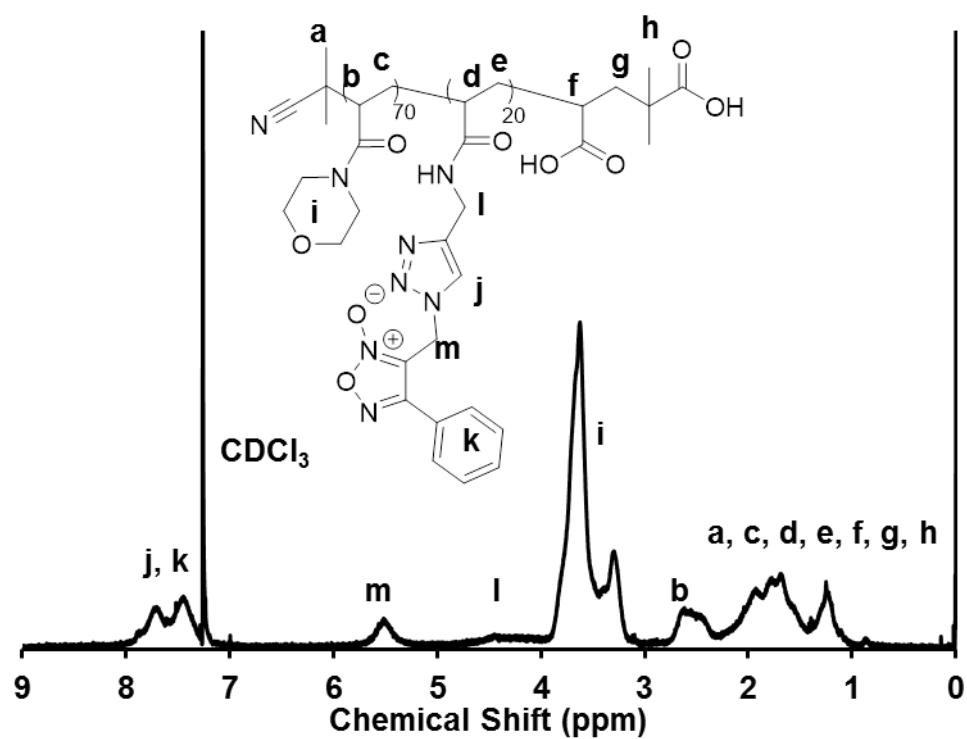
Figure 59. ^{1}H NMR spectrum of PAM-P(furoxan) (27) in CDCl$_3$.
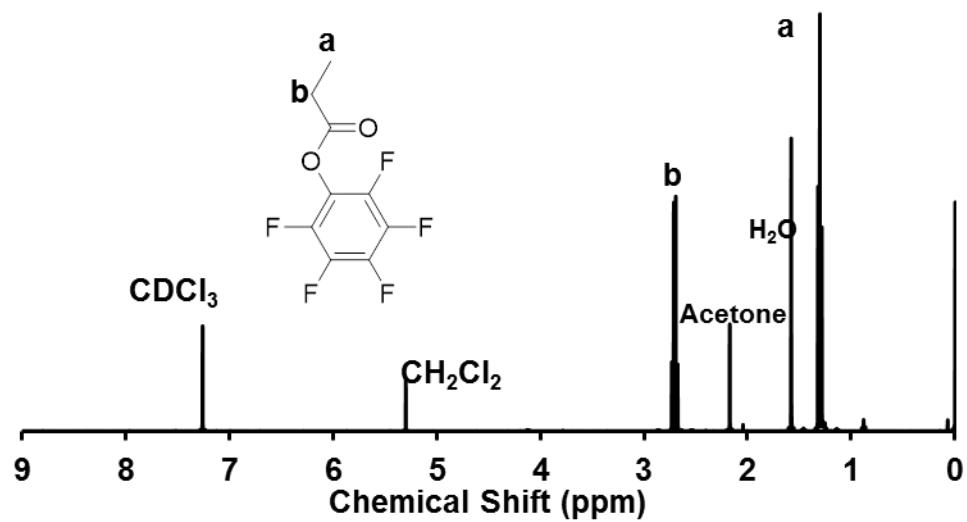

Figure 60. ^{1}H NMR spectrum of perfluorophenyl propionate (28) in CDCl$_3$.

4-Acryloylmorpholine (AM, **16**) was polymerized in DMF at 60°C for 24 h using 2-((((dodecylthio)carbonthioyl)thio)-2-methylpropanoic acid (**14**) as the chain transfer agent (CTA) and AIBN as the radical initiator. The AM concentration was 1 M and the AM/CTA/AIBN ratio was 70/1/0.2. The average degree of polymerization (DP) of the resulting polymer (PAM-CTA, **23**) was 70 according to ^{1}H NMR. The polymerization was carried out under the different conditions as listed in **Table 5**. When the reaction was carried out in DMF at 60 °C with the molar ration of CTA to AIBN of 5 for 24 h, the full conversion of the monomer was observed. Gel permeation chromatography (GPC) showed a unimodal peak with a low polydispersity index (M_w/M_n) of 1.08 showing a narrow size distribution (**Table 6**, **Figure 62**). Then, by using (**23**) as a macro-CTA, pentafluophenyl acrylate (**PA**, **24**) was polymerized to yield PAM-PPA-CTA diblock copolymer (**25**). The polymerization proceeded quantitatively when the PA concentration was 1 M and the PA/PAM/AIBN ratio was 25/1/0.3. The block copolymer had a unimodal size distribution as confirmed by GPC (**Table 6** and **Figure 62**).

Table 5. RAFT polymerization of 4-acryloylmorpholine (AM) with under different conditions.

Solvent[a]	[CTA]/[AIBN][b]	Temp. °C	M_n^c,NMR	M_n/M_w^d,GPC
DMSO	5/1	60	13210	1.06
DMF	5/1	60	14481	1.07
1,4-Dioxane	5/1	60	5305	1.16
1,4-Dioxane	5/1	70	10810	1.13
1,4-Dioxane	3/1	70	14340	1.12

[a] Monomer concentration 1M. Molar ration [Monomer]/[CTA]=100, reaction time is 24 h. [b] Molar ration. [c]. Molecular weight (g/mol) were calculated from the integral ratio of the CH-CH2 signals of PAM and the CH2-CH3 group of the CTA. [d]. Molecular weight (g/mol) and M_n/M_w were determined by GPC using a PEG standard with DMF elution rate is 1 mL/min.
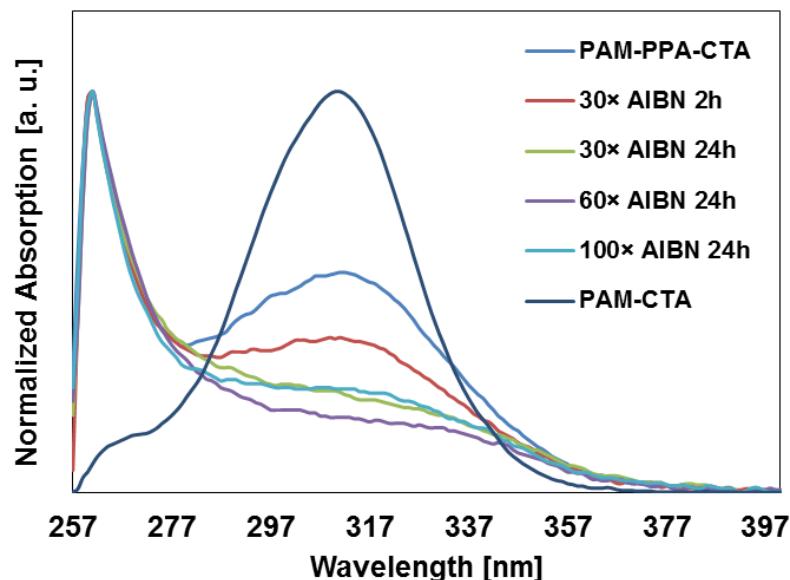
Figure 61. CTA removal of PAM-PPA-CTA (25) by reacting against excess amount of AIBN.

To avoid the formation of thiols by transamidation with the thiocarbonate group during post-modification of the block copolymer, that could potentially lead to dimerization, the CTA end-group was removed by reacting excess amount AIBN at 80 °C. The absorption at 310 nm due to the trithiocarbonates group was decreased with the increase of the AIBN to CTA ratio as observed by UV-Vis spectroscopy (**Figure 61**). This result indicated that the optimal CTA removal efficiency was reacted when 60 times molar equivalents of AIBN to CTA group were applied. Furthermore, GPC showed that no dimerization took place during the end group removal (**Figure 62**).
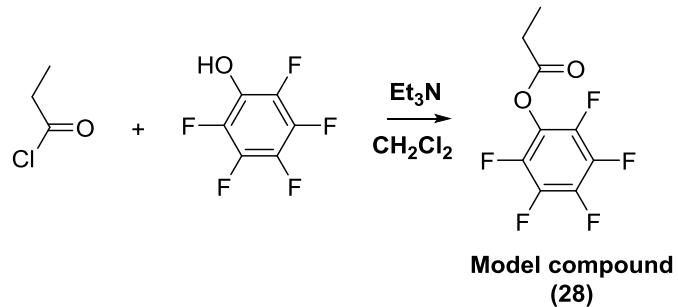
Scheme 9. Synthesis scheme to perfluorophenyl propionate (28).

The successful copolymerization of pentafluophenyl acrylate block was confirmed by ^{1}H NMR showing peaks due to the C$\underline{H}$-CH$_2$ at 3.20-2.70 ppm. Further confirmation was obtained by IR (**Figure 63**). Compound (**28**) was synthesized with the similar pentafluophenyl moiety with PPA block

used to monitor the reaction processing by IR. After copolymerization, the bands at around 1516 cm^{-1} that can be assigned to the ν(C-F) stretching vibration and 1790 cm^{-1} due to the ν(C=O) vibration were observed in the IR spectrum of PAM-PPA (**26**).

Table 6. Molecular Weights of 23, 25, 26 and 27 by ^{1}H NMR and GPC.

| Polymer	$M_{n\ theor}$[a]	$M_{n\ NMR}$[b]	$M_w/M_{n\ GPC}$[c]
23	10247	10247	1.08
25	15245	15245	1.12
26	15024	15024	1.12
27	16678	16678	1.22

a. Theoretical molecular weight (g/mol).
b. Molecular weight (M_n) (g/mol) as calculated by ^{1}H NMR.
c. Molecular weight (M_n) (g/mol) and M_w/M_n were determined by GPC using a PEG standard.
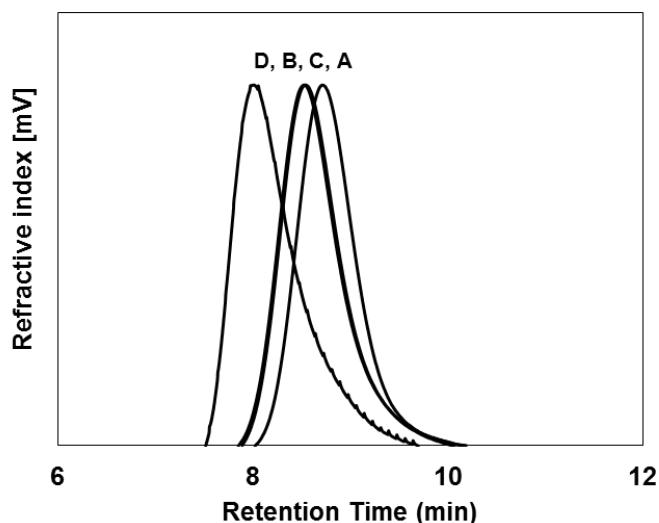
Figure 62. GPC elution profiles of 23 (A), 25 (B), 26 (C), and 27 (D) as measured by the change in refractive index (RI). The elution profiles have been normalized for comparison reasons.
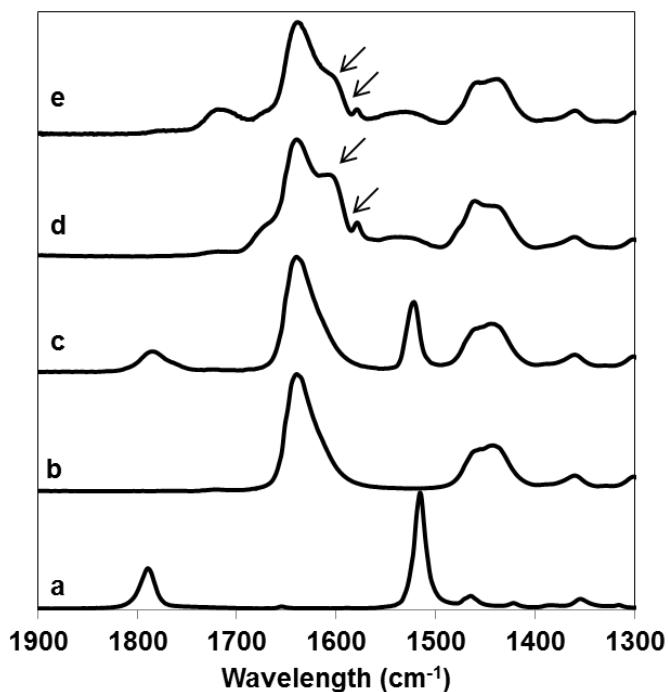
Figure 63. IR spectra of the different intermediates to prepare polymer 27. (a) 28, (b) 23, (c) 26, (d) 27 and (21). The vibration bands of the furoxan ring are indicated by the arrows.

PAM-PPA (**26**) was then conjugated with amine-containing furoxan (**5**) to yield the furoxan-bearing polymer (**27**). The shift of the ν(C=O) stretching band at 1790 cm^{-1} shifted to 1678 cm^{-1} in the IR spectrum and the absence of ν(C-F) as well as C$\underline{H}$-CH$_2$ (PPA) peaks in the ^{1}H NMR spectrum showed successful conjugation of amine-containing furoxan (**5**). The degree of functionalization was 95% as calculated from ^{1}H NMR using the integral values of the CH$_2$-furoxan protons at around 5.6 ppm and the N-CH$_2$-CH$_2$-O of the PAM at 3.9-3.2 ppm. In addition, the IR spectrum showed the shift of ν(C=O) stretching vibration from 1720 to 1715 cm^{-1}

and the appearance of a shoulder and a weak absorption around 1600 cm^{-1} that can be assigned to the C=N stretching vibrations of the furoxan ring which was agreed with the IR spectrum of furoxan bearing copolymer (**21**, **Figure 63**).

Preparation and characterization of the furoxan-bearing micelles

The furoxan-bearing micelles were prepared from block copolymer (**27**) by self-assembly in water. The micelles were about 130 nm in diameter with a narrow size distribution (polydispersity index: 0.123) as determined by DLS (**Figure 64 A**). The spherical morphology of the micelles was confirmed by AFM (**Figure 64B** and **C**).
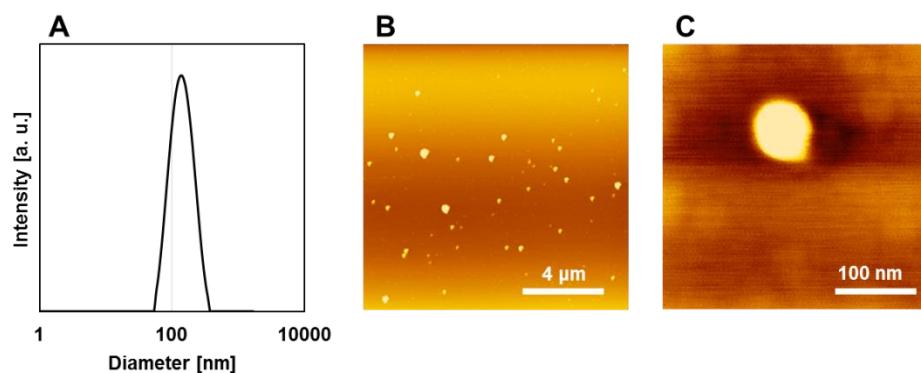


Figure 64. Structural characterization of the Furoxan micelles. (A) Size distribution by DLS. (B) (C) AFM image.

NO release from the micelles

NO release from the micelles in the presence of cysteine at different

concentrations was tested by Griess assay. As shown in **Figure 65A**, micelles release NO in the presence of cysteine and the amount of released NO increases with the increase of the cysteine concentration.
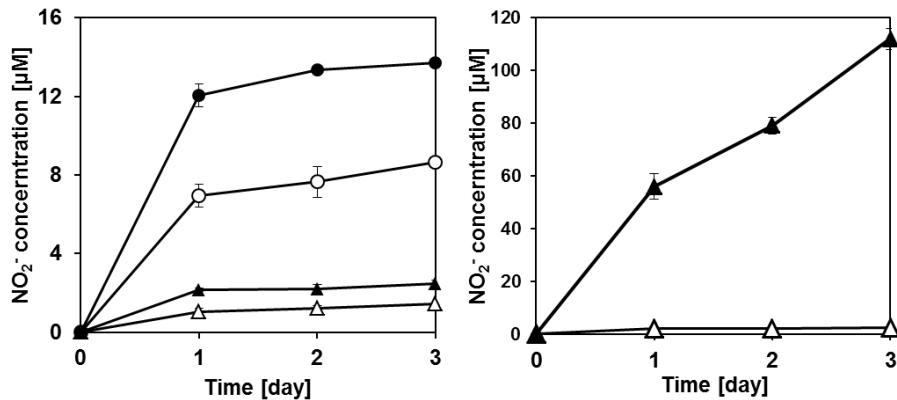
Figure 65. NO release from the micelles. (A) NO release from the furoxan-bearing micelles in the presence of cysteine at different concentrations. The micelles were reacted in 50 mM PBS (pH7.1) with 1.25 (open triangle), 2.5 (closed triangle), 12.5 (open circle) and 25 mM (closed circle) of cysteine (furoxan concentration: 250 μM) at 37°C. At the indicated time points, the nitrite (NO$_2^-$) concentration was measured by the Griess assay. (B) NO release from the micelles (open triangle) and the model compound (5) (closed triangle) in the presence of 2.5 mM cysteine. The micelles and compound (5) were reacted in 50 mM PBS (pH7.1) with 2.5 mM cysteine (furoxan concentration: 250 μM) at 37°C. At the indicated time points, the nitrite (NO$_2^-$) concentration was measured by the Griess assay.

The effect of the micelle structure on NO release was also studied. In this experiment, amine-containing furoxan derivative (**5**) was used as a model compound. As can be seen in **Figure 65B**, there is a significant difference in the amount of NO released between the micelles and

compound (**5**) in the presence of 2.5 mM cysteine. Whereas the total amount of NO release after 3 d reached about 112 µM for amine-containing furoxan (**5**), the micelles at the same furoxan concentration only released about 3 µM. This result may be due to the limited interaction between cysteine and furoxan moieties located within the hydrophobic core of the micelles which is in good agreement with the results obtained in chapter 3.

Conclusion

poly(*N*-acryloylmorpholine)-*b*-poly(pentafluorophenyl acrylate) diblock copolymer was synthesized using the RAFT polymerization of pentafluorophenyl acrylate (PPA) block, which was further modified with amine-containing furoxan to yield the furoxan-bearing block copolymer. The resulting amphiphilic diblock copolymer self-assembled in water to form micelles with the diameter of 130 nm. The micelles released NO in the presence of cysteine.

Chapter 6

Concluding Remarks

In this doctoral thesis, preparation and potential therapeutic application of polymeric furoxan-bearing nanomedicine including PEG-furoxan conjugates and furoxan-bearing micelles were described. Furthermore, an efficient protocol for the removal of copper impurities from polymers during nanomedicine synthesis was developed. The results obtained in each chapter were summarized below.

In chapter 2, "**Nitric oxide-releasing polymeric furoxan conjugates**" was described. Azide- and amine-containing furoxan derivatives with different substituents, phenyl and nitrophenyl, were prepared and conjugated to PEG to yield PEG-furoxan conjugates. The conjugates released NO in the presence of cysteine, glutathione and the cell lysate of murine macrophages, but not FBS, suggesting that NO release from conjugates can be induced by the intracellular components. Both the furoxans and PEG–furoxan conjugates were decomposed in PBS to yield products with no or less NO release activity. However, the PEG-furoxan conjugates slowed down the decomposition of furoxan and released a

significantly higher amount of NO compared to the corresponding furoxans after 24 h of incubation in PBS. Furthermore, the PEG conjugate of furoxan with a phenyl substituent released NO and enhanced the anti-proliferative effect of ibuprofen in HT-29 colon cancer cells.

In chapter 3, "**Furoxan-bearing micelles for nitric oxide delivery**" was described. The furoxan-bearing micelles with a diameter around 50 nm were prepared from amphiphilic block copolymers consisting of a hydrophilic poly(*N*-acryloylmorpholine) and a hydrophobic furoxan-bearing block. The micelle structure slowed down NO release in the presence of cysteine as well as hydrolytic decomposition of the furoxan moiety in physiological buffer solution. Furthermore, the micelles enhanced the IBU-induced anti-proliferative effect in human colon cancer HT-29 cells suggesting a potential use of the micelles in cancer chemotherapy.

In chapter 4, "**Copper removal from polymers by diethyldithiocarbamate complexation**" was described. An efficient protocol was developed for the removal of copper impurities from polymers by complexation with DTC in DMF followed by size exclusion

chromatography using Sephadex LH-20. An advantage of the present method is that it is readily scalable to purify larger amounts of polymers by increasing the column size and amendable for automation using commercial available fraction collectors. Furthermore, since DMF is a good solvent for a wide range of polymers, it is expected that this purification method could be an alternative for copper removal from polymers where current methods fail.

In chapter 5, "**NO-releasing micelles from amphiphilic furoxan-bearing block polymers by modification of poly(N-acryloylmorpholine)-*b*-poly(pentafluorophenyl acrylate) with amine-containing furoxan**" was described. Furoxan-bearing block copolymer was prepared from pentafluorophenyl ester group-bearing block copolymer by reacting with amine-containing furoxan derivative. The polymer formed micelles with diameter of 130 nm by self-assembly in water. The micelles released NO in the presence of cysteine and showed much slower NO release compared to the amine-containing furoxan derivative.

In conclusion, furoxans nanomedicines include micellar type and

PEG-conjugate type was first time developed in this thesis and released NO in the presence of cysteine. The micelle structure of furoxan bearing micelles slowed down the cysteine induced NO release as well as hydrolytic decomposition of the furoxan moiety of PEG-furoxan conjugates and low molecular weight furoxans in physiological buffer solution. Furthermore, furoxan nanomedicines in this thesis enhanced the IBU-induced anti-proliferative effect in human colon cancer HT-29 cells suggesting a potential use of the micelles in cancer chemotherapy. However, for a clinic use of furoxan nanomedicines, one limitation is lack of targeting delivery property. In such case, furoxan micelles are able to be modified with targeting peptides or antibodies reach a targeting delivery application of NO. All in all, there still have abundant of challenges and promising opportunities to all researchers in the further study of development and application of polymeric furoxan nanomedicines.

References

(1) Bredt. D; Snyder. S *Annu. Rev. Biochem.* **1994**, *63*, 175.

(2) Williams, S. B.; Cusco, J. A.; Roddy, M.-A.; Johnstone, M. T.; Creager, M. A. *J. Am. Coll. Cardiol.* **1996**, *27*, 567.

(3) Aram, G.; Potter, J. J.; Liu, X.; Torbenson, M. S.; Mezey, E. *Hepatology* **2008**, *47*, 2051.

(4) Cannon, R. O. *Clin. Chem.* **1998**, *44*, 1809.

(5) Smith, K. J.; Lassmann, H. *Lancet Neurol.* **2002**, *1*, 232.

(6) Simone, M. *Curr. Cancer Drug Targets* **2009**, *9*, 214.

(7) Gasco, A.; Fruttero, R.; Sorba, G.; Stilo, A. D.; Calvino, R. *Pure Appl. Chem.* **2004**, *76*, 9.

(8) Wang, P. G.; Xian, M.; Tang, X.; Wu, X.; Wen, Z.; Cai, T.; Janczuk, A. J. *Chem. Rev.* **2002**, *102*, 1091.

(9) Culotta, E.; Koshland, D. *Science* **1992**, *258*, 1862.

(10) Radomski, M. W.; Palmer, R. M.; Moncada, S. *Proc. Nati. Acad. Sci. U. S. A.* **1990**, *87*, 5193.

(11) Stuehr, D. J. *Annu. Rev. Pharmacol. Toxicol.* **1997**, *37*, 339.

(12) Moncada, S.; Palmer, R. M.; Higgs, E. A. *Pharm. Rev.* **1991**, *43*, 109.

(13) Lundberg, J. O.; Weitzberg, E.; Gladwin, M. T. *Nat. Rev. Drug Discov.* **2008**, *7*, 156.

(14) Björnekan, H.; Petersson, J.; Phillipson, M.; Weitzberg, E.; Holm, L.; Lundberg, J. O. *J. Clin. Invest.* **2004**, *113*, 106.

(15) Änggård, E. *Lancet* **1994**, *343*, 1199.

(16) Calabrese, V.; Mancuso, C.; Calvani, M.; Rizzarelli, E.; Butterfield, D. A.; Stella, A. M. *Nat. Revi. Neurosci.* **2007**, *8*, 766.

(17) Nathan, C. F.; Hibbs, J. B. *Curr. Opin. Immunol.* **1991**, *3*, 65.

(18) Pinsky, D. J.; Naka, Y.; Chowdhury, N. C.; Liao, H.; Oz, M. C.; Michler, R. E.; Kubaszewski, E.; Malinski, T.; Stern, D. M. *Proc. Nati. Acad. Sci. U. S. A.* **1994**, *91*, 12086.

(19) Schulz, R.; Kelm, M.; Heusch, G. *Cardiovasc. Res.* **2004**, *61*, 402.

(20) Barbato, J. E.; Tzeng, E. *J. Vasc. Surg.* **2004**, *40*, 187.

(21) Sergio, H.; Sapna, C.; Benjamin, B. *Int. J. Oncol.* **1992**, *33*, 909.

(22) Bonavida, B.; Baritaki, S.; Huerta-Yepez, S.; Vega, M. I.; Chatterjee, D.; Yeung, K. *Nitric Oxide* **2008**, *19*, 152.

(23) Mocellin, S.; Bronte, V.; Nitti, D. *Med. Res. Rev.* **2007**, *27*, 317.

(24) Rigas, B.; Kashfi, K. *Trends Mol. Med.* **2004**, *10*, 324.

(25) Kelm, M. *Biochim. Biophys. Acta* **1999**, *1411*, 273.

(26) Gasco, A.; Schoenafinger, K. In *Nitric Oxide Donors*; Wiley-VCH Verlag GmbH & Co. KGaA: 2005, p 131.

(27) Boiani, M.; Cerecetto, H.; González, M. *Il Farmaco* **2004**, *59*, 405.

(28) Faigle, J. W.; Blattner, H.; Glatt, H.; Kriemler, H.-P.; Mory, H.; Storni, A.; Winkler, T.; Oesch, F. *Helv. Chim. Acta* **1987**, *70*, 1296.

(29) Ghosh, P. B.; Whitehouse, M. W. *J. Med. Chem.* **1968**, *11*, 305.

(30) Bertinaria, M.; Stilo, A. D.; Tosco, P.; Sorba, G.; Poli, E.; Pozzoli, C.; Coruzzi,

G.; Fruttero, R.; Gasco, A. *Bioorg. Med. Chem.* **2003**, *11*, 1197.

(31) Cerecetto, H.; Di Maio, R.; González, M.; Risso, M.; Saenz, P.; Seoane, G.; Denicola, A.; Peluffo, G.; Quijano, C.; Olea-Azar, C. *J. Med. Chem.* **1999**, *42*, 1941.

(32) Bolt, A. G.; Sleigh, M. J. *Biochem. Pharmacol.* **1974**, *23*, 1969.

(33) Feelisch, M.; Schönafingeri, K.; Noack, H. *Biochem. Pharmacol.* **1992**, *44*, 1149.

(34) Bohn, H.; Brendel, J.; Martorana, P. A.; Schönafinger, K. *Br. J. Pharmacrol.* **1995**, *114*, 1605.

(35) Schiefer, I. T.; VandeVrede, L.; Fa, M.; Arancio, O.; Thatcher, G. R. *J. Med. Chem.* **2012**, *55*, 3076.

(36) Turnbull, C. M.; Cena, C.; Fruttero, R.; Gasco, A.; Rossi, A. G.; Megson, I. L. *Br. J. Pharmacrol.* **2006**, *148*, 517.

(37) Mott, B. T.; Cheng, K. C.; Guha, R.; Kommer, V. P.; Williams, D. L.; Vermeire, J. J.; Cappello, M.; Simeonov, A.; Inglese, J. *Medchemcomm* **2012**, *3*, 1505.

(38) Lolli, M. L.; Cena, C.; Medana, C.; Lazzarato, L.; Morini, G.; Coruzzi, G.; Manarini, S.; Fruttero, R.; Gasco, A. *J. Med. Chem.* **2001**, *44*, 3463.

(39) Cena, C.; Lolli, M. L.; Lazzarato, L.; Guaita, E.; Morini, G.; Coruzzi, G.; McElroy, S. P.; Megson, I. L.; Fruttero, R.; Gasco, A. *J. Med. Chem.* **2003**, *46*, 747.

(40) Ferioli, R.; Folco, G. C.; Ferretti, C.; Gasco, A. M.; Medana, C.; Fruttero, R.; Civelli, M.; Gasco, A. *Br. J. Pharmacrol.* **1995**, *114*, 816.

(41) Moghimi, S. M.; Hunter, A. C.; Murray, J. C. *FASEB J.* **2005**, *19*, 311.

(42) Peer, D.; Karp, J. M.; Hong, S.; Farokhzad, O. C.; Margalit, R.; Langer, R. *Nat. Nanotechnol.* **2007**, *2*, 751.

(43) Park, J. H.; Lee, S.; Kim, J.-H.; Park, K.; Kim, K.; Kwon, I. C. *Prog. Polym.*

Sci. **2008**, *33*, 113.

(44)   Duncan, R.; Ringsdorf, H.; Satchi-Fainaro, R. In *Polymer Therapeutics I*; Satchi-Fainaro, R., Duncan, R., Eds.; Springer Berlin Heidelberg: 2006; Vol. 192, p 1.

(45)   Haag, R.; Kratz, F. *Angew. Chem. Int. Ed.* **2006**, *45*, 1198.

(46)   Bildstein, L.; Dubernet, C.; Couvreur, P. *Adv. Drug Deliv. Rev.* **2011**, *63*, 3.

(47)   Duncan, R. *Nat. Rev. Cancer* **2006**, *6*, 688.

(48)   Kataoka, K.; Harada, A.; Nagasaki, Y. *Adv. Drug Deliv. Rev.* **2001**, *47*, 113.

(49)   Torchilin, V. P. *Expert Opin. Ther. Pat.* **2005**, *15*, 63.

(50)   Savić, R.; Eisenberg, A.; Maysinger, D. *J. Drug Target.* **2006**, *14*, 343.

(51)   Nishiyama, N.; Kataoka, K. In *Polymer Therapeutics II*; Satchi-Fainaro, R., Duncan, R., Eds.; Springer Berlin Heidelberg: 2006; Vol. 193, p 67.

(52)   Noble, C. O.; Kirpotin, D. B.; Hayes, M. E.; Mamot, C.; Hong, K.; Park, J. W.; Benz, C. C.; Marks, J. D.; Drummond, D. C. *Expert Opin. Ther. Targets* **2004**, *8*, 335.

(53)   Barenholz, Y. *Curr. Opin. Colloid Interface Sci.* **2001**, *6*, 66.

(54)   Yang, C.; Fu, Z.-X. *Biomed. Rep.* **2014**, *2*, 335.

(55)   Svenson, S.; Tomalia, D. A. *Adv. Drug Deliv. Rev.* **2005**, *57*, 2106.

(56)   Lee, C. C.; MacKay, J. A.; Frechet, J. M. J.; Szoka, F. C. *Nat. Biotechnol.* **2005**, *23*, 1517.

(57)   Zhou, Y.; Huang, W.; Liu, J.; Zhu, X.; Yan, D. *Adv. Mate.* **2010**, *22*, 4567.

(58)   Bellomo, E. G.; Wyrsta, M. D.; Pakstis, L.; Pochan, D. J.; Deming, T. J. *Nat. Mater.* **2004**, *3*, 244.

(59)   Holowka, E. P.; Sun, V. Z.; Kamei, D. T.; Deming, T. J. *Nat. Mater.* **2007**, *6*, 52.

(60) Rijcken, C. J. F.; Soga, O.; Hennink, W. E.; Nostrum, C. F. v. *J. Control. Release* **2007**, *120*, 131.

(61) Petka, W. A.; Harden, J. L.; McGrath, K. P.; Wirtz, D.; Tirrell, D. A. *Science* **1998**, *281*, 389.

(62) Kretschmann, O.; Choi, S. W.; Miyauchi, M.; Tomatsu, I.; Harada, A.; Ritter, H. *Angew. Chem. Int. Ed.* **2006**, *45*, 4361.

(63) Berndt, I.; Pedersen, J. S.; Richtering, W. *Angew. Chem. Int. Ed.* **2006**, *45*, 1737.

(64) Bertozzi.; R., C. *Acc. Chem. Res.* **2011**, *44*, 651.

(65) Ringsdorf, H. *J. Polym. Sci.Polym. Symp.* **1975**, *51*, 135.

(66) Cabral, H.; Nishiyama, N.; Okazaki, S.; Koyama, H.; Kataoka, K. *J. Control. Release* **2005**, *101*, 223.

(67) Wang, J.; Mongayt, D.; Torchilin, V. P. *J. Drug Target.* **2005**, *13*, 73.

(68) Lukyanov, A. N.; Hartner, W. C.; Torchilin, V. P. *J. Control. Release* **2004**, *94*, 187.

(69) Juliana Saraiva; Samantha S. Marotta-Oliveira; Simone Aparecida Cicillini; Josimar de Oliveira Eloy; Marchetti, J. M. *J. Drug Deliv.* **2011**, *2011*, 1.

(70) Shin, J. H.; Metzger, S. K.; Schoenfisch, M. H. *J. Am. Chem. Soc.* **2007**, *129*, 4612.

(71) Hetrick, E. M.; Shin, J. H.; Stasko, N. A.; Johnson, C. B.; Wespe, D. A.; Holmuhamedov, E.; Schoenfisch, M. H. *ACS Nano* **2008**, *2*, 235.

(72) Polizzi, M. A.; Stasko, N. A.; Schoenfisch, M. H. *Langmuir* **2007**, *23*, 4938.

(73) Molina, M. M.; Seabra, A. B.; de Oliveira, M. G.; Itri, R.; Haddad, P. S. *Mater. Sci. Eng. C* **2013**, *33*, 746.

(74)   Friedman, A. J.; Han, G.; Navati, M. S.; Chacko, M.; Gunther, L.; Alfieri, A.; Friedman, J. M. *Nitric Oxide* **2008**, *19*, 12.

(75)   Weller, R. B. *J. Invest. Dermatol.* **2009**, *129*, 2335.

(76)   Mihu, M. R.; Sandkovsky, U.; Han, G.; Friedman, J. M.; Nosanchuk, J. D.; Martinez, L. R. *Virulence* **2010**, *1*, 62.

(77)   Yoo, J.-W.; Lee, J.-S.; Lee, C. H. *J. Biomed.Mater. Res. A* **2010**, *92A*, 1233.

(78)   Kumar, V.; Hong, S. Y.; Maciag, A. E.; Saavedra, J. E.; Adamson, D. H.; Prud'homme, R. K.; Keefer, L. K.; Chakrapani, H. *Mol. Pharm.* **2010**, *7*, 291.

(79)   Jo, Y. S.; van der Vlies, A. J.; Gantz, J.; Thacher, T. N.; Antonijevic, S.; Cavadini, S.; Demurtas, D.; Stergiopulos, N.; Hubbell, J. A. *J. Am. Chem. Soc.* **2009**, *131*, 14413.

(80)   Hyduke, D. R.; Liao, J. C. *Am. J. Physiol. Heart Circ. Physiol.* **2005**, *288*, H2390.

(81)   Duong, H. T.; Kamarudin, Z. M.; Erlich, R. B.; Li, Y.; Jones, M. W.; Kavallaris, M.; Boyer, C.; Davis, T. P. *Chem. Commun.* **2013**, *49*, 4190.

(82)   Gao, M.; Liu, S.; Fan, A.; Wang, Z.; Zhao, Y. *RSC Adv.* **2015**, *5*, 67041.

(83)   Yu, S. H.; Hu, J.; Ercole, F.; Truong, N. P.; Davis, T. P.; Whittaker, M. R.; Quinn, J. F. *ACS Macro Lett.* **2015**, *4*, 1278.

(84)   Kanayama, N.; Yamaguchi, K.; Nagasaki, Y. *Chem. Lett.* **2010**, *39*, 1008.

(85)   Rothrock, A. R.; Donkers, R. L.; Schoenfisch, M. H. *J. Am. Chem. Soc.* **2005**, *127*, 9362.

(86)   Smith, D. J.; Pulfer, S.; Simmons, M. L.; Hrabie, J. A.; Saavedra, J. E.; Davies, K. M.; Mooradian, D. L.; Hanson, S. R.; Keefer, L. K. *J. Med. Chem.* **1996**, *39*, 1148.

(87)   Kolb, H. C.; Finn, M. G.; Sharpless, K. B. *Angew. Chem. Int. Ed.* **2001**, *40*,

2004.

(88)   Rhiannon, K. I.; Karen, L. W.; Andreas, M. N.; Daniel, J. B.; Matthew, J. K.; Craig, J. H. *Chem. Rev.* **2009**, *109*, 67.

(89)   Meldal, M. *Macromol. Rapid Commun.* **2008**, *29*, 1016.

(90)   Evans, R. A. *Aust. J. Chem.* **2007**, *60*, 384.

(91)   Miranda, K. M.; Espey, M. G.; Wink, D. A. *Nitric Oxide* **2001**, *5*, 62.

(92)   Misko, T. P.; Schilling, R. J.; Salvemini, D.; Moore, W. M.; Currie, M. G. *Anal. Biochem.* **1993**, *214*, 11.

(93)   Thompson, A. S.; Humphrey, G. R.; DeMarco, A. M.; Mathre, D. J.; Grabowski, E. J. J. *J. Org. Chem.* **1993**, *58*, 5886.

(94)   Lieber, E.; Rao, C. N. R.; Chao, T. S.; Hoffman, C. W. W. *Anal. Chem.* **1957**, *29*, 916.

(95)   Boyer, N. E.; Czerniak, G. M.; Gutowsky, H. S.; Snyder, H. R. *J. Am. Chem. Soc.* **1955**, *77*, 4238.

(96)   Kross, R. D.; Fassel, V. A. *J. Am. Chem. Soc.* **1956**, *78*, 4225.

(97)   Zhao, J.; Zhou, M.; Zuo, J.; Xu, X.; Zhang, X.; Yuan, W. *Tetrahedron* **2015**, *71*, 1560.

(98)   Rostovtsev, V. V.; Green, L. G.; Fokin, V. V.; Sharpless, K. B. *Angew. Chem. Int. Ed.* **2002**, *41*, 2596.

(99)   Tsikas, D. *J. Chromatogr. B* **2007**, *851*, 51.

(100)   Kirsch, M.; de Groot, H. *J. Biol. Chem.* **2002**, *277*, 13379.

(101)   Smulik, R.; Dębski, D.; Zielonka, J.; Michałowski, B.; Adamus, J.; Marcinek, A.; Kalyanaraman, B.; Sikora, A. *J. Biol. Chem.* **2014**, *289*, 35570.

(102)   Reisz, J. A.; Bechtold, E.; King, S. B. *Dalton Trans.* **2010**, *39*, 5203.

(103)   Jones, D. P.; Carlson, J. L.; Mody Jr, V. C.; Cai, J.; Lynn, M. J.; Sternberg Jr, P. *Free Rad. Biol. Med.* **2000**, *28*, 625.

(104)   Jones, D. P.; Carlson, J. L.; Samiec, P. S.; Sternberg Jr, P.; Mody Jr, V. C.; Reed, R. L.; Brown, L. A. S. *Clin. Chim. Acta* **1998**, *275*, 175.

(105)   Yap, A. H.; Weinreb, S. M. *Tetrahedron Lett.* **2006**, *47*, 3035.

(106)   Kalisiak, J.; Sharpless, K. B.; Fokin, V. V. *Org. Lett.* **2008**, *10*, 3171.

(107)   Thompson, R. L.; Damodaran, K.; Luebke, D.; Nulwala, H. *Synlett* **2013**, *24*, 1093.

(108)   Loren, J. C.; Krasiński, A.; Fokin, V. V.; Sharpless, K. B. *Synlett* **2005**, *2005*, 2847.

(109)   Ueda, S.; Su, M.; Buchwald, S. L. *Angew. Chem. Int. Ed.* **2011**, *50*, 8944.

(110)   Williams, J. L.; Borgo, S.; Hasan, I.; Castillo, E.; Traganos, F.; Rigas, B. *Cancer Res.* **2001**, *61*, 3285.

(111)   Hickok, J. R.; Thomas, D. D. *Curr. Pharm. Des.* **2010**, *16*, 381.

(112)   Moad, G.; Rizzardo, E.; Thang, S. H. *Aust. J. Chem.* **2012**, *65*, 985.

(113)   Keddie, D. J. *Chem. Soc. Rev.* **2014**, *43*, 496.

(114)   Perrier, S.; Takolpuckdee, P. *J. Polym. Sci. A Poly. Chem.* **2005**, *43*, 5347.

(115)   Moriyama, M.; Metzger, S.; van der Vlies, A. J.; Uyama, H.; Ehrbar, M.; Hasegawa, U. *Adv. Healthc. Mater.* **2015**, *4*, 569.

(116)   Chong, Y. K.; Moad, G.; Rizzardo, E.; Thang, S. H. *Macromolecules* **2007**, *40*, 4446.

(117)   Matyjaszewski, K. *Macromolecules* **2012**, *45*, 4015.

(118)   Gaetke, L. *Toxicology* **2003**, *189*, 147.

(119)   Baskin, J. M.; Prescher, J. A.; Laughlin, S. T.; Agard, N. J.; Chang, P. V.; Miller, I. A.; Lo, A.; Codelli, J. A.; Bertozzi, C. R. *Proc. Nati. Acad. Sci. U. S. A.* **2007**, *104*, 16793.

(120)   Treat, N. J.; Sprafke, H.; Kramer, J. W.; Clark, P. G.; Barton, B. E.; Read de Alaniz, J.; Fors, B. P.; Hawker, C. J. *J. Am. Chem. Soc.* **2014**, *136*, 16096.

(121)   Ydens, I.; Moins, S.; Botteman, F.; Degée, P.; Dubois, P. *E Polymers* **2004**, *4*, 414.

(122)   Matyjaszewski, K.; Pintauer, T.; Gaynor, S. *Macromolecules* **2000**, *33*, 1476.

(123)   Jasinski, N.; Lauer, A.; Stals, P. J. M.; Behrens, S.; Essig, S.; Walther, A.; Goldmann, A. S.; Barner-Kowollik, C. *ACS Macro Lett.* **2015**, *4*, 298.

(124)   Nguyen, L. M.; Dellinger, M. E.; Lee, J. T.; Quinlan, R. A.; Rheingold, A. L.; Pike, R. D. *Inorg. Chim. Acta* **2005**, *358*, 1331.

(125)   Jeliazkova, B. G.; Yordanov, N. D. *Inorg. Chim. Acta* **1993**, *203*, 201.

(126)   Wyatt, P. F. *Analyst* **1953**, *78*, 656.

(127)   Strafford, N.; Wyatt, P. F.; Kershaw, F. G. *Analyst* **1945**, *70*, 232.

(128)   Ellman, G. L. *Arch. Biochem. Biophys.* **1959**, *82*, 70.

(129)   Chan, T. R.; Hilgraf, R.; Sharpless, K. B.; Fokin, V. V. *Org. Lett.* **2004**, *6*, 2853.

(130)   Cavallini, D.; De Marco, C.; Duprè, S.; Rotilio, G. *Arch. Biochem. Biophys.* **1969**, *130*, 354.

(131)   Graisuwan, W.; Zhao, H.; Kiatkamjornwong, S.; Theato, P.; Hoven, V. P. *J.*

Polym. Sci. A Poly. Chem. **2015**, *53*, 1103.

(132)   Woodfield, P. A.; Zhu, Y.; Pei, Y.; Roth, P. J. *Macromolecules* **2014**, *47*, 750.

(133)   Quek, J. Y.; Roth, P. J.; Evans, R. A.; Davis, T. P.; Lowe, A. B. *J. Polym. Sci. A Poly. Chem.* **2013**, *51*, 394.

(134)   Chua, G. B. H.; Roth, P. J.; Duong, H. T. T.; Davis, T. P.; Lowe, A. B. *Macromolecules* **2012**, *45*, 1362.

(135)   Nilles, K.; Theato, P. *J. Polym. Sci. A Poly. Chem.* **2010**, *48*, 3683.

List of Publications

1. Nitric Oxide-releasing Polymeric Furoxan Conjugates

Tengjiao Wang, André J. van der Vlies, Hiroshi Uyama and Urara Hasegawa*

Polymer Chemistry, 2015, 6, 7737-7748.

2. Furoxan-Bearing Micelles for Nitric Oxide Delivery

Urara Hasegawa*, Tengjiao Wang, Jerry J. Chen, Hiroshi Uyama and André J. van der Vlies

Macromolecular Bioscience, 2016, accepted

3. Copper Removal from Polymers by Diethyldithiocarbamate Complexation

Urara Hasegawa*, Tengjiao Wang, Hiroshi Uyama and André J. van der Vlies

Chemistry Letters, 2016, accepted

Acknowledgements

My most sincere gratitude should go to my roommate and also my best buddy, **Mu Han**. He taught me how to swim, how to enjoy the life living in Osaka, how to be optimistic when facing problems. Thanks to his accompany, I feel no longer be boring and lonely apart from research life.

Last but not the least, I send my everlasting feelings of gratefulness and thankfulness to my parents, for their invaluable love and support. The love I owed them could never be paid.

Needless to say more, only a sincere "Thank You"!

Tengjiao Wang

January 2016